THE

LONDON, EDINBURGH, AND DUBLIN

PHILOSOPHICAL MAGAZINE

AND

JOURNAL OF SCIENCE.

[SEVENTH SERIES.]

AUGUST 1929.

XVI. *The Magneto-Optical Dispersion of some Organic Liquids in the Ultra-Violet Region of the Spectrum.* By C. C. Evans, *M.Sc.*, *and* Prof. E. J. Evans, *D.Sc.**

Introduction.

THE magneto-optical rotations of a large number of substances have been determined by several observers. Perkin, in particular, has measured very accurately and compared the magneto-rotary powers of many substances at the wave-length of sodium light.

T. M. Lowry † has determined the magnetic rotations of many organic compounds in the visible spectrum, and others (especially Borel, Meyer, and Richardson) have also studied the problem of magneto-optical dispersion.

Our knowledge, however, of the magneto-rotary dispersion over an extended range of the spectrum (especially in the ultra-violet) is still very incomplete. The present work deals with the determination of the values of Verdet's constants at different wave-lengths in the ultra-violet for four organic liquids, and also embodies the results of an investigation of the refractive indices of three of these liquids. It is a continuation of work carried out by Stephens and Evans ‡, and by Jones and Evans §.

* Communicated by the Authors.
† J. C. S. i. p. 106 (1913).
‡ Phil. Mag., March 1927, p. 546.
§ Phil. Mag., March 1928, p. 593.

From measurements of the magneto-optical dispersion of any substance, it is possible, with a knowledge of its natural dispersion in the same region, to deduce important information with regard to the nature of the resonators in the atoms of the various substances. These resonators are responsible for the magneto-rotary effects, and from observations of the magneto-optical dispersion it is possible to calculate their free periods. The experimental results also afford a means of testing the various theories put forward to account for the magneto-optical properties of substances.

Reference has already been made to Richardson in this branch of work, and if we adopt here the same nomenclature as he used in his papers *, the following method of examining the experimental results in relation to theory will be employed.

Assuming that the natural dispersion of a substance can be represented by an equation of the Ketteler-Helmholtz type, we have

$$n^2-1=b_0+\frac{b_1}{\lambda^2-\lambda_1^2}+\frac{b_2}{\lambda^2-\lambda_2^2}+\ldots, \quad . \quad . \quad (1)$$

where n is the refractive index for wave-length λ ; b_0, b_1, b_2, etc., are constants ; and $\lambda_1, \lambda_2 \ldots$ are the wave-lengths of the absorption bands of the substance.

This equation represents the state of affairs accurately when not too near an absorption band. Now, the rotary power δ of any substance has been shown by Larmor† to be given by the equation

$$\delta=\frac{e}{2mc^2}\lambda\frac{dn}{d\lambda}. \quad . \quad . \quad . \quad . \quad . \quad . \quad (2)$$

c=vel. of light and $\frac{e}{m}$ the ratio of the charge to the mass for all the resonators.

If we suppose that the dispersion of the medium is controlled by a single absorption band, or by a number of such bands for all of which the Zeeman constant is the same, the formula should apply exactly. Assuming, however, that an equation of the same type as equation (2) still applies when $\frac{e}{m}$ has different values for the various reso-

* Phil. Mag. xxxi. pp. 232 & 454.

† 'Æther and Matter,' Appendix F, p. 352.

nators, and substituting the value of $\frac{dn}{d\lambda}$ from (1) in equation (2), it can be shown * that

$$\phi = n\delta\lambda^2 = k_1\left\{\frac{\lambda^2}{\lambda^2-\lambda_1^2}\right\}^2 + k_2\left\{\frac{\lambda^2}{\lambda^2-\lambda_2^2}\right\}^2 + \ldots, \quad (3)$$

where k_1, k_2, etc., are constants.

In the case of media transparent in the visible and infra-red regions $\lambda_1, \lambda_2 \ldots$ will represent ultra-violet free periods. If the substance possesses only one absorption band, which contributes to the magnetic rotation, the equation takes the form:

$$\phi = k_1\left\{\frac{\lambda^2}{\lambda^2-\lambda_1^2}\right\}^2 . \quad . \quad . \quad . \quad . \quad . \quad (4)$$

From two values of the function ϕ corresponding to two values of λ, it is possible to determine the values of k_1 and λ_1 for the region of the spectrum between the two values of λ chosen. If it be found that the experimental results lead to different values of λ_1 depending on the values of λ chosen, and if these values increase progressively as the wave-lengths are taken in regions of shorter and shorter wave-lengths, it can be naturally inferred that the substance possesses more than one ultra-violet free period. In this case the magnetic-rotary dispersion equation assumes the form of equation (3), and as many terms appear on the right-hand side of (3) as there are absorption bands responsible for the rotary effect.

Apparatus.

The General Arrangement.

A detailed account of the apparatus used in this work has already been published †. It will therefore suffice to indicate briefly here the main features.

Light from a tungsten arc falls upon the polarizing unit of the apparatus and then traverses the liquid contained in the polarimeter tube, which is placed symmetrically inside the core of a solenoid. Between the tube and the solenoidal coil is a jacket through which water is passed, to enable constancy of temperature to be maintained.

The polarized beam, after emerging from the liquid, falls upon the analyser and afterwards upon a quartz-fluorite lens, which brings it to a focus at the slit of a quartz spectrograph.

* Richardson, *loc. cit.*

† Stephens and Evans, *loc. cit.*

The Polarimeter.

In these experiments the polarizer was of the Bellingham-Stanley type, suitable for ultra-violet work. It consisted of a quartz lens and a modified Jellet prism *. The beam of light, after emerging from the prism, consisted of two semicircular beams, the vibrations in one half being polarized at a slight angle with those in the other half, the line of demarcation between them being horizontal. The components of the analyser were assembled together with a thin film of glycerine between the faces in contact. The absorption of light in these experiments, due to this film of glycerine, was of no consequence, since the liquids used were themselves much more strongly absorbing. Both the analyser and the quartz-fluorite lens behind it were capable of being independently adjusted, so that the beam of light passed axially through the apparatus.

The Polarimeter Tube.

Throughout the whole investigation the same polarimeter tube was used. It was made of clear fused quartz, having an external diameter of 1 cm., and could contain a column of liquid 30·5 cm. long. The two ends of the tube were closed by fusing on disks of polished fused quartz. These disks rotate polarized light in a magnetic field, so that a correction has to be applied when measuring magnetic rotations of liquids. The values of the rotations of these disks at several wave-lengths were determined experimentally, and a curve drawn, so that the actual correction to be applied at any wave-length could be read off.

The Solenoid and its Magnetic Field.

At the commencement of this research the solenoid used was the identical one employed by Stephens and Evans †. These observers, by measuring the ballistic throw, determined the values of H at several points on the axis of the solenoid, and for the polarimeter tube 30·5 cm. long they deduced a value of 12,445 cm. gauss for ΣHl (where l is the length of the column of liquid over which H can be assumed to be constant).

Faulty insulation, however, necessitated the construction of a new coil after a few months' work. The new coil had the same number of layers of wire as the old one, but

* For details see 'Dictionary of Applied Physics,' iv. p. 476.

† *Loc. cit.*

improvements in the method of insulation altered the dimensions slightly, and therefore the field due to the same current was different.

A very careful series of determinations of the value of ΣHl was undertaken by measuring the magnetic rotations of conductivity water at several wave-lengths and using the known values of Verdet's constants at these points. The mean value thus found was 12,270 cm. gauss. The value calculated theoretically from the dimensions of the coil was 12,260 cm. gauss. Later, the values of H at various points along the axis of the coil were determined by observing the ballistic throws, and the above results were verified. The value finally adopted for ΣHl was 12,270 cm. gauss.

In series with the coil was a battery of 110 volts, a Weston volt-ammeter, and two variable resistances. One of these resistances served as a fine adjusting rheostat to keep the current steady. It is estimated that the current was kept steady at 2 amperes in these experiments to within 1 part in 700 on the average. The ammeter employed was periodically calibrated by comparing its readings with that of a large Weston Standard Ammeter. A reversing key was also introduced into the circuit, and the practical value of reversing the current in the coil will be referred to later.

To minimise difficulties and possible errors due to the heating of the liquid by the passage of the current through the coil, water was allowed to flow through the jacket during the experiments. It was found necessary to allow the current and water to flow for about an hour before taking a photograph, as this ensured a steady thermal state inside the core of the solenoid. The average variation of temperature during exposures was of the order of 0·1° C.

Source of Light and Spectrograph.

Throughout the whole investigation a tungsten arc was used as a source of light. Even with this powerful source of ultra-violet radiation, it was not found possible to work much below ·29 μ with the least absorbing of the liquids used in the present investigation.

The spectrograph employed was of the usual type and consisted of a Cornu quartz prism, together with quartz lenses.

The photographic plates used were either Imperial plates or Wellington Special Rapid plates, and the exposures, two of which were taken on each plate, varied from about 10 minutes at ·4 μ to about 40 minutes at ·29 μ.

Experimental Details.

The two beams of polarized light, after emerging from the polarimeter, appear as two superposed spectra after passing through the Cornu prism. These spectra appear at the camera end separated by a very fine horizontal gap.

In the absence of liquid in the polarimeter tube and the magnetic field, these spectra can be adjusted to be uniformly intense along the whole range. The intensities of the bottom and top halves, however, are not in general equal. They are only equally intense for four definite positions of the analyser with an angle of 90° separating one position from the next. Two of these positions separated from one another by 180° correspond to the maximum intensity, and the other two to positions of minimum intensity. In this latter position the instrument is extremely sensitive, and one of these positions is used as the zero reading of the analyser.

The actual position of the zero was determined by taking a series of photographs corresponding to different settings of the analyser near the position of minimum intensity, and carefully examining the plates. The zero having been fixed, a few photographs were taken in its neighbourhood with the liquid in the tube to ascertain whether or not the sample showed any natural rotation due to the presence of optically active impurities.

In the present work all four liquids were proved to be optically inactive.

When these preliminary observations had been performed, the magnetic rotary experiments were commenced. The analyser was rotated through a known angle θ_1 from the zero, the magnetic field applied, and a stream of water allowed to flow through the jacket. After an interval of about one hour, when temperature conditions were steady, a photograph was taken. During the exposure a constant watch was kept over the reading of the ammeter, the temperature of the water, and the position of the arc light. A second exposure was then taken on the same plate, corresponding to a rotation of θ_1 on the opposite side of the zero, with the magnetic field reversed.

On examining the plate, it is observed that, whilst the upper and lower halves of each spectrum are of very different intensities, there is a line of definite wave-length which has the same intensity in the upper and lower halves of each spectrum. The wave-length of this line is the same within a few Angström units for each direction of the magnetic field. The reversal of the magnetic field supplies a means

of eliminating certain sources of error, such as a slight mistake in the location of the zero position.

The experimental result that the wave-length for equality of intensity was the same for each direction of the field, also shows that the liquids employed did not contain any optically active substances as impurities.

If the mean wave-length as thus determined be denoted by λ, the rotation of the liquid at this wave-length $=\theta_1-\theta_2$, where θ_2 is the magnetic rotation of the quartz disks at wave-length λ. A series of determinations were then made, corresponding to increasing values of θ_1, until the point of equality had shifted to the limit in the ultra-violet.

The values of Verdet's constant δ were calculated from the formula: $\theta=\theta_1-\theta_2=\delta\Sigma Hl$.

Figs. 2, 3, 4, and 5 show the variation of δ with λ for the liquids investigated.

The Measurement of Natural Dispersion.

In the case of the four liquids experimented upon, namely isopropyl alcohol, allyl alcohol, methyl acetate, and ethyl acetate, values of the refractive indices in the ultra-violet could only be obtained for allyl alcohol*.

The values of the refractive indices in the ultra-violet for the other three substances were determined in the following manner:—

The same spectograph was used, with the Cornu prism replaced by a hollow prism closed by plates of polished fused quartz. A liquid whose refractive indices are known over a wide range of wave-lengths was placed in the prism, and a photograph taken with the top half of the slit illuminated by light from an iron arc. The liquid was then extracted from the prism, and the latter, which was rigidly fixed in position, was carefully cleaned and dried. A second photograph was then taken on the same plate, with the liquid whose refractive indices are required placed in the hollow prism. In this case the bottom half of the slit was illuminated by the light from the iron arc.

To find the refractive indices at various wave-lengths for the substances examined, it is only necessary to identify a line of wave-length λ_1, say, in the spectrum due to refraction through the standard liquid which is superimposed upon a line of wave-length λ_2 due to refraction through the substance.

* 'Etudes de Photochemie,' Victor Henri, p. 103.

The refractive index of the substance for wave-length λ_2 is then equal to the refractive index of the standard for wave-length λ_1.

In the present experiments pure ethyl alcohol was found to be a suitable standard liquid, and the refractive indices of isopropyl alcohol, methyl acetate, and ethyl acetate, over the ranges of wave-length required, have been determined with an accuracy of about 1 in 1000.

The values of the refractive indices of ethyl alcohol at various wave-lengths are due to Victor Henri *.

Experimental Results.

Table I. (*a*).

Natural Dispersion.

Isopropyl alcohol.		Methyl acetate.		Ethyl acetate.	
Wave-length.	Refractive Index.	Wave-length.	Refractive index.	Wave-length.	Refractive index.
·4384 μ	$1{\cdot}386_5$	·3975 μ	$1{\cdot}372_5$	·4384 μ	$1{\cdot}379_6$
·3975 μ	$1{\cdot}391_5$	·3813 μ	1·375	·4138 μ	$1{\cdot}381_2$
·3720 μ	$1{\cdot}395_3$	·3560 μ	$1{\cdot}377_3$	·3930 μ	$1{\cdot}383_6$
·3440 μ	$1{\cdot}400_1$	·3491 μ	$1{\cdot}378_5$	·3767 μ	$1{\cdot}385_9$
·3189 μ	1·405	·3307 μ	$1{\cdot}381_9$	·3625 μ	$1{\cdot}387_8$
·3127 μ	$1{\cdot}407_6$	·3195 μ	$1{\cdot}384_3$	·3426 μ	$1{\cdot}391_3$
·2973 μ	$1{\cdot}411_1$	·3101 μ	$1{\cdot}386_6$	·3227 μ	$1{\cdot}395_1$
		·3025 μ	$1{\cdot}388_7$	·3091 μ	$1{\cdot}398_3$
		·2747 μ	$1{\cdot}398_5$	·2973 μ	$1{\cdot}402_1$
				·2880 μ	1·405
Mean Temperature 20° C.				·2830 μ	$1{\cdot}406_9$

For the purpose of calculating the values of Verdet's constants from the magneto-rotary equations in the visible region of the spectrum, a few determinations of the refractive indices of each of the above three liquids were undertaken at well-known visible wave-lengths. These are collected and given in Table I. (*b*).

* 'Etudes de Photochemie,' Victor Henri, p. 61.

TABLE I. (*b*).

Refractive Index.

Wave-length.	Isopropyl alcohol.	Methyl acetate.	Ethyl acetate.
·6678 μ	$1{\cdot}375_3$	$1{\cdot}362_2$	$1{\cdot}371_8$
·6563 μ	$1{\cdot}375_9$	—	—
·5893 μ	$1{\cdot}377_1$	$1{\cdot}363_9$	$1{\cdot}373_7$
·5876 μ	$1{\cdot}377_7$	$1{\cdot}364_3$	1·374
·5461 μ	$1{\cdot}379_8$	$1{\cdot}366_3$	$1{\cdot}376_4$
·5016 μ	$1{\cdot}381_3$	$1{\cdot}367_8$	$1{\cdot}377_8$
·4713 μ	$1{\cdot}383_2$	$1{\cdot}368_5$	$1{\cdot}378_3$
·4472 μ	$1{\cdot}385_3$	1·370	—
	Mean Temp. 20° C.	Mean Temp. 16·8° C.	Mean Temp. 16·2° C.

Fig. 1.

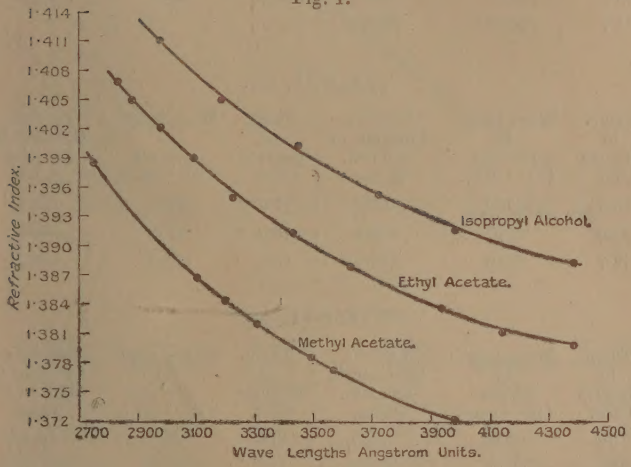

Magnetic Rotary Dispersion.

Isopropyl Alcohol.

Three sets of experiments were carried out on this liquid. The first two sets of results were obtained with the old solenoid, when the value of ΣHl for the polarimeter tube, 30·5 cm. long, was 12,445 cm. gauss. The third set was taken with the new solenoid, which gave for ΣHl the value 12,270 cm. gauss for the same tube. The experimental results are collected in Tables II. (*a*), II. (*b*), and II. (*c*).

The results tabulated in Table II. (*a*) were taken with a specimen of isopropyl alcohol from Poulenc Frères : those in Table II. (*b*) with a redistilled specimen from Dr. Schuchardt, of Görlitz. This latter specimen was also used in determining the results tabulated in Table II. (*c*).

TABLE II. (*a*).

Temp. in degrees Cent.	Wave-length in microns (10^{-4} cm.).	Verdet's Constant in min./cm. gauss.	Temp. in degrees Cent.	Wave-length in microns (10^{-4} cm.).	Verdet's Constant in min./cm. gauss.
16·0	·4400	·0238	15·7	·3586	$·0377_8$
15·7	·4008	·0293	15·5	·3504	$·0402_8$
16·2	·3913	$·0309_4$	15·4	·3415	$·0429_8$
15·5	·3866	$·322_8$	15·7	·3327	$·0458_1$
15·2	·3710	$·0350_6$	15·7	·3318	·0462
15·7	·3616	$·0371_8$			

TABLE II. (*b*).

Temp. in degrees Cent.	Wave-length in microns (10^{-4} cm.).	Verdet's Constant in min./cm. gauss.	Temp. in degrees Cent.	Wave-length in microns (10^{-4} cm.).	Verdet's Constant in min./cm. gauss.
15·0	·4400	·0238	14·9	·3730	$·0347_3$
13.6	·4010	·0293	15·0	·3710	$·0350_5$
13·7	·3940	$·0304_6$	15·0	·3590	·0377

TABLE II. (*c*).

Temp. in degrees Cent.	Wave-length in microns (10^{-4} cm.).	Verdet's Constant in min./cm. gauss.	Temp. in degrees Cent.	Wave-length in microns (10^{-4} cm.).	Verdet's Constant in min./cm. gauss.
10·9	·4380	$·0240_7$	11·0	·3730	$·0347_3$
10·9	·4193	$·0266_8$	11·0	·3590	·0377
11·1	·3995	$·0295_9$	11·1	·3564	$·0387_3$
11·0	·3973	$·0299_1$	11·0	·3495	·0409
11·1	·3877	$·0321_7$	10·8	·3417	·0429
10·9	·3840	·0329	10·8	·3356	·0447

From large-scale copies of the curves illustrated in figs. 1 and 2 a series of values of n, the refractive index, and δ Verdet's constant for isopropyl alcohol were read off ; these are tabulated from Table II. (*d*), and were made use of in attempting to test the results in relation to Larmor's theory.

As a result of this, it was found that the experimental results fitted into a formula of the type :

$$\phi = n\delta\lambda^2 = k_1\left\{\frac{\lambda^2}{\lambda^2 - \lambda_1^2}\right\}^2.$$

Fig. 2.

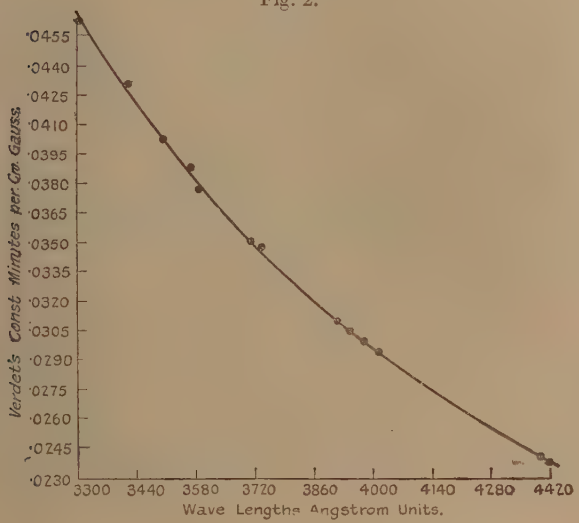

TABLE II. (*d*).

Isopropyl Alcohol.

	Wave-length in microns.	Refractive index.	Verdet's Constant, min./cm. gauss.		Wave-length in microns.	Refractive index.	Verdet's Constant, min./cm. gauss.
(*a*)	·4350 μ	1·3871	$\cdot 0245_1$	(*m*)	·3750 μ	1·3947	·0344
(*b*)	·4300 μ	1·3875	·0251	(*n*)	·3700 μ	1·3954	$\cdot 0355_2$
(*c*)	·4250 μ	1·3880	$\cdot 0257_3$	(*o*)	·3650 μ	1·3962	$\cdot 0366_9$
(*d*)	·4200 μ	1·3887	$\cdot 0263_9$	(*p*)	·3600 μ	1·3970	$\cdot 0379_4$
(*e*)	·4150 μ	1·3892	$\cdot 0271_1$	(*r*)	·3550 μ	1·3979	$\cdot 0393_3$
(*f*)	·4100 μ	1·3899	$\cdot 0278_4$	(*s*)	·3500 μ	1·3988	$\cdot 0405_5$
(*g*)	·4050 μ	1·3905	$\cdot 0286_4$	(*t*)	·3450 μ	1·3997	$\cdot 0419_7$
(*h*)	·4000 μ	1·3912	$\cdot 0294_5$	(*u*)	·3400 μ	1·4007	$\cdot 0434_7$
(*i*)	·3950 μ	1·3920	$\cdot 0303_5$	(*v*)	·3350 μ	1·4018	·0450
(*j*)	·3900 μ	1·3927	$\cdot 0312_5$	(*w*)	·3300 μ	1·4029	·0467
(*k*)	·3850 μ	1·3933	$\cdot 0322_5$	(*y*)	·3250 μ	1·4040	·0485
(*l*)	·3800 μ	1·3939	$\cdot 0333_2$				

The values of the function ϕ were calculated for each wave-length, and by eliminating k_1 from several pairs of these a set of values of λ_1 was obtained.

Eliminating k_1 from	λ_1 (microns).	Eliminating k_1 from	λ_1 (microns).	Eliminating k_1 from	λ_1 (microns).
(*c*) and (*o*)	·1134 μ	(*c*) and (*s*)	·1127 μ	(*c*) and (*w*)	·1139 μ
(*g*) and (*s*)	·1132 μ	(*j*) and (*w*)	·1136 μ	(*e*) and (*v*)	·1125 μ
(*c*) and (*t*)	·1137 μ	(*i*) and (*v*)	·1133 μ	(*i*) and (*w*)	·1132 μ
(*h*) and (*w*)	·1138 μ	(*b*) and (*n*)	·1160 μ	(*b*) and (*o*)	·1148 μ

The mean values of λ_1 from these $=$ ·1137 μ, and using this value of λ_1, the mean value of $k_1 = 5{\cdot}5526 \times 10^{-3}$ when δ is measured in minutes per cm. gauss and λ in microns. The equation therefore finally takes the form:

$$\phi = n\delta\lambda^2 = 5{\cdot}5526 \times 10^{-3} \left\{ \frac{\lambda^2}{\lambda^2 - (\cdot 1137)^2} \right\}^2 \quad . \quad . \quad (a)$$

This equation was used, together with values of n read off from fig. 1, to evaluate δ at a few wave-lengths where experimental determinations had been carried out. The result of such a comparison is shown in Table II. (*e*).

TABLE II. (*e*).

Isopropyl Alcohol.

λ.	δ (observed).	δ (calculated).	λ.	δ (observed).	δ (calculated).
·4400 μ	·0238	$\cdot 0237_5$	·3564 μ	$\cdot 0387_3$	$\cdot 0386_9$
·3866 μ	·0322	$\cdot 0319_6$	·3417 μ	·0429	$\cdot 0429_4$
·3730 μ	$\cdot 0347_3$	$\cdot 0347_7$	·3318 μ	·0462	$\cdot 0461_7$

Lowry and Dickson* have also determined the rotary dispersion of isopropyl alcohol at a few wave-lengths in the visible spectrum. These observers compare the rotary powers at various wave-lengths with that at $\lambda =$ ·5461 μ.

Using values of n obtained from a curve drawn from results tabulated in Table I. (*b*) and equation (*a*) above, δ was calculated for each of these wave-lengths, and the comparison is given below:

* J. C. S. l. p. 1072 (1913).

Wave-length, microns.	Rotary power relative to that at ·5461 μ.	
	Lowry & Dickson.	Present results.
·6708 μ	0·642	0·644
·6438 μ	0·702	0·703
·5893 μ	0·850	0·849
·5086 μ	1·163	1·167
·4800 μ	1·320	1·326
·4359 μ	1·634	1·646

The value of δ for the wave-length of sodium light was calculated from the formula (*a*), and found to be 0·01252 min. per cm. gauss.

Perkin * determined the rotation of isopropyl alcohol at this wave-length relative to water, and quotes the value 0·952. Using the value 0·0131 min. per cm. gauss for δ at ·5893 μ, in the case of water, this gives 0·01247 as the value for isopropyl at this wave-length.

The agreement between the value determined from the formula and the value obtained experimentally by Perkin is satisfactory.

It is interesting to point out that the equation connecting φ with λ in the case of normal propyl alcohol, as determined by Jones and Evans †, is given by

$$\phi = n\delta\lambda^2 = 5{\cdot}34 \times 10^{-3}\left\{\frac{\lambda^2}{\lambda^2-(\cdot 1138)^2}\right\}^2.$$

On comparing the experimental results, it is seen that the absorption bands are situated almost exactly at the same point in the ultra-violet. The values of Verdet's constant for isopropyl alcohol are, on the average, 4 per cent. higher than the corresponding values for normal propyl alcohol: this is also the identical order of difference obtained by Perkin ‡ for these liquids at λ = ·5893 μ.

Allyl Alcohol.

In the present investigation the values of Verdet's constants for allyl alcohol have been determined from ·446 μ to ·2884 μ. The sample was experimented upon before and after a series of successive distillations. The results, in both cases, are identical, and are collected together in Tables III. (*a*) and III. (*b*).

* J. C. S. i. p. 468 (1884).
† *Loc. cit.*
‡ *Loc. cit.*

In Table III. (*c*) the values of Verdet's constants are those for which extremely accurate determinations had been carried out. The values of the refractive indices are those read off from a curve drawn from the results of Victor Henri *.

Here, again, the magnetic dispersion equation possesses only one term on the right-hand side, indicating that the magnetic rotation of allyl alcohol in the ultra-violet region investigated in this work is governed by a single absorption band.

TABLE III. (*a*).

Allyl Alcohol (before distillation).

Temp. in degrees Cent.	Wave-length in microns.	Verdet's Constant in min./cm. gauss.	Temp. in degrees Cent.	Wave-length in microns.	Verdet's Constant in min./cm. gauss.
11·1	·4460	$·0311_3$	11·2	·3689	$·0500_1$
10·9	·4282	·0344	11·2	·3649	$·0516_4$
10·8	·4229	$·0354_9$	11·2	·3593	$·0532_4$
10·8	·4145	$·0371_1$	11·1	·3560	$·0548_6$
11·0	·4136	$·0374_7$	11·2	·3520	$·0546_7$
10·8	·4073	$·0387_1$	11·2	·3472	$·0584_9$
11·0	·4012	$·0403_3$	11·1	·3416	·0605
11·0	·3985	$·0411_8$	11·0	·3382	$·0625_3$
10·9	·3940	$·0419_5$	11·0	·3346	$·0645_5$
11·0	·3890	$·0435_6$	11·0	·3299	$·0671_4$
11·0	·3828	$·0451_7$	11·0	·3240	$·0702_7$
11·2	·3783	$·0467_9$	10·8	·3181	$·0751_2$
11·2	·3736	$·0483_9$			

TABLE III. (*b*).

Allyl Alcohol (after distillation).

Temp. in degrees Cent.	Wave-length in microns.	Verdet's Constant in min./cm. gauss.	Temp. in degrees Cent.	Wave-length in microns.	Verdet's Constant in min./cm. gauss.
9·2	·3207	·0727	11·3	·2998	$·0892_3$
9·3	·3181	$·0751_2$	11·3	·2957	$·0916_8$
9·8	·3098	$·0807_9$	11·0	·2943	$·0933_7$
10·5	·3057	·0836	11·0	·2884	$·0992_6$

* *Loc. cit.* p. 103.

TABLE III. (*c*).

Allyl Alcohol.

	Wave-length in microns.	Refractive index. "n."	Verdet's Constant in min./cm. gauss.
(*a*)	·4282	1·4299	·0344
(*b*)	·3783	1·4366	$\cdot 0467_9$
(*c*)	·3299	1·4496	$\cdot 0671_4$
(*d*)	·2943	1·4658	$\cdot 0933_7$

Fig. 3.

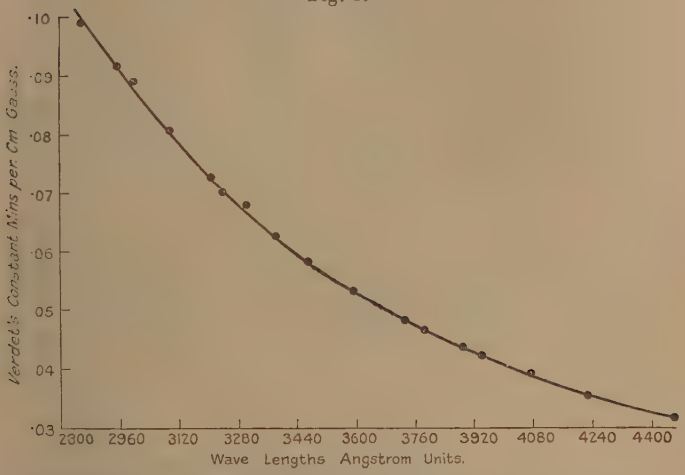

The following values of λ_1, the wave-length of the absorption band for allyl alcohol, were calculated by solving equation (4).

Eliminating k_1 from	λ_1 in microns.
(*a*) and (*b*)	·1365
(*b*) and (*c*)	·1363
(*c*) and (*d*)	·1384
(*b*) and (*d*)	·1375
(*a*) and (*d*)	·1372

These give for λ_1 a mean value $= \cdot 1372\,\mu$, and the mean value of $k_1 = 7 \cdot 24 \times 10^{-3}$. These values of λ_1 and k_1 are also the identical values obtained from the mean of more than 20 solutions of equation (4), using values δ and n from the respective dispersion curves.

The final equation for this liquid, therefore, is

$$\phi = n\delta\lambda^2 = 7 \cdot 24 \times 10^{-3} \left\{ \frac{\lambda^2}{\lambda^2 - (\cdot 1372)^2} \right\}^2.$$

In Table III. (*d*) below, a comparison is given between the values of Verdet's constants as determined experimentally and those calculated from the above formula.

TABLE III. (*d*).

Wave-length.	δ (calculated).	δ (observed).	Wave-length.	δ (calculated).	δ (observed).
·4229 μ	$\cdot0353_5$	$\cdot0354_9$	·3593 μ	$\cdot0532_5$	$\cdot0532_4$
·4012 μ	$\cdot0402_6$	$\cdot0403_3$	·3472 μ	$\cdot0584_1$	$\cdot0584_8$
·3890 μ	·0435	$\cdot0435_8$	·2957 μ	$\cdot0917_8$	$\cdot0916_8$
·3736 μ	$\cdot0482_1$	$\cdot0483_9$			

The above equation was used to calculate the values of Verdet's constant for the green and violet mercury lines at ·5461 μ and ·4359 μ. In this way it was found that the ratio

$$\frac{\delta_{\cdot4359}}{\delta_{\cdot5461}} = 1\cdot690.$$

Lowry *, who has determined the rotation of allyl alcohol for six wave-lengths in the visible spectrum (previously referred to), has found for this ratio the value 1·672. He expressed his results in the form of an empirical relation :

$$\alpha = \frac{k}{\lambda^2 - \lambda_0^2}$$

where α is the rotation for wave-length λ, k a constant, and λ_0 the wave-length of the absorption band. The absorption band from his value of λ_0^2 (·0293) is situated at ·1710 μ. According to the measurements of Victor Henri † on natural dispersion, the strong absorption band is calculated to be at ·1588 μ, whilst in the present experiments the absorption band is found to be at ·1372 μ.

The value of Verdet's constant at the wave-length of sodium light, according to the formula derived from the present work, = $\cdot0165_2$ minute per cm. gauss ; the value given by Perkin's ‡ results at 13° C. = ·01639.

Methyl Acetate.

The magnetic rotations of methyl acetate have been examined in the present work from ·44 μ to ·2951 μ, and the experimental results appear in Table IV. (*a*). Combining these results with the data in Table I., according to Larmor's § theory, it was discovered that one absorption

* *Loc. cit.* † *Loc. cit.* ‡ *Loc. cit.* § *Loc. cit.*

band was responsible for the magneto-rotary effects of this liquid in the region of the spectrum investigated.

TABLE IV. (*a*).

Methyl Acetate.

Temp. in degrees Cent.	Wave-length (microns).	Verdet's Constant, min./cm. gauss.	Temp. in degrees Cent.	Wave-length (microns).	Verdet's Constant, min./cm. gauss.
11·7	·4386	·0200	11·7	·3465	$\cdot 0346_3$
11·7	·4238	$\cdot 0216_1$	11·7	·3423	$\cdot 0356_2$
11·7	·4050	·0240	11·7	·3340	$\cdot 0376_2$
11·6	·3992	$\cdot 0247_4$	11·7	·3277	$\cdot 0396_3$
11·7	·3908	·0256	11·6	·3248	$\cdot 0404_9$
11·6	·3806	$\cdot 0275_2$	11·7	·3230	$\cdot 0410_4$
11·7	·3754	$\cdot 0284_8$	11·8	·3170	$\cdot 0428_2$
11·7	·3675	$\cdot 0300_6$	11·7	·3109	·0449
11·7	·3654	$\cdot 0304_2$	11·7	·3079	$\cdot 0461_7$
11·7	·3620	·0310	11·6	·3064	$\cdot 0467_3$
11·6	·3568	$\cdot 0323_4$	11·7	·2020	$\cdot 0484_3$
11·7	·3507	$\cdot 0336_1$	11·6	970	$\cdot 0506_8$

Fig. 4.

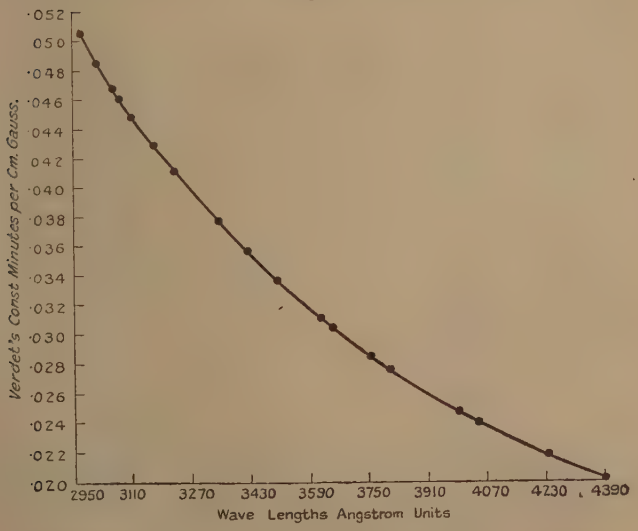

Table IV. (*b*) contains results read off from figs. 1 and 4.

TABLE IV. (*b*).

	Wave-length in microns.	Verdet's Constant, min./cm. gauss.	Refractive index.		Wave-length in microns.	Verdet's Constant, min./cm. gauss.	Refractive index.
(*a*)	·4000	$\cdot 0246_2$	1·3721	(*n*)	·3450	$\cdot 0349_8$	1·3792
(*b*)	·3950	·0253	1·3727	(*o*)	·3400	$\cdot 0362_2$	1·3801
(*c*)	·3900	$\cdot 0260_3$	1·3732	(*p*)	·3350	$\cdot 0375_2$	1·3811
(*d*)	·3850	$\cdot 0268_2$	1·3737	(*q*)	·3300	·0389	1·3821
(*e*)	·3800	$\cdot 0276_3$	1·3743	(*r*)	·3250	$\cdot 0403_8$	1·3833
(*f*)	·3750	$\cdot 0285_8$	1·3749	(*s*)	·3200	$\cdot 0419_2$	1·3845
(*g*)	·3700	$\cdot 0295_4$	1·3756	(*t*)	·3150	$\cdot 0435_6$	1·3858
(*h*)	·3650	·0305	1·3762	(*u*)	·3100	$\cdot 0452_6$	1·3871
(*k*)	·3600	$\cdot 0315_4$	1·3769	(*v*)	·3050	$\cdot 0472_5$	1·3885
(*l*)	·3550	$\cdot 0325_8$	1·3776	(*w*)	·3000	·0494	1·3900
(*m*)	·3500	$\cdot 0337_8$	1·3783	(*z*)	·2950	·0516	1·3916

Using the above results and solving the dispersion equation as before, we have the following values of λ_1 for the wave-length of the absorption band in the case of methyl acetate :—

Eliminating k_1 from	λ_1 (microns).	Eliminating k_1 from	λ_1 (microns).	Eliminating k from	λ_1 (microns).
(*a*) and (*w*)	·1109	(*b*) and (*q*)	·1121	(*g*) and (*z*)	·1108
(*b*) and (*p*)	·1129	(*g*) and (*n*)	·1117	(*k*) and (*s*)	·1091
(*a*) and (*p*)	·1116	(*f*) and (*v*)	·1103	(*a*) and (*o*)	·1139
(*a*) and (*r*)	·1109	(*d*) and (*t*)	·1114	(*d*) and (*v*)	·1113
(*a*) and (*m*)	·1129	(*c*) and (*r*)	·1139	(*c*) and (*s*)	·1119

These give $\cdot 1117\,\mu$ as a mean value of λ_1, and for k_1, the constant in the dispersion equation, the calculated mean is equal to $4\cdot 587 \times 10^{-3}$.

The equation, therefore, finally takes the form

$$\phi = n\delta\lambda^2 = 4\cdot 587 \times 10^{-3} \left\{ \frac{\lambda^2}{\lambda^2 - (\cdot 1117)^2} \right\}.$$

A comparison between the values of Verdet's constant calculated from this formula, and the values obtained experimentally, is given in Table IV. (*c*) below.

TABLE IV. (*c*).

Methyl Acetate.

λ.	δ (calculated).	δ (observed).	λ.	δ (calculated).	δ (observed).
·3026	$·0484_2$	$·0484_3$	·3423	$·0355_4$	$·0356_2$
·3170	$·0429_5$	$·0428_2$	·3675	$·0299_7$	$·0300_8$
·3230	·0410	$·0410_4$	·4386	·0199	·0200

Unfortunately, no strict comparison can be made between the values of Verdet's constant as calculated from the formula derived from this work and that as determined by Perkin *, since the present determinations have been performed at 11·6° C. and Perkin † worked at 22° C. The value of δ, Perkin ‡ gives at ·5893 μ = ·0102 min. per cm. gauss at 22° C., whilst the value calculated from the present results = ·0104 min. per cm. gauss at 11·6° C.

Ethyl Acetate.

In the case of ethyl acetate the magnetic rotations were determined from ·4404 μ to ·3091 μ; the results are collected together in Table V. (*a*).

As in the case of the other three organic liquids tested, it was found possible to account for these results on the assumption of one strong ultra-violet absorption band.

TABLE V. (*a*).

Ethyl Acetate.

Temp. in degrees Cent.	Wave-length in microns.	Verdet's Constant in min./cm. gauss.	Temp. in degrees Cent.	Wave-length in microns.	Verdet's Constant in min./cm. gauss.
11·6	·4406	$·0207_2$	11·6	·3605	$·0331_1$
11·6	·4305	$·0219_1$	11·6	·3546	$·0346_4$
11·6	·4075	$·0246_9$	11·6	·3476	$·0362_5$
11·6	·3995	$·0258_0$	11·6	·3529	$·0349_5$
11·6	·3920	$·0270_9$	11·6	·3407	$·0379_4$
11·6	·3850	·0283	11·6	·3346	$·0397_8$
11·6	·3785	$·0294_2$	11·7	·3270	$·0417_8$
11·6	·3725	$·0307_1$	11·6	·3206	$·0439_5$
11·6	·3660	$·0319_1$	11·6	·3152	$·0459_3$
11·6	·3657	$·0319_2$	11·6	·3103	$·0477_6$

* *Loc. cit.* p. 494. † *Loc. cit.* ‡ *Loc. cit.*

Fig. 5.

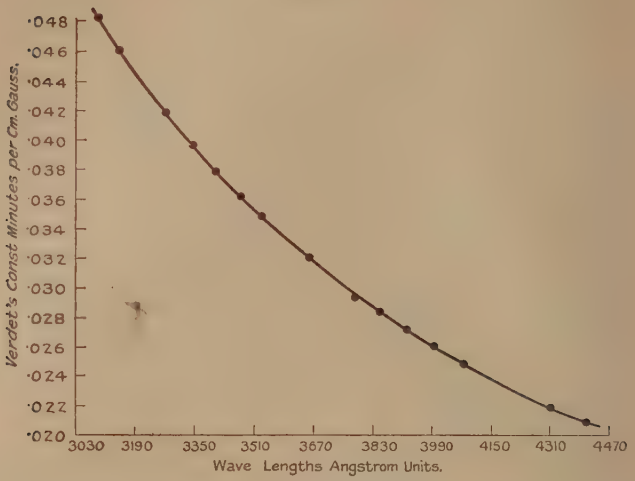

The results tabulated in Table V. (*b*) are those read off from figs. 1 and 5, and were made use of in calculating the value of λ_1 for ethyl acetate.

TABLE V. (*b*).

Ethyl Acetate.

	Wave-length in microns.	Verdet's Constant, min./cm. gauss.	Refractive index.		Wave-length in microns.	Verdet's Constant, min./cm. gauss.	Refractive index.
(*a*)	·4200	$\cdot 0231_8$	1·3808	(*m*)	·3600	$\cdot 0331_8$	1·3880
(*b*)	·4150	$\cdot 0237_4$	1·3812	(*n*)	·3550	$\cdot 0342_6$	1·3889
(*c*)	·4100	$\cdot 0243_6$	1·3817	(*o*)	·3500	$\cdot 0355_4$	1·3898
(*d*)	·4050	$\cdot 0250_4$	1·3821	(*p*)	·3450	$\cdot 0367_8$	1·3908
(*e*)	·4000	$\cdot 0257_4$	1·3826	(*q*)	·3400	$\cdot 0380_5$	1·3918
(*f*)	·3950	$\cdot 0264_8$	1·3832	(*r*)	·3350	$\cdot 0394_8$	1·3928
(*g*)	·3900	$\cdot 0273_6$	1·3837	(*s*)	·3300	$\cdot 0409_4$	1·3939
(*h*)	·3850	$\cdot 0282_5$	1·3843	(*t*)	·3250	·0425	1·3951
(*i*)	·3800	$\cdot 0291_2$	1·3850	(*u*)	·3200	$\cdot 0442_4$	1·3964
(*j*)	·3750	$\cdot 0300_6$	1·3857	(*v*)	·3150	$\cdot 0460_6$	1·3976
(*k*)	·3700	$\cdot 0310_8$	1·3864	(*w*)	·3100	$\cdot 0478_3$	1·3990
(*l*)	·3650	$\cdot 0320_3$	1·3872				

Eliminating k_1 from	λ_1 (microns).	Eliminating k_1 from	λ_1 (microns).	Eliminating k_1 from	λ_1 (microns).
(*e*) and (*g*)	·1164	(*a*) and (*w*)	·1113	(*c*) and (*n*)	·1153
(*p*) and (*b*)	·1146	(*c*) and (*w*)	·1134	(*g*) and (*r*)	·1153
(*j*) and (*u*)	·1136	(*b*) and (*t*)	·1127	(*o*) and (*v*)	·1119
(*b*) and (*q*)	·1134	(*g*) and (*u*)	·1147	(*e*) and (*k*)	·1156
(*c*) and (*s*)	·1143	(*g*) and (*v*)	·1147	(*k*) and (*w*)	·1113
(*e*) and (*s*)	·1156	(*b*) and (*l*)	·1143		

The mean value of λ_1 from the above $= \cdot1140\,\mu$, and the mean value of $k_1 = 4\cdot825 \times 10^{-3}$.

Thus the dispersion equation is.

$$\phi = n\delta\lambda^2 = 4\cdot825 \times 10^{-3} \left\{ \frac{\lambda^2}{\lambda^2 - (\cdot1140)^2} \right\}^2.$$

Table V. (*c*) shows a comparison between results calculated from the above equation and those determined experimentally.

TABLE V. (*c*).

Ethyl Acetate.

λ.	δ (calculated).	δ (observed).	λ.	δ (calculated).	δ (observed).
·4406 μ	·0207	$\cdot0206_3$	·3476 μ	$\cdot0360_7$	$\cdot0362_5$
·4305 μ	$\cdot0218_3$	·0219	·3529 μ	$\cdot0347_8$	$\cdot0349_5$
·4075 μ	$\cdot0247_5$	$\cdot0246_9$	·3270 μ	$\cdot0419_3$	0417_8
·3725 μ	$\cdot0305_5$	$\cdot0307_1$			

Perkin's * values for the specific rotation at ·5893 μ, in the case of ethyl acetate, are 0·8315 at 10·5° C. and 0·8295 at 14·5° C. These give values of 0·01089 and 0·01087 respectively for δ in minutes per cm. gauss.

The value calculated from the formula derived here = 0·01092 at 11·7° C.

SUMMARY.

(*a*) The magneto-optical rotations of isopropyl alcohol, allyl alcohol, methyl acetate, and ethyl acetate have been determined for various wave-lengths in the violet and near ultra-violet regions of the spectrum.

The refractive indices of isopropyl alcohol and of methyl and ethyl acetates have also been determined in the visible and near ultra-violet regions of the spectrum.

(*b*) The magneto-rotary dispersion of isopropyl alcohol and of allyl alcohol for the ranges of wave-length investigated can be represented by the equations:

$$\phi = n\delta\lambda^2 = 5{\cdot}5526 \times 10^{-3} \left\{ \frac{\lambda^2}{\lambda^2 - (\cdot 1137)^2} \right\}^2$$

and $$\phi = n\delta\lambda^2 = 7{\cdot}24 \times 10^{-3} \left\{ \frac{\lambda^2}{\lambda^2 - (\cdot 1372)^2} \right\}^2$$

respectively, where n is the refractive index and δ Verdet's constant in minutes per cm. gauss for wave-length λ. The strong ultra-violet absorption bands which control the magnetic rotation in the case of isopropyl alcohol and allyl alcohol have wave-lengths $\cdot 1137\,\mu$ and $\cdot 1372\,\mu$ respectively.

(*c*) The magnetic-rotary dispersion of methyl and ethyl acetates for the ranges of wave-lengths investigated can be represented by the equations:

$$\phi = n\delta\lambda^2 = 4{\cdot}587 \times 10^{-3} \left\{ \frac{\lambda^2}{\lambda^2 - (\cdot 1117)^2} \right\}^2$$

and $$\phi = n\delta\lambda^2 = 4{\cdot}825 \times 10^{-3} \left\{ \frac{\lambda^2}{\lambda^2 - (\cdot 1140)^2} \right\}^2$$

respectively.

The wave-lengths of the absorption bands which control the magneto-optical rotation of methyl and ethyl acetates are $\cdot 1117\,\mu$ and $\cdot 1140\,\mu$ respectively.

Swansea,
January 1929.

XVII. *An Apparatus for the Measurement of Magnetic Susceptibility.* *By* W. Sucksmith, *B.Sc., Lecturer in Physics, University of Bristol* *.

IN connexion with another investigation the writer found it necessary to measure the magnetic susceptibilities of a number of paramagnetic substances. As the method employed embodies only very simple apparatus and is capable of measuring moderate susceptibilities with a fair degree of accuracy, it seemed worth while to deal with it in a separate communication.

* Communicated by the Author

Existing Apparatus and Methods.

The method most generally useful is that of Faraday, in which the force on a small specimen placed in a non-uniform field is measured. If an isotropic substance of mass m and susceptibility χ is placed in a non-uniform field H whose gradient perpendicular to the magnetic lines of force is $\frac{d\mathrm{H}}{dx}$, the force experienced along the x-axis is given by

$$\mathrm{F}_x = \chi m \mathrm{H} \frac{d\mathrm{H}}{dx}.$$

In the early experiments of Curie the substance was placed on the arm of a torsion-balance, and the force measured by the displacement experienced by the specimen. The displacement was kept small, otherwise the value of $\mathrm{H}\frac{d\mathrm{H}}{dx}$ varies considerably. The best position for the specimen is the point at which this is a maximum, so that errors due to accidental displacement from this position are reduced to a minimum. The susceptibility can be readily calculated from the constants of the system together with a knowledge of H and $\frac{d\mathrm{H}}{dx}$. The accurate determination of $\frac{d\mathrm{H}}{dx}$ is, however, rather difficult, and late experimenters have avoided it by comparing the susceptibility of the substance under examination with that of a standard substance placed in the same position, the susceptibility of which had been determined by other means (*e. g.* the Quincke ascension method for liquids, which has the advantage of employing a uniform field). With a torsion-balance the great sensitivity obtainable is offset by the difficulty of placing the comparison substance in exactly the same position as that occupied by the specimen, together with the unavoidably long period of oscillation of the system.

Weiss and his collaborators have developed an apparatus which is capable of considerable accuracy, the most recent form of which is due to Foex and Forrer *. The torsion-balance is replaced by a movable pendular system which carries the specimen. The moving system is suspended by fine threads so as to allow motion only in one direction. Thus, under the action of the magnetic field the system moves horizontally against the gravitational control of the

* *Journ. de Phys.* vol. vii. p. 180 (1926).

system in a direction perpendicular to the lines of force. A null method is used, and the magnetic force is compensated by the electro-dynamic force exerted between a coil carried on the moving system and a fixed permanent magnet. The latter force varied approximately linearly with the current carried by the coil. To indicate the zero of the system a Kelvin double-suspension mirror of special type was used, the supporting threads being 4 mm. apart. The authors claim an accuracy of 1 part in 750 in a measurement on 0·35 gram of a substance of susceptibility $0{\cdot}55\times10^{-6}$, the force being less than 3 dynes. The accuracy and sensitivity appear to be as great as is necessary, but these appear to be somewhat counterbalanced by the elaborate nature of the apparatus and the reliance placed on the relationship between restoring force and the current in the restoring coil. In addition, the apparatus is bulky, since the restoring coil should be well removed from the region of stray field of the magnet, though correction can be made for the residue of this. The suspensions are apparently of the order of 60 cm. in length.

For many purposes an accuracy of $\frac{1}{2}$ to 1 per cent. is quite sufficient, and it appeared possible to the writer to design an apparatus that would meet this requirement and at the same time eliminate the necessity of using restoring forces by making the displacements very small.

Description of Method.

The method depends on the deformation of a circular ring of strip phosphor-bronze fixed at the top and subjected to a force at the bottom. The applied force is due to the action of a magnetic field on a specimen under investigation. If such a ring is clamped in a vertical plane at its highest point, and a force P applied at the bottom of the ring vertically downwards, then the radial displacement u at any point is given by

$$u=\frac{\mathrm{P}r^3}{4\mathrm{EI}}\left\{\theta\sin\theta+\cos\theta-\frac{4}{\pi}\right\},$$

where r = radius of the ring,

I = the moment of inertia of cross-section of the ring,

E = Young's Modulus,

and θ = angle between the radius through the point considered and the horizontal.

When $\theta = 90°$, then the displacement of the lowest point relative to the point of support

$$= \frac{Pr^3}{2EI}\left\{\frac{\pi}{2} - \frac{4}{\pi}\right\} = \frac{0{\cdot}298\,Pr^3}{2EI}.$$

The angle turned through by the tangent to the ring is, to a first approximation, given by

$$\phi = \frac{1}{r} \cdot \frac{du}{d\theta} = \frac{Pr^2}{4EI}(\theta \cos\theta).$$

This is a maximum at about 49°, whence

$$\phi = \frac{0{\cdot}561\,Pr^2}{4EI}.$$

Two mirrors, facing each other, are placed at the points B and C (see figure), where the angular displacement is a

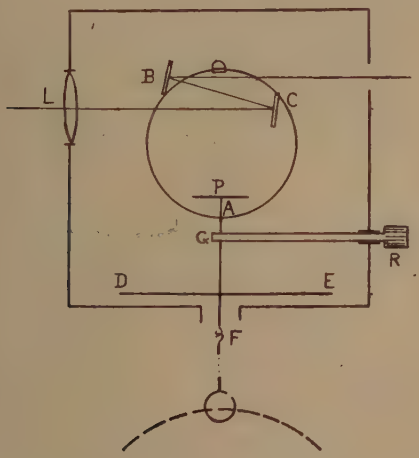

maximum. Light from a distant source passes through the lens L, and if, after reflexion at the two mirrors, it is focussed on a vertical scale D cm. away, then the scale-displacement corresponding to the force P is given by

$$v = \phi(4D + 2d),$$

where d is the distance between the mirrors at B and C.

In terms of the constants of the system

$$v = \frac{(4D + 2d)0{\cdot}561\,Pr^2}{4EI}.$$

Hence

$$\frac{v}{u} = \frac{0{\cdot}943(4D + 2d)}{r}.$$

Since P is the magnetic force exerted on a body in a non-uniform magnetic field, u must be kept small, *i. e.* the ratio v/u should be as large as conveniently possible. The values chosen were $r = 2{\cdot}5$ cm., and D a distance of about 1 metre. This gives a scale-displacement about 150 times that of the body. For a source a lamp with a straight metal filament was found most satisfactory. With a distance D of 100 cm. the lens which gives best definition of the image is one of 50-cm. focus, so that the distance of the source is about 1 metre from the lens and the magnification of the image unity. Further, as the size of the mirrors governs the effective lens aperture, these should be as large as conveniently possible. These were made by chemically silvering selected plate-glass $10 \times 10 \times 1$ mm. In lieu of a scale, a microscope with vertical traverse is focussed on the image of the filament. Under these conditions it is easy with a little practice to read the position of the image to 0·01 mm., which corresponds to a displacement of the specimen of 0·000007 cm.

From the lower extremity of the ring hangs a copper wire carrying a light mica damping-vane D E. The specimen carrier for powdered material and liquids is a thin-walled glass phial at the end of an extension of thin glass tube. This hangs from the lower extremity of the copper wire at F. The joints at A and F are cemented rigid with shellac.

The whole apparatus is enclosed in a brass box $10 \times 10 \times 13$ cm. The support for the ring is a circular brass rod fitted into a friction-tight brass tube. This allows of approximately horizontal adjustment along or perpendicular to the lines of magnetic force. The dotted outline of pole-pieces is shown in the figure, so that for a paramagnetic substance the magnetic force is vertically downwards. In the tests to be described, plane pole-pieces of diameter 10 cm., 3 cm. apart, were used, thus ensuring a reasonable volume over which $H\frac{dH}{dx}$ is appreciably constant. The separation of 3 cm. is sufficient to allow the specimen to be enclosed in the usual apparatus

for high- or low-temperature work. The current used was 15 amperes, which gave a value of $H\frac{dH}{dx}$ of about 10^7.

Since the accuracy of the method depends on the linear relationship between force and displacement, tests were made to verify this. By putting weights on the small mica "scale-pan" P (see figure), this was shown to hold to within 1 part in 1000 for scale-displacements up to 3 cm. (3000 scale-divisions), which is more than adequate for the purposes of the apparatus. The setting of the specimen in the position of maximum $H\frac{dH}{dx}$ is carried out by levelling-screws on the electromagnet. If necessary more accurate setting can be made by slightly loading the scale-pan P. For subsequent measurements with different masses of materials for comparison, the same position of the image is maintained by loading or unloading the scale-pan. This is an accurate criterion of the setting of the phial in the same position. Independent settings of a specimen of paramagnetic material gave the same deflexion within 1 part in 500. The zero is extremely stable, and after a first preliminary deflexion due to the magnetic field, there is practically no sign of elastic fatigue. The times of oscillation of the systems used varied from 1/15 to 1/5 second, so that equilibrium is reached very quickly and a set of readings can be taken in a very short time.

To test the apparatus for accuracy in the actual measurement of magnetic susceptibility, the four substances shown in the table were chosen as being of various orders of susceptibility, about which different experimenters give results in good agreement. The first three materials, in the anhydrous state, were measured on a ring of phosphor-bronze 0·13 mm. thick by 3·0 mm. wide. One of these, $NiSO_4$, was measured on a weaker ring ($0{\cdot}10 \times 2{\cdot}0$ mm.), as also was $NiSO_4 . 7H_2O$. On a third ring ($0{\cdot}065 \times 2{\cdot}0$ mm.) pure water was used *. The second column gives the scale-deflexion for the weight used, the fourth column the scale-deflexion per gram of material. Column 5 gives the weight-calibration of the system, *i. e.* the scale-deflexion per gram weight of load placed in the pan P. This allows the results with different rings to be brought to a common basis

* In the case of this ring, the shape became somewhat elongated under the weight it had to carry. This was easily remedied by shaping the strip so that under a mean load it was approximately circular.

Substance.	v (cm.).	w (weight).	$v/w = V$.	W (cm.).	V/W.	$\chi' \times 10^6$.	$\chi \times 10^6$.
$MnCl_2$	1·304	0·1815	7·182	5·760	1·248	112·2	114·8 *, 111·8 †
,, ...	0·971	0·1355	7·167	5·760	1·244		
$CoCl_2$	1·165	0·1870	6·230	5·760	1·081	97·4	99·7 *, 95·0 †
$NiSO_4$	0·253	0·1515	1·670	5·760	0·290	26·1	26·5 ‡, 26·2 †
,, ...	0·812	0·1835	4·425	15·30	0·289	26·0	
$NiSO_4 . 7H_2O$ ...	0·659	0·2450	2·690	15·30	0·176	15·85	15·7 ‡, 15·5 §
H_2O	0·301	0·491	0·613	76·70	0·00799	0·720 ‖	

* Theodorides, *Arch. de Genève*, vol. iii. p. 161 (1921).
† Ishawara, Sci. Rep. Tohoku, vol. iii. p. 243 (1915).
‡ Jackson, Phil. Trans. A, vol. cciv. p. 1 (1924).
§ Onnes & Hof, see Jackson (*ibid.*).
‖ Taken as standard.

for comparison, which is expressed in column 6 as the force (in grams weight) per gram of specimen. In the seventh column the results are expressed as susceptibilities, the standard used being pure water ($\chi = 0{\cdot}72 \times 10^{-6}$). The most reliable results of experimenters are added for comparison in the last column, all results being reduced to 14° C., the temperature at which the measurements were made.

There is usually a field-gradient along the lines of force, such that $H \frac{dH}{dy}$ (where the y-axis is along the lines of force) is zero midway between the poles, with increasing positive values as the pole-pieces are approached. In other words, a paramagnetic specimen is in a position of unstable equilibrium as regards horizontal displacement, and may, if this force is sufficiently large, be drawn laterally to one or other of the pole-pieces. This fault is experienced for the largest deflexions (above about 500 scale-divisions), and is eliminated as follows :—Parallel to the lines of force a single cocoon silk fibre is fixed between the two adjustable rods R, which were each 5 cm. from the suspending ring. The rods are drawn towards the extension A F until the fibre just touches, where it is fixed by a speck of shellac. This addition neither alters the uniformitv of deflexion with force nor is the sensitivity appreciably changed. With it the deflexions for four successive increments of 0·02 gram were 5·64, 5·66, 5·64, and 5·64 mm. respectively, whilst prior to the attachment of the fibre the mean deflexion was 5·67 mm.

Summary and Conclusions.

A simple apparatus admitting of rapid measurement of magnetic susceptibilities is described. An accuracy of $\frac{1}{2}$ per cent. is obtained on substances of moderate specific susceptibility, whilst for susceptibilities of the order 10^{-6}, measurements can be made to 1 per cent. on half a gram of material. The force experienced by a specimen in a non-homogeneous magnetic field produces a very small movement of the specimen, thus eliminating the necessity for a null method. The movement, which is directly proportional to the magnetic force, is magnified to a suitable value for observation. The method could be easily adapted to measurements of the large forces on paramagnetic substances at very low temperatures.

XVIII. *A Class of Artificial Lines containing a Class of Phase-shifting Networks.* *By* A. C. Bartlett, B.A.* (Communication from the Staff of the Research Laboratories of the General Electric Co., Ltd., Wembley.)

THE class of artificial lines to be described is constructed of sections of which a typical half-section is shown in fig. 1. A complete artificial-line section is made by taking another identical half-section and connecting T_1' to T_1', T_2' to T_2', etc. The constants can be stated in terms of simple continuants. As a special case there occurs a class of phase-shifting artificial lines, *i.e.*, whose characteristic impedances

Fig. 1.

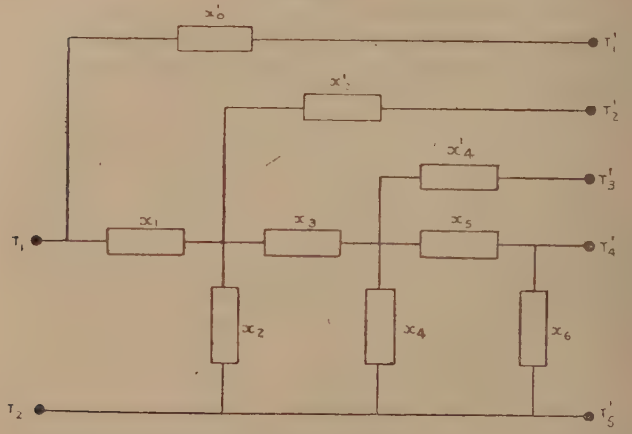

are pure resistances at all frequencies, whose attenuation constants are zero at all frequencies, and whose phase constants vary with frequency. Such networks are becoming of importance in long-distance telephony. The half-section of the artificial line to be considered consists of a series of impedances x_1, x_3, $x_5 \ldots x_{2n-1}$, of shunt impedances x_2, $x_4 \ldots x_{2n}$, and cross impedances x_0', $x_2' \ldots x'_{2(n-1)}$; fig. 1 illustrates the case $n=3$.

Applying a theorem previously given†, if Z_0 and θ are the constants of this section, then $Z_0 \coth \frac{\theta}{2}$ is the impedance

* Communicated by C. C. Paterson, Director.
† Phil. Mag., Nov. 1927.

of the half-section of fig. 1 measured at T_1T_2 with the terminal $T_1'T_2'$ ..... free, and so is the impedance of the ladder network

Fig. 2 *a*.

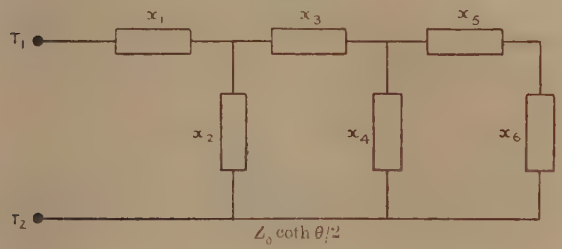

of fig. 2 *a*. Similarly, $Z_0 \tanh \theta/2$ is the impedance of the network of fig. 1 with the terminals $T_1'T_2'$, etc., connected together, which can be re-drawn as the ladder network shown in fig. 2 *b*.

Fig. 2 *b*.

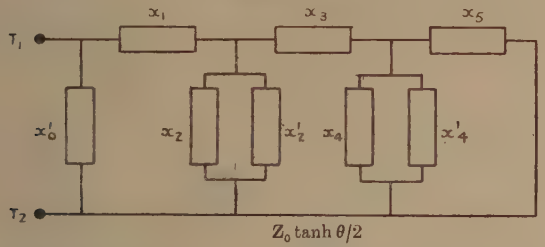

Let the impedances of x_1, x_3, x_5, etc., be a_1, a_3, a_5, etc., of x_0', x_2, x_2', x_4, x_4', etc.. be $1/a_0'$, $1/a_2$, $1/a_2'$, $1/a_4$, $1/a_4'$, etc.; then the constants can be readily determined in terms of simple continuants *. $Z_0 \coth \theta/2$ is equal to the impedance of the network of fig. 2 *a*, which is

$$\frac{K(a_1, a_2, a_3 \ldots\ldots a_{2n})}{K(a_2, a_3 \ldots\ldots\ldots a_{2n})}, \quad \ldots\ldots \quad (1)$$

while in a similar way from fig. 2 *b*,

$$Z_0 \tanh \theta/2 = \frac{K(a_1, (a_2+a_2'), a_3, (a_4+a_4'), \ldots, a_{2n-1})}{K(a_0', a_1, (a_2+a_2'), a_3, \ldots\ldots\ldots, a_{2n-1})}. \quad (2)$$

These two equations determine Z_0 and θ for the general case.

* Post Office Electr. Eng. Journal, Jan. 1926.

Consider next the special case where x_1, x_3, x_5, ... x_{2-n1} are all numerical multiples of one type of impedance X, and are b_1X, b_2X, b_5X, etc., respectively. Let the other x's be all numerical multiples of another impedance Y, which is equal to Q^2/X, where Q is any impedance, so that a_0', a_2, a_2', a_4, etc., will be $b_0'X/Q^2$, b_2X/Q^2, $b_2'X/Q^2$, b_4X/Q^2, etc. Now let the b's be chosen so that

$$b_0' = b_1,$$
$$b_1 = b_2,$$
$$b_3 = b_2 + b_2',$$
$$b_3 = b_4,$$
$$b_5 = b_4 + b_4'.$$
$$b_5 = b_6,$$

etc., etc.

It will be seen, after inserting these values in (1) and (2), that with the b's so chosen the two networks of fig. 2*a* and fig. 2*b* are mutually reciprocal with respect to the impedance Q, *i.e.*, the product of their impedances is Q^2, and therefore, for this artificial line, $Z_0 = Q$. Now let Q be a resistance R and X any pure reactance ladder network, then $Y = \frac{R^2}{X}$ is a physically realizable pure reactance network. The artificial-line section thus obtained therefore has a characteristic impedance R at all frequencies. Since $Z_0 \tanh \theta/2$ is the impedance of an entirely reactive network, it must be a pure imaginary, and thus, since $Z_0 = R$ and is real, $\tanh \theta/2$ and therefore θ must be pure imaginaries.

Thus the artificial line has zero attenuation at all frequencies, and is a pure phase-shifting network. The special case also leads to a class of artificial lines having the same characteristic impedance as a uniform line ; for choosing the b's as before and choosing X and Y so that their product is

$$(R + jpL)/(S + jpC),$$

which can be done in an infinite number of ways, it is seen that the characteristic impedance of the artificial line is

$$\sqrt{\frac{R + jpL}{S + jpC}}.$$

XIX. *On the Modes of Vibration of a Quartz Crystal.* By J. W. Harding, *B.Sc., and* F. W. G. White, *B.Sc., Senior Scholar in Physics, Victoria University College, Wellington, N.Z.**

[Plates I.–V.]

Introduction.

THE existence of nodes and antinodes on the surface of an oscillating quartz crystal has been demonstrated by A. Crossley (P. I. R. E., April 1928), using ferro-ferricyanide solution as an indicator. It is stated that lycopodium powder was tried but was thrown off, leaving no trace on the crystal. Using a fairly thick crystal, the present writers have found lycopodium powder very effective, and a comprehensive study of the various patterns formed on the crystal surface for different modes of vibration has been carried out. Special care has been taken to trace the connexion between the modes of vibration of the faces and the air-currents which may issue from those faces.

Method of obtaining Figures.

The crystal was placed either between two vertical plane electrodes, in which case the top face was left clear, or, when it was necessary to use horizontal electrodes, the crystal was set oscillating, and then the electrode was gently pushed off the surface as far as possible and the lycopodium powder scattered in a fine layer by means of a small brush. Care had to be exercised that such patterns were not modified by air-streams issuing from beneath the electrode. The crystal was frequently cleaned by immersion in carbon tetrachloride, and it was noticed that vigorous oscillation was generally accompanied by a spark discharge between the electrodes and the quartz surface with consequent production of ozone. A large black film was sometimes placed between the brass plate acting as the lower electrode and the crystal in order to obtain better photographs of the wave-patterns. The electric field was applied parallel to the three different axes in turn, and the patterns, together with the corresponding frequencies, were recorded. The size of the crystal used throughout these investigations was 4 cm. × 3·5 cm. × 2·5 cm.

* Communicated by Sir W. H. Bragg, K.B.E., F.R.S.

At first the simple self-maintained circuit was used with the crystal in the grid circuit, and the plate circuit tuned to resonance with the crystal frequency. This circuit was afterwards modified to that shown (fig. 1). This circuit oscillated

Fig. 1.

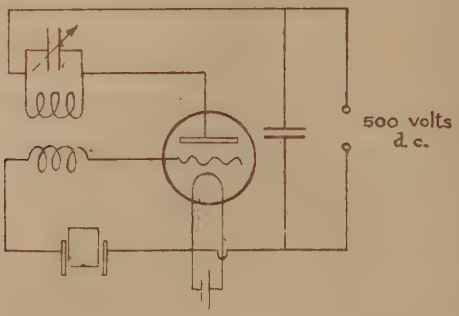

at definite frequencies only, corresponding to natural frequencies of the crystal, but, owing to the reactive effect of the grid coil, the oscillations were much stronger and much more easily maintained.

Fig. 2.

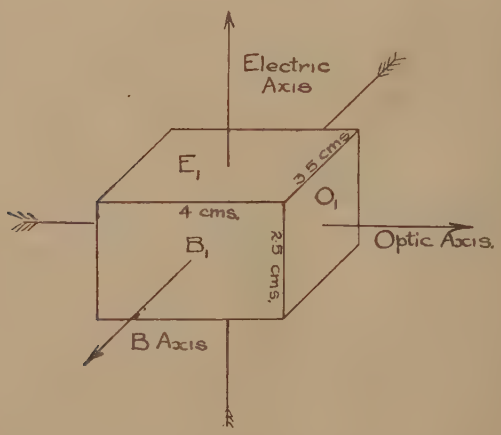

The method adopted of naming the faces in accordance with the three principal axes will be sufficiently clear from the diagram (fig. 2).

Description of Patterns.

1. *Field parallel to Electric Axis. Longitudinal Vibrations.*

The following faces are described with reference to figs. 3 and 5 :—

Face B_1.—The mode of vibration is very complicated. On the left the powder streams off in the direction shown, forming strong air-currents from the side faces. There are

Fig. 3.

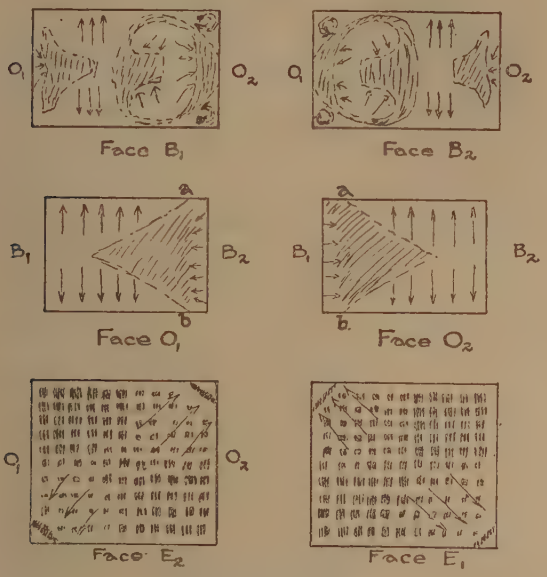

Field parallel to E axis.
Longitudinal mode.

other movements, as indicated by the arrows in the diagram, including the rotatory motion in the two right-hand corners. No air-currents issue from this face.

Face B_2.—Similar figure to above, with the orientation shown.

Face O_1.—The powder collects as shown on the right-hand side. There is a slight inward movement of powder on the right, while the powder streams off on the left in the direction of the arrows, forming strong air-currents from the side faces ;

but there is no air-stream from this face itself. The nodes at *a* and *b* correspond to the two nodes across the corners of the E faces, as will be seen from the model. If a block of ebonite is supported a few millimetres from one of the side faces, the lycopodium powder can be seen suspended in the form of flat disks in mid-air at the nodes between the crystal and the block. It should be noted that this supports the assumption that the checker-board pattern of the E faces is maintained while the other faces are being examined, since the disks form along definite pencils in air above certain squares of the pattern.

Face O_2.—The pattern on this face is similar to the above, with the orientation shown.

Face E_1.—The powder collects in a checker-board pattern with two nodes across opposite corners. There is a small movement of the dust at these corners towards the two nodes, probably due to the presence of two strong air-streams issuing upwards most strongly from the regions indicated; but there was no sign of an air-current from the sides in this case. As the condenser is turned the two nodes move inwards, and the rest of the powder moves outwards to form the ellipse of the other mode of vibration (see below).

Face E_2.—A similar figure, with the orientation shown.

Typical dust-figures are shown in the photographs of Pl. I.

2. *Field parallel to the Electric Axis. Transverse Vibrations.*

The following faces are described with reference to figs. 4 and 6 :—

Face B_1.—A general checker-board pattern. On the left-hand side the powder collects, but on the right it streams off in the direction of the arrows, and is also shot up into the air at a distance of several centimetres over this half of the crystal, since a current of air issues vertically from almost the whole of the right-hand side of this face. There is also an air-current from the side face, as shown, and a slight movement on the left-hand side along the edges is indicated by the arrows.

Face B_2.—The pattern is as described above, with the orientation indicated.

Face O_1.—On the right-hand side the powder collects in a checker-board pattern which moves in the direction of the arrows. This does not mean that the nodes change position, but that the powder is continually replaced by fresh supplies from the left. The powder flakes are shot into the air over

Fig. 4.

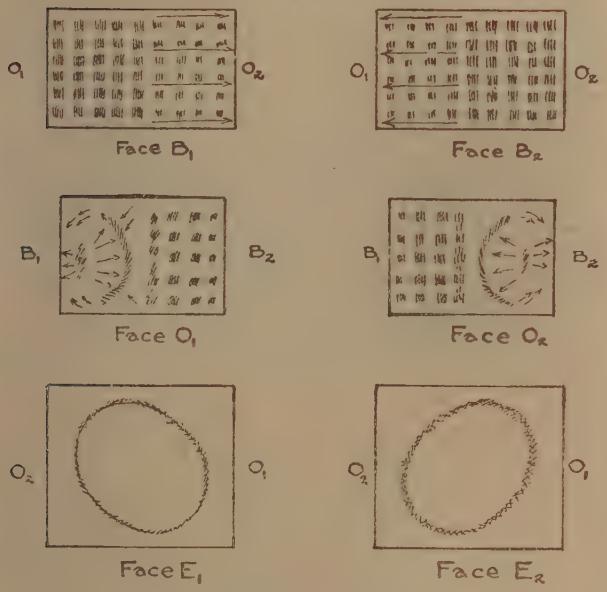

Field parallel to E axis.
Transverse mode.

Fig. 5.

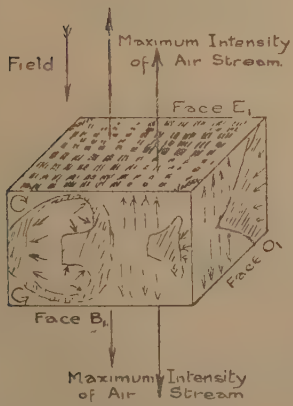

Longitudinal mode.

this face, the movement being most violent on the extreme right. Elsewhere the movement of the powder as it is sprinkled on is indicated as arrows, and there is an air-current from the right-hand B face.

Face O_2.—The figure is similar to that just described, orientated as shown.

Face E_1.—The powder moves in the direction of the arrows to form an ellipse of major axis 3 cm. and minor axis 2·5 cm. The major axis does not coincide with the diagonal of the rectangular face. This ellipse is very clearly defined if very little powder is used, and its dimensions may be accurately measured. Strong air-currents are produced from the side faces in the positions indicated.

Face E_2.—The same figure, orientated as shown.

Typical dust-figures are shown in photographs of Pl. II.

Fig. 6.

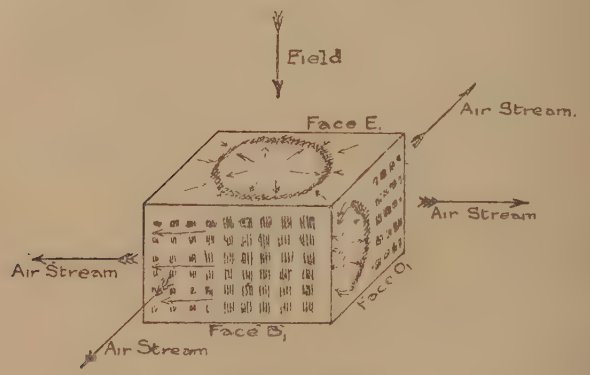

Transverse mode.

Photographs of Air-streams and Standing Waves.

In order to show the radiation of ultrasonic waves from certain sides of the crystal, several photographs were taken of the dust-pattern formed on a smooth horizontal surface round the crystal. If an obstacle is so placed as to reflect the waves, both the standing wave-pattern is obtained and also the air-streams noted by Meissner (P. I. R. E., April 1927). It is important to notice that the emission of ultrasonic waves and air-currents is always associated with the presence of the checker-board pattern on the radiating face.

In Pl. I., C and D show standing waves and air-streams

emitted from the E surfaces of the crystal. In these photographs the dust-figures surrounding the crystal are taken at a distance of about a centimetre below the upper surface, and show the air-stream emerging from the right-hand side. If the film is now moved down towards the lower face, the stronger air-current would now appear on the left side, corresponding to a reversal of the dust-pattern of the upper face on the lower surface.

When the crystal is oscillating longitudinally, air-streams and sound-waves emerge from the E surfaces only.

In Pl. II., A and C, ultrasonic waves are shown radiated from the B and O faces of the crystal. Photograph B shows the air-stream coming from the B face at about 5 mm. below the upper surface. Since the dust-pattern is reversed on the lower face, this air-stream will issue from the opposite B face at a similar distance from the lower face. These photographs, showing simultaneously both the pattern on a face and the air-streams issuing on adjacent sides, are particularly valuable in building up a model.

The various figures described above can be pieced together to form a model to illustrate the resultant pattern over all the faces simultaneously when the crystal is vibrating in the longitudinal or in the transverse mode, corresponding to two distinct vibration frequencies. This is shown in figs. 5 and 6.

Along certain nodes, such as the ellipse on face E, when the transverse mode is used, the powder tends to stick to the crystal face. Thus, if this particular surface is vertical, the powder running down the side will stick along the node-forming parts of the pattern on the side. This fact, as well as the existence of the air-streams, indicates that the same pattern is maintained when the crystal is turned on to a new side.

3. *Field parallel to the* B *Axis. Longitudinal Vibrations.*

The faces are described with reference to figs. 7and 9 :—

Face E_1.—There are nodes across the face and at the corners, as shown. Elsewhere the powder moves in the manner indicated by the arrows. There is a collection of powder at *a* and *b* corresponding to the collection of powder near *a* and *b* on the O faces, and there are air-streams from the side B faces, as indicated.

Face E_2.—The same pattern, with the orientation with respect to the O faces shown by the letters in brackets.

Face B_1.—On the lower half the powder forms into thick streams with a suggestion of the checker-board pattern, and

moves in the direction of the arrows. There is a small node at *a* which apparently extends up the middle of the face. At the top end the powder tends to collect, with a slow movement in the direction of the arrows. The whole pattern is difficult to obtain owing to the modifying effect of an air-current which comes mainly from the centre and lower half.

Face B_2.—The same figure, with similar orientation with respect to the E faces.

Face O_1.—The powder collects along O *a* and O *b*, corresponding to the position of the nodes on the E faces (see below), and there is a node up the middle of the face. The powder on the top half streams off rapidly in the direction of the arrows.

Fig. 7.

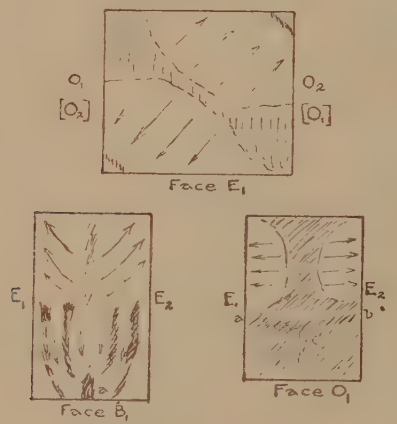

Field parallel to B axis.
Longitudinal mode.

Face O_2.—The same figure, with similar orientation with respect to the E faces.

Typical dust-figures are shown in the photographs of Pl. III.

4. *Field parallel to the B Axis. Transverse Vibrations.*

The faces are described with reference to figs. 8 and 10:—

Face E_1.—As the powder is scattered, it forms a checker pattern, and moves everywhere towards the distinct

nodal lines shown. Air-currents issue from this face, mainly from the corners.

Face E_2.—The same figure, orientated as shown by the letters in brackets.

Fig. 8.

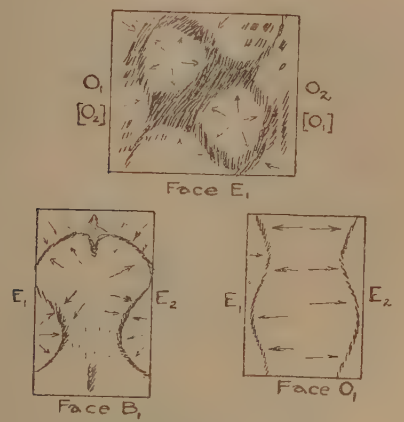

Field parallel to B axis.
Transverse mode.

Fig. 9.

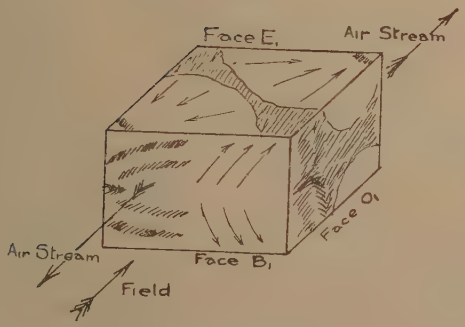

Longitudinal mode.

Face B_1.—The powder forms the nodal lines shown with a faint line up the centre, and dust moves everywhere towards the two outer lines. The nodes at the edges of the face join

up with corresponding nodal lines on the E faces, as can be seen from the model (fig. 10).

Face B_2.—The same figure, with similar orientation.

Face O_1.—If very little powder is applied, just the two outer lines are obtained. If more, the powder collects heavily in the centre, with a movement everywhere towards the nodal lines.

Face O_2.—The same figure, with similar orientation.

Typical dust-figures are shown in the photographs of Pl. IV.

Fig. 10.

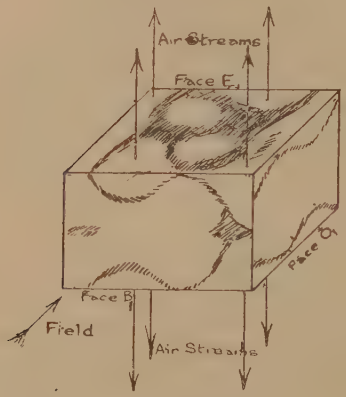

Transverse mode.

Photographs of Air-streams and Standing Waves.

In Pl. V. are two photographs, showing simultaneously the patterns on the B faces with the air-streams emitted from the E sides. The apparent intensity of the emitted currents, as indicated by the dust-pattern, will depend on the position of the film on which the powder is scattered. In A the film has been placed over the brass electrode and the crystal has been removed. The pattern is seen to have formed underneath the crystal. B shows the pattern on top of the crystal for the same arrangement.

As in the preceding case, these patterns may be pieced together to form the two models given in figs. 9 and 10.

Vibrations with the Field parallel to the Optic Axis.

No vibrations could be induced in the crystal with the electric field parallel to this axis.

Summary.

Four models showing the possible normal modes of vibration of the crystal have been constructed—a longitudinal and a transverse mode for each of the two directions of the alternating field.

Two general features are evident from these models :—

(1) The presence of the checker-board pattern on a face indicates that an air-stream is issuing from that face.

(2) In all four models the pattern on the E faces has the same orientation on looking right through the crystal, while the patterns on opposite B and O faces are reversed.

The checker-board pattern is apparently the only one which has as yet received attention in the few publications on this subject. Crossley's experiments, using various solutions, cited in the Introduction, appear inconclusive in establishing the form of this pattern, but the general features are clearly indicated in the description of the "hillocks" over the crystal vibrating in transformer oil.

The modes of vibration are rather more complicated than one would expect, and the writers feel that it is rather premature to discuss this subject more fully until further research has been carried out, using crystals of different dimensions, and preferably employing independent methods as a confirmation of these results. Further work along these lines is now in progress.

In conclusion the authors wish to thank Prof. D. C. H. Florance for providing the facilities for carrying out this research, and the New Zealand Institute for a grant towards the cost of the necessary apparatus.

Victoria University College,
Dec. 1928.

XX. *Notes on Surface-Tension.* *By* ALFRED W. PORTER, *D.Sc., F.R.S., F.Inst.P., Emeritus Professor of Physics in the University of London* *.

IV. *The Mechanics of Drops Pendant from Cylindrical Tubes.*

IN Note II. (Phil. Mag. vii. p. 624, 1929) the method of dimensions was applied briefly to drops from cylindrical tubes. In the present note an examination will be made of the mechanics of a sustained drop for such a tube.

In practice it may be convenient to feed fresh fluid into the drop in such a way that there is no free surface in the fluid into the tube. If this is done the pressure cannot be observed directly. It is best in a theoretical inquiry to imagine it fed in through a capillary dipping into the tube but letting the free surface be observed. It will be assumed that the liquid wets the tube and that its angle of contact is zero.

The drop can be observed as it grows. Casual observation shows that two cases can arise. When the drop begins to grow it makes contact with the end face of the tube The outside edge is, of course, never a mathematical line, but is more or less rounded off, even in the case of a carefully ground "tip." The result is that the angle that the liquid makes with the *horizonal* at the point of contact is capable of varying between 0° and 90°. The more vertical the contact the greater the weight that can be sustained, though it must be borne in mind that the actual weight depends not only upon the tension, but also on the curvatures of the liquid surface where it touches. Meanwhile the point P (fig. 1) moves along the curved edge. In the case of a tube of several millimetres radius the drop falls just as it gets round the edge.

When a small tube is used the process does not stop there ; but at a certain point—probably when P reaches the outer edge—the liquid *suddenly* leaps up so as to occupy a position such as Q, vibrating briskly before settling down : indicating that it has reached a stable position. With fresh accretion of liquid the point Q moves *downwards* until at last the drop breaks away when the edge is arrived at once more.

* Communicated by the Author.

We will consider this second case first, and assume that the contact is already made at such a point as Q. It will further be assumed, at first, that the tube-wall is infinitely thin. The external forces on the liquid (neglecting $a-r$)

Fig. 1.

are $2\pi\sigma a$ at BB (fig. 2) and $2\pi\sigma a$ at AA, the atmospheric pressure cutting itself out on the whole. If W is the weight of the liquid below AA, and w that above AA, we have for equilibrium

$$W + w = 4\pi\sigma a.$$

Fig. 2.

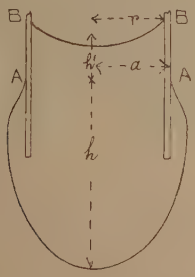

If h' is the "equivalent" height of the column w (*i. e.* the actual height $+\frac{1}{3}$ radius approximately), $w = h'\pi a^2 g\rho$ and

$$W = 4\pi\sigma a - h'\pi a^2 g\rho$$

or

$$\frac{W}{2\pi\sigma a} = 2 - \frac{h'a}{2\beta^2}, \quad \ldots \quad (1)$$

where $\beta^2 = \sigma/g\rho$. Thus a determination of h' (as in Sentis's method) gives a connexion between W and β.

Again considering the level AA, the external forces are $2\pi a\sigma$ and $-\pi a^2\left(\frac{\sigma}{a}-\frac{\sigma}{c}\right)$, where c is the radius of the curvature at A in the plane of the diagram reckoned positive when concave outwards. Therefore

$$W = 2\pi a\sigma - \pi a^2\left(\frac{\sigma}{a}-\frac{\sigma}{c}\right)$$

or

$$\frac{W}{\pi\sigma a} = 1 + \frac{a}{c} \quad . \quad . \quad . \quad . \quad . \quad . \quad . \quad (2)$$

Hence a determination of c would give W for a liquid of known surface-tension.

No one of the approximate equations that have been given to the contour of a surface enables us to determine the value of c corresponding to a given value of a. Even Rayleigh's final equation (see Note I.) *, when the signs are adjusted to suit the case of the denser fluid being on the concave side, gives a contour asymptotic to the axis instead of to the outside of the tube. In order to obtain information in regard to contours which rigorously satisfy the differential equation, it is necessary to resort to a graphical method. Such a method was proposed by Lord Kelvin and placed in the hands of John Perry in 1874, and described before the Royal Institution, January 29th, 1886, together with diagrams drawn by Perry; reproductions of these drawings were first published in 'Nature' for 1886 (see also Kelvin, Popular Lectures and Addresses, vol. i.).

The method depends on the equation :

$$\frac{d\sin\theta}{dx} + \frac{\sin\theta}{x} = \frac{1}{a} - \frac{1}{c} + \frac{y}{\beta^2}$$

which expresses the fact that the total curvature increases at a uniform rate with increase in depth y. The curvature in the plane of the diagram is initially $\frac{1}{c}$; the curvature in the rectangular plane starts with the value $\frac{1}{a}$ and is at each point the reciprocal of the distance to the axis along the normal to the curve. Starting with the value $\frac{1}{c}$, a short

* *Loc. cit.*

length of the curve is drawn as a circular arc ; the normal distance of its end point from the axis is measured and also y ; whence the new value of c can be calculated and a further short length of the contour is drawn and so on.

In practice, in order to obtain diagrams holding for any value of β it is best to employ the reduced coordinates introduced by Bashforth and Adams. Each length is divided by B and taken as a new coordinate ; whence, representing those with a suffix r

$$\frac{d \sin \theta}{dx_r} + \frac{\sin \theta}{x_r} = \frac{1}{a_r} - \frac{1}{c_r} + y_r. \quad . \quad . \quad . \quad (3)$$

The suffixes can all be dropped until the end of the inquiry, when the lengths in the diagram can be transformed in the requisite ratio to suit any particular value of β.

By this graphical method the accompanying diagrams (fig. 3) have been constructed. They are for values of $a_r = 1, 0{\cdot}5, 0{\cdot}2, 0{\cdot}1, 0{\cdot}05$. In each case an initial value of c was assumed and the construction carried out from the top downwards*. The most characteristic (and unsuspected) result obtained was that unless a particular value of c, for a given a, happened to be selected, the contour refused to approach the axis normally at the bottom. If too small a value was selected, the curve turned upwards as the axis was approached, as in the dotted curve H ; if too large a value, it turned downwards, as in the dotted curve G, and then away from the axis. Hence the remarkable conclusion :— *In the assumed conditions and for a given outside radius of the tube one and one only initial curvature corresponds to a pendant-drop of a definite fluid in equilibrium.*

And in consequence : In the assumed conditions for a given material, one and only one weight of pendant-drop can be in equilibrium near the end of a tube of given outside radius of curvature, namely such that

$$\frac{W}{\pi \sigma a} = 1 + \frac{a}{c}, \quad . \quad . \quad . \quad . \quad . \quad . \quad . \quad (4)$$

where c is the unique value corresponding to a.

The foregoing account all refers to the case for which the tube has an infinitely thin wall. The solution obtained is correspondingly ideal. The assertion that there is one and only one weight of drop sustainable is so contrary to experimental experience (in which we examine a pendant-drop

* The reverse sense would have been much more convenient, but the construction then becomes "unstable"—any accidental departure from the correct line leads to still further departures.

Fig. 3.

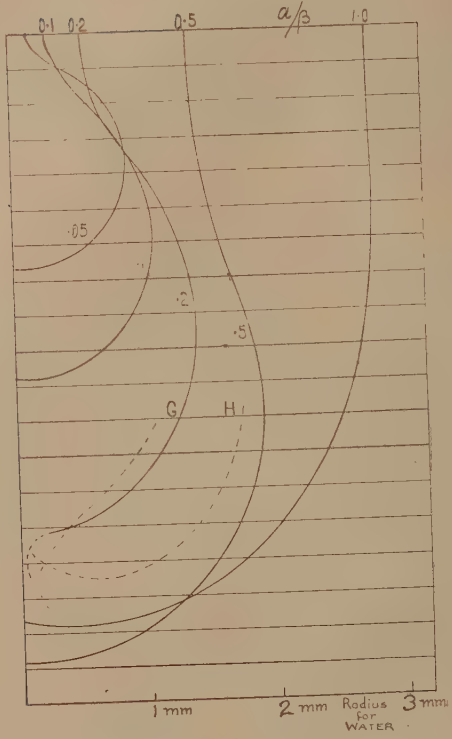

Fig. 4.

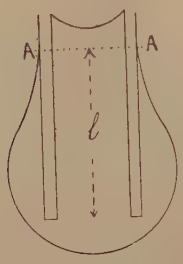

growing as fresh liquid is fed into it) that it is necessary to inquire into the way in which ideality is departed from in practice.

Experience shows that, when the sides of the tube are wetted, the drop extends some small distance along them, as shown in figure 4. In some cases, particularly for small drops, the wall reaches almost to the bottom of the drop. As fresh liquid is fed in, the level AA lowers. The force sustaining the drop is no longer $2\pi a\sigma$ together with the inside force at AA acting downwards, viz., $\pi r^2\left(\frac{\sigma}{a}-\frac{\sigma}{c}\right)$, because there is a downward force in the liquid at the bottom *horizontal* surface of the wall. Moreover, the weight of liquid sustained is no longer $g\rho V$, where V is the volume inside the contour of the drop, but V is less by the volume of wall immersed. If the sustained drop has a weight W',

$$W'=g\rho(V-\pi(a^2-r^2)l)$$

$$=2\pi a\sigma-\pi r^2\sigma\left(\frac{1}{a}-\frac{1}{c}\right)-\left(\sigma\left(\frac{1}{a}-\frac{1}{c}\right)+g\rho l\right)(\pi a^2-\pi r^2)$$

$$=\pi a\sigma\left(1+\frac{a}{c}-\frac{l}{\beta^2}\frac{a^2-r^2}{a}\right).$$

As fresh water is added the length l diminishes and the *greatest* weight sustainable is

$$W'=\pi a\sigma\left(1+\frac{a}{c}\right);$$

that is, it is the unique value sustainable for the given radius of curvature c corresponding to a in the case of an infinitely thin-walled tube.

These statements appear to be exact; but, of course, they must not be applied to the *fallen* drop because of uncertainty as to the exact position at which the drop nips off. In the case of a narrow tube this appears to be very close to the end of the tube; for a wide tube, however, it appears to be lower down, and there is a considerable remnant left behind when the fall occurs. It seems probable that this "remnant" consists in parts of fresh liquid which has moved downwards out of the tube during the process of rupture.

The non-dimensional term $W/(a\sigma)$ is the one considered by Rayleigh (see Note II., *loc. cit.*).

For fallen drops, its value for different reduced radii of tube (a/β) was determined by Rayleigh and extended values have been obtained by Harkins and Brown (J. Am. Ch.

Soc. xli. p. 499, 1919). It is interesting to compare these values with the corresponding values determined from equation (4), in which the values of c are obtained by the graphical method. In reality the graphical method can only give exact values with immense labour because the selection of values of c is made by trial and error; each trial involves the construction of a complete curve. Only approximate values have yet been determined; the direction in which they require correction is indicated by a + or −. The accompanying table shows the results for the Rayleigh number divided by 2π.

Rayleigh number/2π.

$\frac{a}{\beta}$.	Static drop.	Fallen drop. H and B.
·025*	·92−*	·924
·05	·85−	—
·10	·78−	·805
·20	·745+	·741
·50	·65	·652
1·00	·58−	·599

* Not shown on fig. 3.

It is not suggested that the static values compete in accuracy with those for the fallen drop. The table is given as indicating for the first time the basis for an interpretation of these numbers. The link between the two sets must be concerned with the precise mode in which instability sets in and the changes of contour which ensue.

87 Parliament Hill Mansions, N.W. 5.
May 23, 1929.

XXI. *Simple Examples of Adiabatic Invariance.*

By W. B. Morton, *M.A., Queen's University, Belfast* †.

THE principle of adiabatic invariance of periodic systems plays an important part in the modern dynamics of the atom. In its simplest form, as applied to systems with one degree of freedom, it states that the action through a period remains the same when secular changes take place in the physical characteristics of the system. The meaning of

† Communicated by the Author.

this statement is easily understood, but the general proof of the theorem involves dynamical reasoning of a somewhat difficult kind. Under these circumstances there may be some advantage in multiplying illustrations of the theory which can be investigated by elementary methods. The classical example, and the only one treated in the accounts which I have read, is the small oscillation of a simple pendulum which is slowly pulled up through its point of support. This was the subject of a question put by Planck and answered by Einstein at the Solvay Conference in 1911. In the present note three cases are treated :—

(1) A simple pendulum swinging through an arc of any extent, and passing into complete revolutions. The bob is supposed to be constrained to move on the circle, so that in cases in which the string would become slack it is replaced by a weightless rod. Alternatively the particle may be supposed to move in a smooth circular tube, or as a bead on a wire, the tube or wire contracting slowly.

(2) A simple oscillator.

(3) A particle describing a planetary orbit.

In each case the slow changes are taken to affect all the magnitudes which enter as constants in the problem. The mass of the particle may be supposed to acquire additions by moving through a dusty or saturated atmosphere, and slow changes to take place in the values of gravity, the stiffness of the spring, and the strength of the centre of force.

(1) *Simple Pendulum.*

Let the thread, of length l, receive a small change of length δl when the inclination to the vertical is θ. The work done upon the system is

$$-\mathrm{T}\delta l = -(mg\cos\theta + mv^2/l)\delta l.$$

The first term is equal to the increase of the potential energy of the bob which is raised vertically through $-\delta l\cos\theta$, so the second term represents the addition to the kinetic energy, or

$$\delta(\tfrac{1}{2}mv^2) = -mv^2\,.\,\delta l/l,$$

$$\delta v/v = -\delta l/l.$$

Next suppose that, in the same position, the bob picks up a small particle δm, previously at rest. Conservation of momentum gives

$$\delta(mv)=0, \quad \delta v/v=-\delta m/m.$$

Combining the two effects, we have

$$\delta v/v=-\delta l/l-\delta m/m.$$

Let h be the height of the level of no velocity above the lowest position of the bob. The motion is expressed by means of elliptic functions with $k^2=h/2l$ when the pendulum is oscillating, and $k^2=2l/h$ when it is making complete revolutions.

In order to include both types of motion we may use $h/2l$, instead of the angular amplitude of the oscillations, to characterize the extent of the motion In the critical case $h=2l$, although the period is infinite, the action is finite, and its value for the half-period of the oscillations passes continuously into that for the complete period of the rotations.

The connexion between θ and the time is given by the equation

$$\sin\tfrac{1}{2}\theta=k\,\mathrm{sn}\,nt$$

for oscillations, and

$$\sin\tfrac{1}{2}\theta=\mathrm{sn}\,(nt/k)$$

for revolutions, where $n=\sqrt{(g/l)}$. The half-period of the oscillations is $2\mathrm{K}/n$ and the whole period of the revolutions $2k\mathrm{K}/n$.

Taking first the oscillatory motion, we have

$$\begin{aligned} v^2&=2g(h-l+l\cos\theta)\\ &=4gl(k^2-\sin^2\tfrac{1}{2}\theta)\\ &=4gl\,k^2\,\mathrm{cn}^2\,nt. \end{aligned}$$

The action taken through a half-period is

$$\int mv^2dt=8mgllk^2\int_0^{\mathrm{K}/n}\mathrm{cn}^2\,nt\,dt=8mg^{\frac{1}{2}}l^{\frac{3}{2}}(\mathrm{E}-k'^2\mathrm{K}).$$

If small changes in g and l are effected at position θ, we have

$$\begin{aligned} 2\delta v/v&=\delta g/g+\delta l/l+2k\,\delta k/(k^2-\sin^2\tfrac{1}{2}\theta)\\ &=\delta g/g+\delta l/l+8gl\,k\,\delta k/v^2. \end{aligned}$$

When the former expression for $\delta v/v$ is combined with this, we have

$$\delta m/m+\delta g/2g+3\delta l/2l+4gl\,k\,\delta k/v^2=0.$$

Now suppose the changes to be brought about so gradually that an increment, such as δl, which is a small fraction of the whole l, is spread over a large number of oscillations. We must then, before integrating the last equation, replace v^2 in its last term by the time-average. The expression for this is got at once from the action already obtained on removing the mass factor and dividing by the time; this gives

$$4gl(\mathrm{E}-k'^2\mathrm{K})/\mathrm{K}.$$

The last term becomes

$$k\,\mathrm{K}\,\delta k/(\mathrm{E}-k'^2\mathrm{K});$$

but

$$\frac{d}{dk}(\mathrm{E}-k'^2\mathrm{K})=k\mathrm{K}.$$

The last term, like the others, is thus a logarithmic differential, and the integral of the equation is

$$mg^{\frac{1}{2}}l^{\frac{3}{2}}(\mathrm{E}-k'^2\mathrm{K})=\text{const.},$$

or the action remains unchanged throughout the slow process of change in length, mass, and gravity.

For small oscillations $k=\frac{1}{4}\alpha^2$, where α is the amplitude,

$$\mathrm{K}=\tfrac{1}{2}\pi\left(1+\frac{1}{16}\alpha^2\right),$$

$$\mathrm{E}=\tfrac{1}{2}\pi\left(1-\frac{1}{16}\alpha^2\right),$$

$$\mathrm{E}-k'^2\,\mathrm{K}=\frac{1}{16}\pi\alpha^2.$$

The result is that $m^2gl^3\alpha^4=\text{const.}$ in adiabatic change.

When the pendulum is describing complete circles, we have

$$v^2=4gl(k^{-2}-\sin^2\tfrac{1}{2}\theta)$$

$$=4glk^{-2}\,\mathrm{dn}^2(nt/k).$$

The action through a complete revolution is

$$8mg^{\frac{1}{2}}l^{\frac{3}{2}}\mathrm{E}/k;$$

the average value of v^2 is $4gl\mathrm{E}/k^2\mathrm{K}$.

$$2\delta v/v=\delta g/g+\delta l/l-2\delta k/k(1-k^2\sin^2\tfrac{1}{2}\theta)$$

$$=\delta g/g+\delta l/l-8gl\,\delta k/k^3v^2.$$

$$\delta m/m+\delta g/2g+3\delta l/2l-4gl\,\delta k/k^3v^2=0.$$

When the average value is substituted in the last term this has the form

$$-\mathrm{K}\delta k/k\mathrm{E}.$$

Now $$\frac{d}{dk}(\mathrm{E}/k)=-\mathrm{K}/k^2,$$

so $$-\mathrm{K}\delta k/k\mathrm{E}=\delta\log(\mathrm{E}/k).$$

The integral again expresses the invariance of the action.

In the earlier statements of quantum theory the constancy was ascribed to the energy of an oscillator divided by its

Fig. 1.

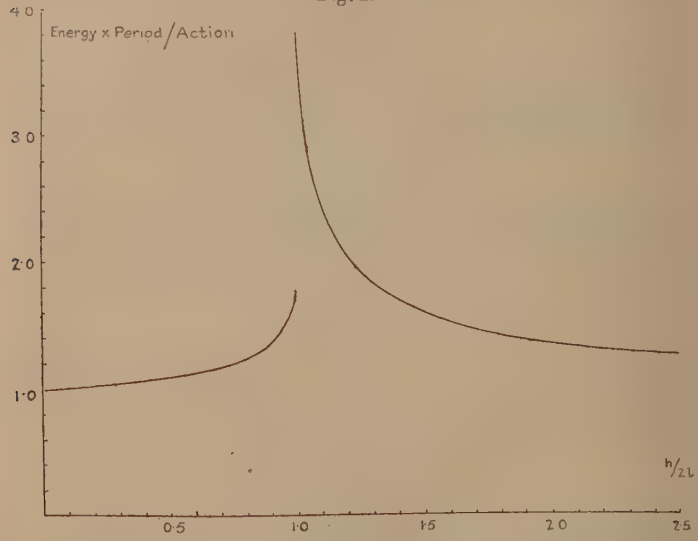

frequency, or energy multiplied by period. For a pendulum this is equivalent to constancy of the phase-integral only in the limit of small oscillations. In general, the magnitude, energy × period, bears to the action through the period the ratio

$$k^2\mathrm{K}/2(\mathrm{E}-k'^2\mathrm{K}),$$

which increases from unity to a logarithmic infinity with increasing amplitude, as shown on fig. 1. In complete revolutions it again approaches unity as the rate is increased.

The connexion between the amplitude and the length of a gradually shortening pendulum is shown on fig. 2, along with a continuation for the motion in complete circles. The

abscissa for both parts is the height of the level of no velocity above the lowest point expressed in terms of the diameter of the circle. Thus the first part is the graph of $(E-k'^2K)^{-\frac{2}{3}}$ against k^2, and the second that of $(E/k)^{-\frac{2}{3}}$ against $1/k^2$. Values of the amplitude $\alpha = \cos^{-1}(1-2k^2)$ are marked for the oscillatory portion. The vertical scale is such that unity is the length of the pendulum which just makes complete revolutions. A gap is left at the point corresponding to this length, where the curves should join, because both curves turn round rapidly to a vertical tangent close to this point, the tangent of the slope approaching infinity in a

Fig. 2.

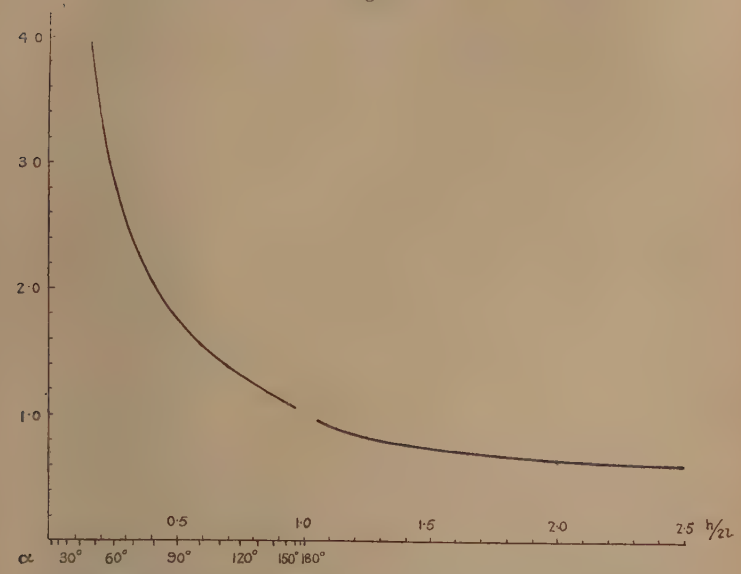

logarithmic manner. The left-hand curve has an inflexion in the neighbourhood of $\frac{1}{2}\alpha = 75°$, $k^2 = \cdot 933$.

It is interesting to compare with the above theory the course of events when the small changes in length are always effected at the same angular position of the pendulum. We have, then, to integrate

$$\delta m/m + \delta g/2g + 3\delta l/2l + k\delta k/(k^2 - \sin^2\tfrac{1}{2}\theta) = 0,$$

treating θ as a constant, which gives

$$m^2gl^3(k^2 - \sin^2\tfrac{1}{2}\theta) = \text{const.}$$

or

$$m^2gl^3(\cos\theta - \cos\alpha) = \text{const.}$$

Thus a continual shortening applied at the end of the swing has no effect on the angular amplitude of the motion, while the most rapid increase is produced when the small pulls are made at the central position. General ideas regarding resonance would lead us to expect that in general the timed impulses would be more effective than those evenly distributed in the adiabatic mode. This is illustrated in fig. 3, in which is showed the connexion between length and angular amplitude for a pendulum which originally swings to 10° on each side. The upper curve gives the result when

Fig. 3.

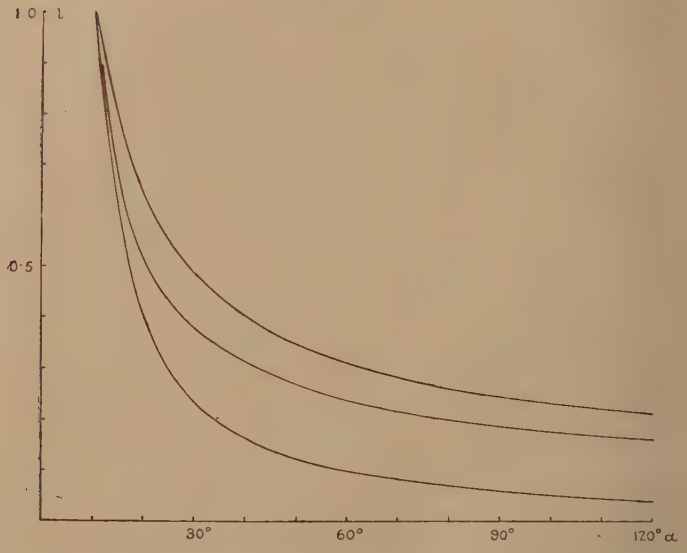

the impulses are applied at $\theta=0$, the middle one that for $\theta=7\frac{1}{2}°$, and the lowest for the adiabatic change.

Since the effect vanishes when θ is the amplitude, there must be some point near the end of the swing where the timed impulses are comparable in effect to the irregular ones. We may arbitrarily define the two cases as equivalent when the critical motion, of complete revolutions with zero velocity at the highest point, is reached with the same length of pendulum in both cases. This gives

$$\cos\theta=\{\cos\alpha+(\mathrm{E}-k'^2\mathrm{K})^2\}/\{1-(\mathrm{E}-k'^2\mathrm{K})^2\}.$$

This is shown on fig. 4, where θ is plotted against the angular amplitude α. The distance of the curve below the straight line shows how far from the end of the swing the timed impulses must be applied in order to be equivalent to the irregular. Incidentally this graph affords an extreme example of the slowness of approach to a logarithmic infinity. It is difficult to believe that when $\alpha = 180^\circ$ is reached the curve runs up to the terminal point of the straight line.

Fig. 4.

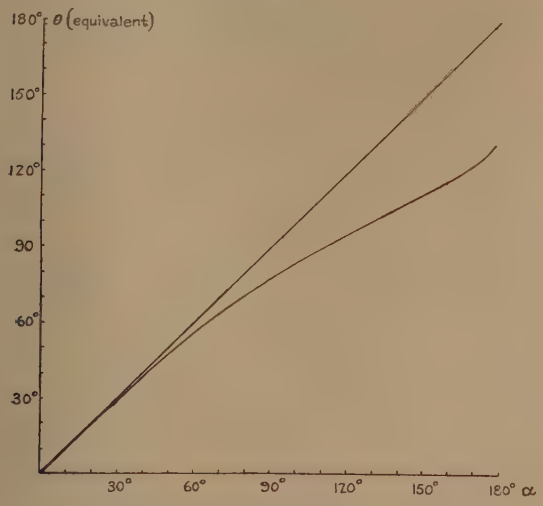

(2) *Simple Harmonic Oscillator.*

If the mass of the oscillating particle is m and the stiffness of the spring is k, so that the equation of motion is

$$m\ddot{x} + kx = 0,$$

then the velocity is given by

$$v^2 = k(a^2 - x^2)/m,$$

where a is the amplitude.

If, at a given position x, the mass and spring and velocity are slightly changed, the resultant change of amplitude is given by

$$2a\,\delta a/(a^2 - x^2) = 2\delta v/v + \delta m/m - \delta k/k.$$

If the alteration in v is due to the picking up of a small mass δm, we have

$$\delta v/v = -\delta m/m.$$

The relation then becomes

$$2\delta a/(a^2-x^2)+\delta m/m+\delta k/k=0.$$

When the alterations of mass and stiffness are always made at the same position of the particle, this leads to

$$mk(a^2-x^2)=\text{const.};$$

but when they are distributed in a random manner through a long time, the time-average of $(a^2 - x^2)$ being $\frac{1}{2}a^2$, we have

$$mka^4=\text{const.}$$

In agreement with this the action through the period

$$2\pi\sqrt{(m/k)}$$

is $$\int m\dot{v}^2\,dt=\int ka^2\cos^2(t\sqrt{k/m})\,dt=\pi\sqrt{(mk)}\,.\,a^2.$$

(3) *Planetary Orbit.*

The same analysis can be applied to the modification of a planetary orbit under slow accretion of mass and a gradual change in the strength of the centre of force. We have

$$v^2=\mu(2/r-1/a),$$

so $$\delta a/a^2=v^2(2\delta r/v-\delta\mu/\mu)/\mu=-(v^2/\mu)(2\delta m/m+\delta\mu/\mu).$$

It is easy to show that $\int r^{-1}dt$ round the orbit has the value $2\pi\sqrt{(a/\mu)}$, from which it follows that the action is $2\pi m\sqrt{(\mu a)}$, and that the average value of v^2 is μ/a. When this is inserted, the differential equation becomes

$$\delta a/a+\delta\mu/\mu+2\delta m/m=0,$$

expressing the adiabatic invariance.

This is a case of two degrees of freedom, and the theory requires the invariance of the two separate phase-integrals

$$\int m\dot{r}\,dr \quad\text{and}\quad \int mr^2\dot{\theta}\,d\theta,$$

which together make up the action. It is obvious that the alterations of μ and m do not affect the angular momentum round the centre, and so the θ-integral is unchanged; the invariance of the r-integral follows.

XXII. *Significance of X-Ray Analysis of Alkali Sulphates.* By A. E. H. Tutton, *M.A., D.Sc., F.R.S.**

THE X-ray analysis of the orthorhombic normal sulphates of potassium, rubidium, cæsium, and ammonium has proved to be of special interest from several points of view. It was first undertaken—in response to a request made to Sir William Bragg, early in the year 1916, when the value of the X-ray spectrometric method had proved itself—by Messrs. (now Professors) A. Ogg and F. Lloyd Hopwood †, then working in Sir William Bragg's laboratory. They used some of the same crystals as had been employed by the author in the detailed crystallographic and physical investigations of these salts.

So long ago as the year 1894 ‡ the relative dimensions and volumes of the unit cells of the space-lattices of the three alkali metallic salts had been determined by combining the crystal axial ratios with the densities of the crystals; and similar constants for ammonium sulphate were added in 1903 §. These strictly relative and truly comparable spatial constants, since known as "topic axial ratios," are rigidly valid when the crystalline substances compared are, as in the group in question, isomorphous in the strict sense known as "eutropic," the individual members of the series only differing by containing different elements of the same family group and type of series (odd or even) of the periodic classification, the system and class of symmetry and the structural space-group being identical. The actual values of these constants are given in the following table, χ, ψ, and ω representing the relative lengths of the edges of the rectangular unit cell of the orthorhombic space-lattice (No. 10 of Bravais), and V the relative volumes of the cells (the molecular volumes M/d). Two sets of the constants are given, the first set being the direct results of the use of the formulæ (given below) for the relative edge-lengths of the orthorhombic (rectangular) cell, a, b, and c being the crystal axial ratios.

$$\chi = \sqrt[3]{\frac{a^2 V}{c}}, \qquad \psi = \sqrt[3]{\frac{V}{ac}}, \qquad \omega = \sqrt[3]{\frac{c^2 V}{a}}.$$

* Communicated by the Author.
† Phil. Mag. xxxii. p. 518 (1916).
‡ Journ. Chem. Soc. lxv. p. 660 (1894).
§ *Idem*, lxxxiii. p. 1067 (1903).

Molecular Volumes and Topic Axial Ratios (Tutton).

Salt.	Mol. vol.	Direct results of formulæ.			ψ for $K_2SO_4=1$.		
		χ.	ψ.	ω.	χ.	ψ.	ω.
K_2SO_4	64·91	3·0617 : 5·3460 : 3·9657			0·5727 : 1·0000 : 0·7418		
Rb_2SO_4	73·34	3·1778 : 5·5528 : 4·1562			0·5944 : 1·0387 : 0·7774		
$(NH_4)_2SO_4$ ...	74·04	3·1788 : 5·6413 : 4·1289			0·5946 : 1·0552 : 0·7723		
Cs_2SO_4	84·58	3·3215 : 5·8149 : 4·3792			0·6213 : 1·0877 : 0·8191		

Absolute Dimensions of Space-lattice Cell (Ogg and Hopwood).

Salt.	Length of sides of unit cell in Å. U. (10^{-8} cm.).			Volume of unit cell.
K_2SO_4	5·731	10·008	7·424	$425·73\times10^{-24}$ c.c.
Rb_2SO_4	5·949	10·394	7·780	$481·14\times10^{-24}$ „
$(NH_4)_2SO_4$	5·951	10·560	7·729	$485·71\times10^{-24}$ „
Cs_2SO_4	6·218	10·884	8·198	$554·88\times10^{-24}$ „

The second set is a simplified one, obtained from the first by dividing throughout by the value of ψ for potassium sulphate, and of course the numbers have precisely the same relations. Below these in the table are given the absolute dimensions and volumes of the unit cells, as determined in 1916 (*loc. cit.*) by Ogg and Hopwood as the result of their X-ray analysis, and confirmed and repeated by Prof. Ogg in his recent (1928) paper * in the Philosophical Magazine, describing further work in the Physics Department of the University of Cape Town. In this later memoir Prof. Ogg confirms the fact that the structure is based on a simple orthorhombic space-lattice, the rectangular one (No. 10), with four molecules of $R_2'SO_4$ to the cell, and decides that the space-group is V_h^{16}. The positions of the metallic atoms have been located, as also those of the tetrahedral SO_4 groups (the S atom at the centre of the tetrahedron and the four oxygen atoms at the corners in each case, as shown for other sulphates by Bradley, James and Wood, and Wasastjerna) in the cases of the sulphates of potassium, rubidium, and cæsium. The NH_4 groups in the case of ammonium sulphate are also shown to be tetrahedral, with the N atom at the centre of the tetrahedron and the four hydrogen atoms at the corners, the whole group NH_4 replacing the alkali metal.

* Phil. Mag. [7] v. p. 354 (1928).

Now, it is very satisfactory, and of great importance, that these facts have been independently confirmed by W. Taylor and T. Boyer, working in Prof. W. L. Bragg's laboratory at the University of Manchester, in a memoir * giving the results of an exhaustive X-ray analysis of cæsium and ammonium sulphates. They also find the space-group to be V_h^{16}, the space-lattice to be the orthorhombic (rectangular) one, and the cell to contain four molecules; and they indicate a similar allocation of metallic atoms or NH_4 groups, and of the SO_4 groups. They have redetermined the cell dimensions, and give them as under :—

Salt.	Length of sides of unit cell in Å.U.			Differences from Ogg and Hopwood.		
	a.	*b.*	*c.*	*a.*	*b.*	*c.*
Cs_2SO_4.....	6·24	10·92	8·22	0·02	0·04	0·02
$NH_4)_2SO_4$	5·98	10·62	7·78	0·03	0·06	0·05

The agreement between the results of these two independent investigations is thus very satisfactory, the maximum difference being only half a *per cent.*

Two further memoirs on the structure of the sulphates of potassium, rubidium, and cæsium by F. P. Goeder †, of the University of Chicago, were published in 1927 and 1928, giving some results obtained by the Laue spot-method. The same conclusion is arrived at that a rectangular orthorhombic space-lattice with four molecules to the unit cell is the basis of the structure, but the space-group is said to be V_h^{13}, while agreeing that the SO_4 group is tetrahedral, with the sulphur atom at the centre of the tetrahedron. No such detailed study by the X-ray spectrometer of the reflected spectra and their intensities, nor the use of the other available methods of investigation by X-rays, such as were carried out by Prof. Ogg and by Messrs. Taylor and Boyer, appear to have been made, so that the balance of evidence is so far in favour of the space-group V_h^{16}. Moreover, both Prof. Ogg and Messrs. Taylor and Boyer have made use of the results of Hartree ‡, and of those of James and Wood §, for the scattering functions of potassium and sulphur, in arriving at their conclusions.

* Mem. and Proc. Manchester Lit. and Phil. Soc. lxxii. p. 125 (1928).
† Proc. Nat. Acad. of Sci. of the U.S. America, xiii. p. 793 (1927), and xiv. p. 766 (1928).
‡ Phil. Mag. i. p. 289 (1925).
§ Proc. Roy. Soc. cxix. p. 598 (1925).

Two main facts which have been clearly proved by the detailed crystallographic and physical investigations of these anhydrous normal rhombic sulphates of the alkalies, and their selenate analogues, as well as of the monoclinic double sulphates and selenates with $6H_2O$, in which these salts are combined with one or other of eight dyad-acting metals (Mg, Zn, Fe, Ni, Co, Mn, Cu, or Cd), are clinched by these structure results of X-ray analysis. (1) There is a progression (increase) in the edge-dimensions and volumes of the unit cells of the space-lattice as one alkali metal of higher atomic weight or atomic number replaces the one below it in order, the rubidium salt in every case standing intermediate in regard to these structural constants, between the potassium and cæsium salts, usually somewhat nearer to the former, the progression being an accelerating one. (2) The crystals of the ammonium salt are very closely isostructural with those of the rubidium salt, the volumes and cell edge dimensions being almost identical. That is, the ammonium group NH_4 replaces the alkali metallic atom so well that in the case of the middle member of the series of salts, the rubidium salt, the cell dimensions are scarcely changed at all. It is somewhat remarkable that this should be so, the ammonium salt not being eutropically but only generally isomorphous with the metallic salts. It is obvious that the tetrahedral NH_4 group goes into the same space as a rubidium atom. That this is so Prof. Ogg now shows very clearly in his two models, illustrated in his 1928 memoir on plates v. and vi.

It was this fact of the isostructure of the ammonium and rubidium salts which had proved a stumbling block to the acceptance of the celebrated Valency Volume Theory of Crystal Structure, on the basis of which the ammonium salt cell should be twice as large as the rubidium one, the valency volumes of Rb_2SO_4 and $(NH_4)_2SO_4$ being 12 and 24. From quite other considerations, especially the ready formation of mixed crystals, it was not likely that the scale on which the metallic and ammonium salts were constructed was different, and consequently that the crystals were not strictly comparable, topic axial ratios being only valid for similar structures; but in any case the crucial test afforded by the new X-ray method, which gave us the absolute and not merely the relative cell dimensions, was of the greatest importance as being decisive on this point. The decision which it gave has, however, been so clear and unambiguous that there can be no doubt left that the structures are exactly analogous, and that the absolute as well as the

relative cell dimensions and volumes of the ammonium and rubidium salts are really practically identical.

But size of atom does come into the question, yet is not determined by the valency electrons chemically active outside the last complete shell of electrons, but by the size of that completed shell, which in turn depends on how many shells of electrons the atoms of that element possess. In the case of the alkali metals the outermost complete shell is that of the inert element of the argon group which immediately precedes it in the periodic table, namely, argon (atomic number 18) in the case of potassium (atomic number 19), krypton (36) in the case of rubidium (37), and xenon (54) in the case of cæsium (55). Now, krypton has either one or two (according to the particular version of the atomic structure theory we adopt) more shells of electrons than argon, and again xenon possesses one or two more than krypton, so that one or two complete shells are added each time we pass from potassium to rubidium and from the latter to cæsium, an addition in each case of 18 electrons. This progressive enlargement of the atom, with all its necessary consequences as regards chemical (particularly electropositive) and physical properties, offers at once an explanation of the progressive increase in the cell dimensions of the crystal space-lattices of the salts of these alkali metals. Moreover, it is noteworthy that all the investigators who have been attempting to determine the sizes of the chemical atoms unite in showing that in a family group such as that of the alkali metals, and in compounds which are truly analogous in structure such as these sulphates and selenates, the atomic size is certainly progressive with the atomic number. This is true whether, for instance, we consider the atomic diameters for the alkali metals given by W. L. Bragg (and either his original or his modified ones), by Niggli in numerous recent memoirs, or most recently of all by V. M. Goldschmidt *, the atom (or "ion" if that term be preferred) of rubidium being invariably found to be of intermediate size and electropositive character as compared with the smaller atoms of potassium or the larger ones of cæsium, the most electropositive of all the elements.

It has also to be remembered that this property of the size of the structural unit cells is only one among many crystal properties, although one which has become very prominent owing to the new field of work opened up by the use of X-rays. The crystal angles, the refractive indices,

* *Ber. der deutsch. chem. Ges.* Jahrg. 60, Heft 5, p. 1263 (1997) and later papers.

the optic axial angles, the dimensions of the optical ellipsoid, and even its position when variable (in the monoclinic series), the thermal expansion, and in fact every detail of the physical properties of the crystals which have been studied, have all been shown to be progressive with the atomic number of the alkali metal. Moreover, this is not alone true for these rhombic sulphates and selenates, and for the monoclinic double salts which they form with the salts of the dyad-acting metals; it is true for all other series of compounds for which the structure has been proved to be strictly analogous and comparable throughout the series. The rhombic perchlorates of the alkalies are pre-eminently such a series, the crystal morphology of which has been determined by Barker *, and the physical properties of the crystals still more recently † by the author; and a similar progression of all properties and constants in the eutropic potassium, rubidium, and cæsium salts, and isostructure of the rubidium and ammonium salts, have been observed exactly as in the cases of the sulphates and selenates. A series of double chromates of the alkalies with magnesium chromate has likewise been studied in collaboration with Miss Mary Porter ‡, and Miss Porter has since § also investigated a series of ditartrates of the alkali metals, with analogous results in all cases.

Hence the fact is fully substantiated that whenever an unbroken strictly structurally comparable series of eutropically isomorphous compounds is investigated, the whole of the morphological and physical properties of their crystals are found to be functions of the atomic numbers and atomic weights of the interchangeable family-group elements which give rise to the series.

It was formerly supposed to throw doubt on this law that the alkali halides did not conform to it. But the advent of X-ray analysis has given a clear explanation of this fact by showing that the type of structure suddenly changes between rubidium and cæsium chlorides (or bromides or iodides). For whereas potassium and rubidium chloride possess the rock-salt structure, that of the centred-face cube, with four molecules of the salt to the unit cell, cæsium chloride possesses the structure of the centred cube, with only a single molecule to the cell. The discovery of this fact affords, indeed, only a further confirmation of the law, for

* *Zeitschr. für Kryst.* xliii. p. 529 (1907), and xlv. p. 17 (1908).
† Proc. Roy. Soc. A, cxi. p. 462 (1926).
‡ Min. Mag. xvi. p. 169 (1912).
§ *Zeitschr. für Kryst.* lxviii. p. 531 (1928).

this series of alkali halides is an exception because it is not structurally analogous throughout.

This beautiful law of progression with the atomic number of the interchangeable elements in a truly structurally analogous series of isomorphous substances, due fundamentally to the progressive change in atomic structure on the part of the interchangeable elements, receives also remarkable confirmation as regards crystal angles in the case of the hexagonal ethyl sulphates of the rare earths studied by F. M. Jaeger *, $R_2'''(SO_4 . C_2H_5)_6 . 18H_2O$, in which R''' may be any one of the rare-earth elements; for the angular differences between twelve of these salts proved to be so small as to lie within the limits of experimental error (a very few minutes), and the ratio of the axes $c : a$ was found to be identical within $\pm$ 0·0012. The reason is that in this remarkable group of rare-earth elements additions of electrons, as we proceed along the list of elements in order of atomic number, are not made as usual, to the outer shell, but to the interior of the atomic structure, causing the remarkable similarity of so many of the compounds of these elements, and the very great labour entailed in separating them from their natural ores and from each other.

Finally, it may with confidence be stated that this law of progression of the crystallographic properties with atomic number, in a eutropic isomorphous series, forms the ultimate proof of the law of Haüy, so long a matter of controversy, that to every definite chemical substance crystallizing in any but the cubic system of symmetry (in which the high symmetry itself fixes the invariable angles) there appertains a particular crystalline form (or forms, if polymorphous), peculiar to and characteristic of the substance. For even in these most closely of all related substances the crystal constants vary, and do so in accordance with the law of progression according to atomic number.

The full confirmation of the law, which is now afforded by X-ray analysis, is thus a matter for deep satisfaction, showing that the advances made in the last half century in pure crystallography are truly founded and may be received with every confidence.

* *Recueil des trav. chim. des Pays-Bas*, xxxiii. p. 343 (1914).

XXIII. *Linear Adsorption.* *By* R. S. Bradley *.

1. *The Three-phase Line.*

IT is only comparatively recently that attention has been directed to an important boundary region, that between two interfaces. The number of molecules concerned, relatively to the number in the surface, is very small. The three-phase line becomes important, however, as a seat of reaction. Thus Volmer † assumes that reaction in the system solid surface-solid surface-gas occurs by adsorption of the gas on the solid surfaces, and by the motion of the adsorbed gas to the reaction line. Such a motion could be observed in the formation of iodine films on mercury. The normal solid reaction is, of course, primarily an interface phenomenon, in that it is concerned primarily with the advance of a reaction wall, and only secondarily with the conditions at the edge of that wall.

We have another experimental edge study in the observation of Estermann ‡ that the critical condensation temperature for a pointed trace of Cd atoms on glass is lower for the point than for the centre of the trace.

Schwab and Pietsch § have formulated equations for adsorption at a line analogous to those holding for the interaction of molecules between phases of three and of two dimensions. They assume a gas equation for the molecules in a line of the same form as for those in a surface. They also obtain the Langmuir adsorption isotherm and the corresponding equation for adsorption at a line by a thermodynamic cycle, involving calculations of ΔA.

In this paper adsorption at a line will be studied from the standpoint of surface thermodynamic activity, an expression for which is derived in section 2. In section 3 this will be applied to study Langmuir's adsorption isotherm. In section 4 a similar process will be used to obtain the adsorption isotherm for a line.

* Communicated by the Author.

† Volmer, *Zeit. Phys. Chem.* cxv. p. 253 (1925); cxix. p. 46 (1926).

‡ Estermann, *Zeit. f. Phys.* xxxiii. p. 320 (1925).

§ Schwab and Pietsch, *Zeit. Phys. Chem.* B. i. p. 385 (1928); B. ii. p. 262 (1929).

2. *The Thermodynamic Surface Activity.*

The free energy F′ per gm. mol. in the surface is $\int A\,dF$, where A is the area per gm. mol., F the two-dimensional pressure. Since

$$F(A-B) = RT,$$

where B is a constant,

$$RT\log a_s = F'-F_0' = RT\log\frac{RT}{A-B} + \frac{BRT}{A-B}$$

$$= RT\log F + BF. \quad . \quad . \quad . \quad (1)$$

Here a_s is the surface activity, and the standard state for F′ is defined by the limits $F' \to F_0'$ when $\frac{A-B}{A} \to 1$, $A \to \frac{RT}{F}$, $a_s \to F$.

H, the heat content per gm. mol., is easily derivable from the equation for a_s,

$$H = F' - T\frac{dF'}{dT}$$

$$= BF - BT\frac{dF}{dT} - RT^2\frac{d\log F}{dT}$$

$$= -RT.$$

3. *The Langmuir Adsorption Isotherm.*

The free energy per gm. mol. of a perfect gas is given by

$$(F'-F_0')\ 3\text{-dimensional gas} = RT\log p,$$

where p is the pressure. For a two-dimensional gas we have equation (1). Hence for the partition of molecules between regions of two and of three dimensions,

$$RT\log\frac{RT}{A-B} + \frac{BRT}{A-B} = RT\log p + K_1,$$

where K_1 is the difference between the free energies in the standard states. Hence, writing $S = \frac{1}{A}$, the surface concentration in gm. mols. per cm.^{2},

$$\log p\left(\frac{1-SB}{S}\right) = \frac{SB}{1-SB} + K_2,$$

where K_2 is a constant, equal to $(F_{0_2}' - F_{0_3}')/RT + \log RT$. When $\frac{SB}{1-SB}$ is small compared with K_2, which will in general hold for S small compared with $\frac{1}{B}$, we get the Langmuir isotherm

$$\frac{\text{constant}}{p} = \frac{1}{S} - \text{constant},$$

i. e., the substance then distributes itself between the two regions according to the modified distribution law,

$$\frac{p}{S/1-SB} = \text{constant},$$

where $\frac{S}{1-SB} = S'$ appears as the effective surface concentration.

4. *Adsorption at a Line.*

A similar method may be applied to adsorption at a line. Here

$$RT \log a_l = RT \log RTL' + RTB^{\frac{1}{2}}L',$$

where a_l is the linear activity, L′ the effective linear concentration in gm. mols. per cm., given by

$$L' = \frac{L}{1-LB^{\frac{1}{2}}},$$

L being the linear concentration. Hence

$$RT \log \frac{S'}{L'} = RTB^{\frac{1}{2}}L' - RTBS + K_3.$$

This reduces, as before, to the approximate distribution law

$$\frac{L'}{S'} = \text{constant} = e^{\frac{\Delta F_0}{RT}}.$$

ΔF_0 being the increase in free energy for the change line $\rightarrow$ surface in the standard states.

The University, Leeds.
May 1929.

XXIV. *Densitometer Curves of the Green Mercury Line.* *By* R. W. Wood, *Johns Hopkins University* *.

Metcalfe and Venkatesachar (Proc. Roy. Soc. cv. p. 520) found evidences of absorption by feebly-excited mercury vapour of the light of all of the satellites of the green mercury line with the exception of −0·237, which failed to confirm the claim of McLennan, Ainslie, and Miss Cale (Proc. Roy. Soc. cii. p. 33) that none of the satellites was absorbed with the exception of the unresolved ones −·008 and +·008, for which absorption was inferred from the circumstance that it was never possible to obliterate completely the main or central strong component, the unabsorbed edges being assumed to represent the satellites reported by Janicki and Nagaoka.

The observations of all these investigators were made with interference spectroscopes, and the spectra yielded by these instruments can be interpreted only after careful study. When modified by absorption they become still more confused, and in very few cases give any clear picture of the group of lines.

Having recently made densitometer curves with a new Moll registering photometer spectrograms of the green mercury line made some years ago with a large plane grating and a lens of very long focus, it has seemed worth while to put them on record, as I do not remember ever having seen a record of the structure of the line which shows such perfect resolution. These curves are reproduced on the figure in register, one above the other.

The lower curve was made from a photograph taken with the light of a glass Cooper-Hewitt mercury arc which emerged through the side of the tube; the upper was made with the tube "end-on," the light coming out through the negative electrode bulb.

The former gives the true structure of the line, the latter the structure as modified by absorption in the long column of luminous vapour. No trace of the satellite +0·124 appears in the lower photograph on account of its relative faintness. The small irregularities in the base line are due to the grain of the plate of course. In the upper photograph this satellite is well developed, which shows that it is absorbed to a much less degree than satellite +0·128, which

* Communicated by the Author.

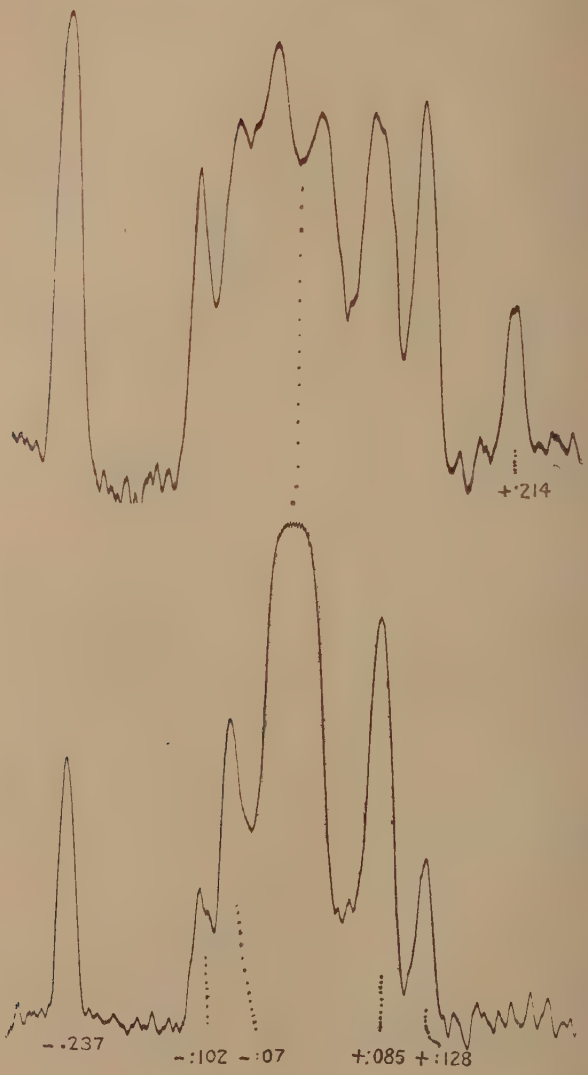
+·214
-·237
-·102
-·07
+·085
+·128

in turn is less absorbed than +0·085, the two latter having practically the same intensity when modified by absorption.

The satellites −0·102 and −0·07 are also very nearly equalized by the absorption, while −0·237 becomes the strongest component of all, which confirms Metcalfe and Venkatesachar's observation that this line was not absorbed at all.

The unsymmetrical reversal of the central or main component appears to be clearly indicated, but it must be remembered that this component is not single.

The photographs were made in the fifth order of a 7-inch plane grating ruled with 15,000 lines to the inch and an achromatic lens of 40-foot focus.

As is well known from the investigations of Nagaoka, recently confirmed most beautifully by Hansen with a Fabry and Perot interferometer and water-cooled arc of special construction (so I am informed), the central component consists of five lines sharp and well resolved.

XXV. *Spectra of High-frequency Discharge in O_2 and CO.*

By. R. W. Wood, *Johns Hopkins University* *.

[Plate VI.]

A BRIEF account of some preliminary experiments, made in collaboration with A. L. Loomis, on high-frequency discharges in very highly exhausted tubes was published in 'Nature' in 1926. The tubes were exhausted at a high temperature with a molecular pump, until they were in the condition usually described as non-conducting, sealed from the pump, and excited through external electrodes by an oscillator giving a 3-metre wave.

References to earlier work in which this type of excitation had been employed were given in this note. The peculiar ruby-red fluorescence of the glass, which was observed by one of us many years ago during experiments with very long hydrogen tubes, when the hydrogen was replaced by oxygen, was found in the case of these high-frequency discharges, which showed the peculiar green colour characteristic of oxygen. This red fluorescence appeared in soft-glass, pyrex, and fused quartz tubes, and appeared to be due to the impact of cathode rays (*i.e.* electrons) in the presence of

* Communicated by the Author.

oxygen, as the fluorescent patches could be moved from one place to another by the approach of a magnet. The discharge is characterized by the appearance of luminous masses shaped like stream-lined bodies, *i. e.* with a blunt cone in front and tapering to a long pointed tail.

I have recently taken up the matter again, and find that the red fluorescence does not appear until the glass has been acted upon for some time by the discharge.

When the current is first applied to the tube through a single wire wrapped around it with one turn only, the discharge is bluish and exhibits the secondary spectrum of hydrogen. This is replaced in a few minutes by the greenish-yellow discharge of oxygen, and the spectroscope shows the four strong negative bands in the green-red region which are characteristic of the gas. The oxygen is evidently derived from the decomposition of SiO_2, as it appears in quartz tubes as well as in glass. After 4 or 5 minutes' operation the walls show a pink fluorescence, which presently becomes ruby-red, the oxygen pressure having risen in the meantime. If, now, the wire loop is moved to the other end of the tube, localizing the discharge in this region, no fluorescence is observed at first, though the pressure of the gas is the same.

A photograph of the discharge is reproduced on Pl. VI. fig. 1. In this case the luminous gas masses were spherical instead of stream-lined. The distribution of luminosity in the tube was very sensitive to the position of the electrode loop: moving it along the tube for a distance of a millimetre or two was sufficient to abolish the spheres, or cause their appearance in different regions.

The most interesting feature, however, and the one which forms the principal subject of this paper was revealed when a spectroscopic examination of the discharge was made. An image of one of the luminous spheres and the region above and below it was formed on the slit of a spectrograph with an achromatic lens, and the resulting spectrogram showed that the spectrum was made up of both lines and bands, the bands appearing enormously enhanced in the spectral images of the sphere. In other words, the sphere is delineated only by the light of the bands, and hence is a phenomenon associated with gas molecules and not with atoms. This indicated that the sphere would be invisible if viewed through a filter transmitting no light of the band spectrum. Glass coloured with nickel oxide and opaque to visible light was found to fulfil this condition, and a photograph of the discharge made with it is reproduced on Pl. VI.

fig. 2. As is apparent, the spheres have vanished. The same thing could be observed visually, though less perfectly, with a filter of a deep violet colour. The spectrum is reproduced in Pl. VI. fig. 3.

It was clear from visual observations that the light of the negative oxygen bands was concentrated in the sphere, while the atomic lines showed no such concentration. These bands do not show on the photograph reproduced, which was made on an ordinary photographic plate, non-sensitive in this region. The nature of the bands in the violet region was not immediately apparent. They were unfamiliar to me, but Professor A. Fowler, to whom I showed the plate, speedily identified them as the "comet-tail" bands, which he was the first to obtain with a terrestrial source. They are characteristic of discharges in carbon monoxide at very low pressure and are emitted by the singly-ionized molecule. Prof. Fowler very kindly measured one of the plates for me (on which there was an iron comparison spectrum) and identified most of the lines. The striking feature of the photograph is that the intensity distribution along the lines from top to bottom is not the same even for the lines due to O_{II}.

The upper of the two spheres was the one focussed on the slit (the electrode wire appears a little above the sphere in Pl. VI. figs. 1 and 2), and owing to the two inversions of the image, one by the lens and the other by the spectrograph, "above" and "below" correspond in the photographs and the spectrogram.

We see at once that the maximum intensity of the lines 4417, 4641, and 4650, all due to doubly-ionized oxygen O_{II}, is distinctly below the sphere, which is sharply defined in the comet-tail bands 4542 and 4273, while the line 4319, also due to O_{II}, has its region of maximum intensity much higher up, the distribution of intensity along the line being similar to that of the line 4368, due to O_I. In the case of the double line between 4474 (unidentified) and 4523 (probably O_I, but possibly a line of the Ångström band) the intensity maximum is still more elevated. These lines also appear to be due to O_{II}: that is, to the same type of atom as the one giving the line 4650, which has its intensity maximum at the bottom. Obviously we must study these differences in relation to the different spectral terms of O_{II}, but it is not worth while to do this until photographs have been made with higher dispersion, and of *both* of the spheres, to determine whether 4650 is brightest at the side of the sphere away from the electrode or on the side adjacent to the

portion of the discharge between the two spheres. It will be necessary also to study the effects with two electrodes.

The spheres are perfectly steady, no change in their appearance or position having been noticed during the half-hour exposure of the spectrogram.

If a magnet is brought up slowly the sphere gradually contracts to a point and vanishes, reappearing and increasing in diameter as the magnet is withdrawn. It will be interesting also to see the effects of obstacles such as thin glass rods or wire supported in various positions inside of the tube, and it seems highly probable that a further study of the spectra of these remarkable discharges will throw some light on their mechanism.

London.
June 8th, 1929.

XXVI. *Talbot's Law in connexion with Photo-electric Cells.* *By* G. H. Carruthers *.

[Plate VII.]

WITH reference to Dr. Campbell's comments † on the paper by Carruthers and Harrison on this subject ‡, and to the reply by Harrison and Stiles §, an account of some experiments on this subject with the aid of an oscillograph may be of interest, as they confirm that the "fatigue" effect discussed in these communications does not occur to any appreciable extent in any single exposure of a cell by a rotating sector.

The experiments were made with an oscillograph of the Wood type ‖. To obtain with this instrument a deflexion of the cathode stream of 10 mm., which is convenient for measuring purposes, a potential difference of about 10 volts must be applied to the electrostatic deflecting plates. To obtain this change with the photo-electric cells employed, which had a dark resistance of approximately infinity and a resistance when exposed to the illumination employed of the order of 10^{12} ohms, it was necessary to use a very high

* Communicated by the Author.
† Phil. Mag. viii. p. 63 (1929).
‡ Phil. Mag. vii. p. 792 (1929).
§ Phil. Mag. viii. p. 64 (1929).
‖ Journ. Institution of Electrical Engineers, lxiii. p. 1046 (1925).

resistance in series with the cell if subsequent amplification were to be avoided. Amplification by means of thermionic valves seemed undesirable in experiments of this nature owing to the possible introduction of distortion, and preliminary experiments were made by connecting a cell in series with a xylol-alcohol resistance of 10^{12} ohms. The ends of the liquid resistance were connected to the electrostatic deflecting plates of the oscillograph. The source of illumination was a 12–14-volt 48-watt gas-filled lamp. Between the lamp and the cell was arranged a small electric motor, to the shaft of which sectors of various angular apertures could be secured.

Figs. 1 and 2 (Pl. VII.) are records taken with a 60°-sector occulting the cell 100 times a second and 70 times a second respectively. The cell used was the cæsium cell used in the previous experiments, which exhibited distinct non-proportionality between photo-electric current and illumination. At the beginning of the records, which is on the left-hand side, the cell is in darkness. At A the cell is exposed to the illumination, and results in a deflexion of the cathode beam, shown downwards in the photographs, and at B the cell is occulted by the sector. Both records show a distinct lag of the apparatus in the recording of the photo-electric current. This lag was due to two causes: in the first place, the capacity of the leads and electrodes of the cell, amounting perhaps to 100 cm., that is 10^{-10} farad, discharging through the high resistance of 10^{10} or 10^{12} ohms will produce a time-lag of 1–100 seconds. In the second place, an apparent lag would be introduced by the light not being occulted instantaneously by the sector disk, but being gradually cut off as the sector moves between the light-source and the cell. To eliminate the latter effect a lens was introduced between the lamp and the sector to project an image of the single filament lamp on the sector disk. Thus, when the sector rotated, an almost instantaneous cut-off of the light was obtained. To eliminate the lag due to the high resistance, recourse was had to valve amplification. The first valve circuit employed is shown in the figure. The liquid resistance of 10^{12} ohms was replaced by a 5-megohm resistance, the junction point of the latter with the cell being connected to the grid of a thermionic valve. The other end of the resistance was connected through a biasing battery with a fine adjustment to the filament of the valve. A $\frac{1}{4}$ of a megohm resistance was placed in the anode circuit, and a micro-ammeter was also included to indicate when the grid bias was correctly adjusted for the valve to be working on

the straight part of its characteristic. The earthed plate of the oscillograph was connected through a biasing battery to one end of the $\frac{1}{4}$-megohm resistance, and the second plate to the junction of the $\frac{1}{4}$-megohm resistance and the anode. A separate biasing battery, which is not shown, was employed to avoid any disturbing effects due to the varying load on the valve high-tension supply.

Figs. 3 and 4 (Pl. VII.) are records taken with these modifications in the apparatus. Fig. 3 is a record of the non-proportional cell, and fig. 4 is a record of a cell for which the proportionality between photo-electric current and illumination strictly holds. At A the cell is exposed, and at B it is occulted by the sector. It will be noticed that

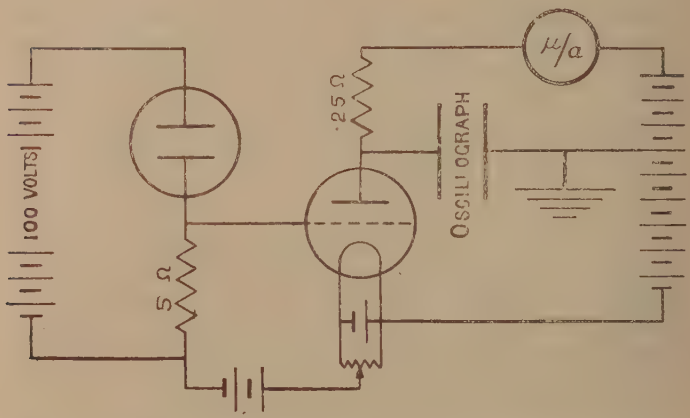

the deflexion when the cell is exposed is now in an upward direction in the photograph, this reversal being due to the introduction of the valve.

Employing one-valve amplification necessitated the use of a resistance, in series with the cell, sufficiently high to cause an appreciable lag, which is evident in the photograph. To eliminate this lag the 5-megohm resistance was replaced by a 2-megohm resistance, and two valves were used for the amplification. The type of record obtained with this arrangement is shown in fig. 5 (Pl. VII.), which is a record obtained with a non-proportional cell. As before, B indicates the point when the cell is occulted by the sector, and A the point when the cell is exposed. Superimposed on this record are two others showing the photo-electric current when the cell

is exposed to a steady illumination and when the cell is in the dark. The parallelism of the light and dark trammels thus obtained with the light and dark deflexions of the record when the cell was alternately illuminated and occulted by the sector-shutter indicates that there is no measurable fatigue in any one of these exposures, which were of the order of a fiftieth of a second. It follows that this "fatigue" or change of emission in non-proportional cells takes place over a number of such exposures corresponding to a period of exposure of $\frac{1}{2}$ to 5 seconds, as indicated by the galvanometer results mentioned in the last paragraph of the paper.

XXVII. *Notes on some Geometrical Radiation Problems.* *By* O. A. Saunders, *B.A., M.Sc., Fuel Research Division, Department of Scientific and Industrial Research* *.

Note I.

1. THE expressions obtained by Professor E. A. Milne in his recent paper † on the radiation transmitted through a pair of parallel circular apertures may be deduced more simply as particular cases of the following more general result :—

"If two apertures (not necessarily plane) are such that their bounding lines lie entirely on one and the same sphere, the radiation transmitted per second through both of them is given by

$$R = I\frac{S_1 S_2}{4\rho^2}, \quad \ldots\ldots \quad (1)$$

where S_1 and S_2 are the surface areas of the parts of the sphere cut off by the bounding lines of the apertures, and ρ is the radius of the sphere."

As in Professor Milne's paper, the radiation falling on the first aperture is supposed to be incident from all directions in which, according to the geometry of the system, it is possible for radiation to pass directly through both apertures ; I is the normal intensity at any point in the incident beam.

2. To prove this result, suppose that dS_1, dS_2 represent elements of area of a spherical surface at two points P_1, P_2.

* Communicated by Prof. E. A. Milne.

† Phil. Mag. [7] vii. p. 273 (Feb. 1929).

The radiant intensity transmitted through both elementary areas is given by

$$\frac{I \cos \zeta_1 . \cos \zeta_2 . dS_1 . dS_2}{P_1 P_2^2},$$

where ζ_1 and ζ_2 denote the angles made with P_1P_2 by the normals to the surface at P_1 and P_2 respectively.

Since the surface is spherical, $\zeta_1 = \zeta_2$ and

$$\cos \zeta_1 = \cos \zeta_2 = \frac{P_1P_2}{2\rho},$$

whence the transmitted radiation is

$$\frac{I\, dS_1\, dS_2}{4\rho^2}.$$

By integration, therefore, the intensity transmitted in series through two finite areas forming parts of a spherical surface is $IS_1S_2/4\rho^2$, where S_1, S_2 are the areas considered, measured upon the surface of the sphere.

Since the transmitted intensity depends only upon the bounding lines of the apertures, and not upon the shapes of the surfaces which are supposed to fill the apertures for the purpose of integration, the result is established.

3. In the particular case considered by Professor Milne, the two parallel circles clearly lie on a sphere whose centre is at O (see fig. 1), where OA = OC.

By the usual solid angle formula the surface areas of the caps cut off from this sphere by the planes of the apertures are given by

$$S_1 = 2\pi\rho^2(1-\cos\phi_1), \qquad S_2 = 2\pi\rho^2(1-\cos\phi_2),$$

where ϕ_1, ϕ_2 denote the angles marked in the figure. The transmitted radiation R is therefore, by (1), equal to

$$\pi^2\rho^2 I(1-\cos\phi_1)(1-\cos\phi_2) = 4\pi^2\rho^2 I \sin^2 \tfrac{1}{2}\phi_1 . \sin^2 \tfrac{1}{2}\phi_2.$$

The intensity transmitted through the aperture CD alone when the screen containing AB is absent is

$$\pi I . \pi\rho^2 \sin^2 \phi_2.$$

Hence the fractional reduction in the radiation reaching CD, caused by the screen containing AB, is

$$\frac{\sin^2 \tfrac{1}{2}\phi_1}{\cos^2 \tfrac{1}{2}\phi_2}. \quad . \quad . \quad . \quad . \quad . \quad . \quad . \quad (2)$$

This is identical with expression (5) in Professor Milne's paper, for it is clear from the figure that, since A, B, C, D are concyclic,

$$\phi_1 = \overset{\wedge}{\mathrm{EOA}} = \tfrac{1}{2}\overset{\wedge}{\mathrm{BOA}} = \overset{\wedge}{\mathrm{BCA}} = \theta - \phi$$

and

$$\phi_2 = \overset{\wedge}{\mathrm{FOC}} = \tfrac{1}{2}\overset{\wedge}{\mathrm{DOC}} = \overset{\wedge}{\mathrm{DAC}} = \theta + \phi,$$

where θ and ϕ are the angles given in Professor Milne's trigonometrical interpretation, and are marked in fig. 1.

Fig. 1.

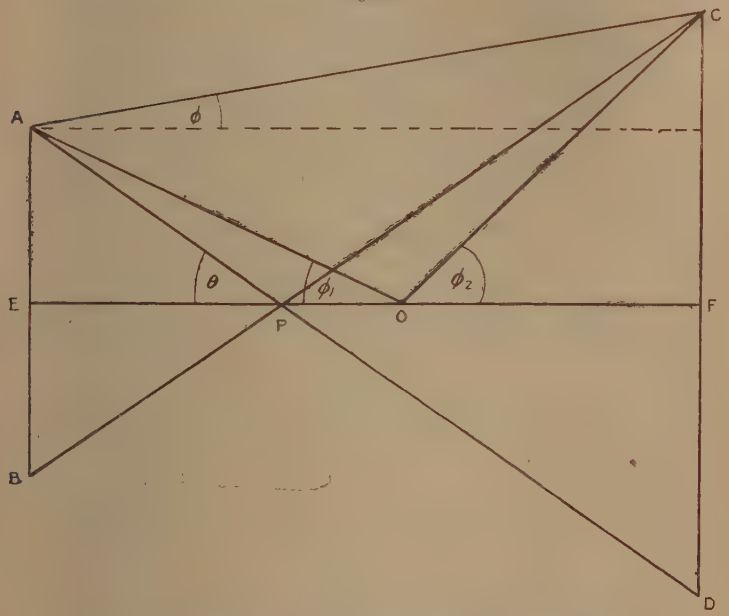

The other formulæ are, of course, easily deduced from (2). Equation (2) provides a very simple trigonometrical method of expressing the intensity transmitted through both apertures.

4. Several points of interest arise from the general result (1).

In the first place, it will be noted that the value of R is independent of the relative positions of the two apertures, provided, of course, that their bounding lines always remain on the same sphere. In other words, if a complete sphere

of thin material be taken and two apertures be cut in its surface at different positions, the intensity of the radiation transmitted through both apertures depends only on their spherical areas, and not upon their shapes and relative positions.

In the particular case when the apertures are circular and equal, a further result of some interest readily follows. The intensity transmitted through two equal parallel circular apertures with their planes at right angles to their line of centres is the same as that transmitted through the same two apertures when placed so that their circular boundaries have a common tangent, and with their planes at an angle $\pi - 2\theta$ to one another, where θ is the angle subtended by the radius of either aperture at the mid-point of the line joining their centres when the apertures are in the parallel position; θ has the same meaning as in Professor Milne's paper.

Finally, if the distance apart of the apertures in the parallel position is equal to the diameter of either, $\theta = \pi/4$ and the transmitted intensity is the same as when the apertures are placed so as to have a common tangent and with planes at *right angles*.

5. The case of two square apertures considered by Dr. Richardson * cannot, of course, be solved in the above manner, since four lines forming a square cannot lie on a sphere.

The peculiar simplicity of the calculation of the transmitted radiation when the boundary lines of the apertures lie on a sphere might be utilized in practice when it is desired to limit a beam of radiation by means of a pair of apertures.

Note II.—*Radiation from a Concave Surface forming part of a Sphere.*

1. The properties of a spherical surface described in Note I. enable a simple expression to be given for the total rate of emission, including all multiple reflexions, of radiation from a diffusely reflecting concave surface of uniform curvature.

2. The fraction of the radiation from an elementary area dS_1 at P_1, which is intercepted by other parts of the surface and thus fails to escape directly, is equal to

$$\frac{1}{\pi}\int \frac{\cos\zeta_1 . \cos\zeta_2 . dS_2}{P_1P_2^2}, \quad \ldots\ldots \quad (3)$$

* Phil. Mag. [7] vi. p. 1019 (Nov. 1928).

where ζ_1 and ζ_2 represent, as before, the angles between P_1P_2 and the normals at P_1 and P_2 respectively, and the integral is taken over the whole surface.

As in Note I., since the surface is part of a sphere, this expression reduces to

$$\frac{S}{4\pi\rho^2}, \quad \ldots\ldots\ldots \quad (4)$$

where S = spherical area of whole surface,

ρ = radius of sphere.

This result is independent of the position of P_1; therefore the fraction of the total emission from the whole surface which *escapes* without striking other parts of the surface is

$$1-\frac{S}{4\pi\rho^2}.$$

Further, each element of area diffusely reflects a fraction $1-e$ of the radiation which is incident upon it from other parts of the surface, e being the uniform surface emissivity. Since the value of the integral (3) is independent of the position of P_1, it follows immediately that each element of area receives the same amount of radiation from the rest of the surface, and consequently the once-reflected radiation is uniformly distributed over the surface. Further, the distribution of intensity about the normal direction is the same for the diffusely-reflected radiation as for the original emission. Hence the fraction of the once-reflected radiation which escapes without striking other parts of the surface is also given by (4). Similarly for the multiply-reflected radiation.

The fraction of the emitted radiation finally escaping, including all multiple reflexions, is therefore

$$\left(1-\frac{S}{4\pi\rho^2}\right)\left[1-\frac{S(1-e)}{4\pi\rho^2}+\frac{S^2(1-e)^2}{16\pi^2\rho^4}+\ldots\right] = \frac{1-\frac{S}{4\pi\rho^2}}{1-\frac{S(1-e)}{4\pi\rho^2}}. \quad (5)$$

This result is independent of the shape of the surface, provided that it has uniform curvature (radius ρ) and total curved surface area S.

3. The "effective emissivity e'" of the concave surface may conveniently be defined as the ratio of the emitted

intensity to that which would be given out by a black surface ($e=1$) of the same shape and size. From (5), remembering that a grey surface only emits e times as much radiation as a black surface, it follows that

$$e' = \frac{e}{1-\frac{S(1-e)}{4\pi\rho^2}}. \quad \ldots\ldots (6)$$

For a hemisphere this reduces to $2e/(1+e)$.

It will be noted that the effective emissivity is increased by reducing ρ, the radius of curvature. This is the principle underlying the well-known increase in radiating power which results from "pitting" or grooving a surface.

4. As $S \to 4\pi\rho^2$, the sphere tending to become complete, $e' \to 1$ whatever the value of e (provided $e \neq 0$), corresponding, of course, to the black-body enclosure. Expression (6) may be applied to determine the departure from the true black-body intensity in the case of the radiation escaping through an aperture of any shape cut in the side of a uniform temperature spherical enclosure whose internal surface is diffusely reflecting and has emissivity e.

For a circular aperture 2 in. in diameter in the side of a sphere of diameter 6 in. and emissivity 0·5, the emitted intensity is within 3 per cent. of that of a black body.

XXVIII. *Solute Molecular Volumes in Relation to Solvation and Ionization.* *By* Sir D. Orme Masson, *K.B.E., F.R.S.**

The Molecular Volume of a Solute Substance.

IT is a familiar fact that this is easily deduced from the composition and specific gravity of the solution if it be assumed that the solvent retains its original volume unchanged, *i.e.*, that the whole contraction (or expansion) on mixing belongs to the solute. On that assumption, if the solvent be water,

$$\phi = \frac{M}{d_w}\left(\frac{1}{ps} - \frac{1-p}{p}\right),$$

where M is the molecular weight of the solute, d_w the density

* Communicated by the Author.

of water at the temperature of observation, p the weight of solute per unit weight of solution, and s the specific gravity (d_t^t) of the solution. As, however, the above assumption is not necessarily true, ϕ is generally called the "apparent" molecular volume of the solute.

More than one way in which the water may suffer change of volume suggests itself. In the first place it may be diminished in quantity by solvate formation. If so, two possibilities have to be considered. Either (1) all the solute molecules will form some definite hydrate and thus destroy, as solvent, an amount of water strictly proportional to the concentration, from extreme dilution up to the point where the whole mixture has the composition of that hydrate, or (2) the average composition of the mixed hydrates present will vary continuously with the concentration. In the second place, apart from quantity, the solvent water may suffer physical changes as the result of admixtures. It has been proved that compressed gases do so, and it may well be argued that the effect should be greater in the liquid state. If so, every property of the water must alter with the concentration, including not only its specific volume but its degree of association and all related characters; and every study of aqueous solutions has, in fact, to deal with a new solvent at each concentration. Yet such a study may, though it neglects this possibility, be justified if it leads to a simple generalization; for in that event it would seem that the physical changes of solvent are relatively negligible in comparison with others that are taken into account.

In the present case evidence has been found to support the following statements. Where water is mixed with a soluble substance the change of volume that occurs is the sum of two changes. One is that due to the formation of a hydrate from its constituent molecules; the other is caused by the dilution of that hydrate with excess of water or with excess of the other component, *e.g.*, at the highest concentration of sulphuric acid. The former may be called the "chemical effect," as it is mainly that, though it also includes in most cases a volume change due to passage from the solid to the liquid state. The latter may provisionally be distinguished as the "physical effect." The chemical effect may be a contraction accompanied by heat evolution or an expansion accompanied by heat absorption; the physical effect is always a contraction, presumably with a corresponding heat evolution. The net effect may be either contraction with rise of temperature, as in the case of

sulphuric acid, or expansion with fall of temperature, as in that of ammonium chloride. The particular hydrate which forms the solute through a range of concentrations down to infinite dilution is, in some cases, the monohydrate; in others it is a higher hydrate. In most of the cases studied the substance is not sufficiently soluble to allow the point to be reached, which may be called the "hydrate point," at which the whole solution has the hydrate composition; but in some it is possible to find a range of higher concentrations through which that hydrate is mixed with a lower one, or a final stage in which the mixture contains mono-hydrate and anhydrous substance. Limits of solubility apart, therefore, there must be always two ranges, and there may be one or more intermediate ones.

In accordance with this view, it is easy to convert the apparent molecular volume (ϕ) of the anhydrous solute into what, if it be accepted, is the true molecular volume (ϕ') of the hydrate actually present. For, in estimating ϕ, it was assumed that a mixture of n molecules of anhydrous substance with n_w molecules of water contains all the latter with their unchanged original volume, viz., $\frac{18{\cdot}016}{d_w} . n_w$ c.c., whereas it really contains this number less xn and their volume is $\frac{18{\cdot}016}{d_w}(n_w - xn)$, where x is an integer indicated by the composition of the hydrate in question. It follows, of course, that $\phi' = \phi + \frac{18{\cdot}016}{d_w} x$. The "chemical effect" (contraction or expansion, as the case may be) is included in ϕ, which is thus never identical with the original anhydrous molecular volume. It includes also the "physical effect," which is always a contraction and the magnitude of which increases with dilution.

The complexity of the solute hydrate (*i. e.*, the value of x) can be definitely determined only in those cases where the solubility is great enough to enable the "hydrate point" to be reached and passed. Where this is not the case, however, the volume study does enable one to give a maximum possible value to x; and, of course, other considerations may help to decide its most probable value. But it will be shown that the interpretation of observed volume change—of the "physical effect" which follows the "chemical effect"—is less affected by any such uncertainty than might have been expected.

The Relation of Solute Molecular Volume to Concentration.

In all, twenty-eight cases have been studied, for which recorded density tables apparently offered suitable data. All but four of these belong to the class of good electrolytes; and twenty-two of them have been here found to conform to the rule that ϕ is a linear function of $n^{1.2}$, where n is the molar concentration (gram-molecules per litre). The two exceptions, magnesium nitrate and sodium acetate, seem to be abnormal, each in a different way, and may be set aside as requiring further investigation; and on the basis of the twenty-two other cases the generalization may be hazarded tentatively that, in the absence of unknown complicating conditions, the following equation holds for good electrolytes:

$$\phi=\left(\frac{1}{ps}-\frac{1-p}{p}\right)\cdot\frac{\mathrm{M}}{d_w}=a+bn^{1/2},$$

where a and b are constants characteristic of the salt dissolved. The other four cases, viz., phosphoric acid, acetic acid, sucrose, and glycerol, are as yet too few to justify a similar generalization, even tentative, for poor electrolytes; but they will be discussed more fully later.

It follows from what has been stated already that the equation for the hydrated solute is

$$\phi'=\phi+\frac{18{\cdot}016}{d_w}x=a'+bn^{1/2},$$

where

$$a'=a+\frac{18{\cdot}016}{d_w}x,$$

and is therefore also a constant. When $n=0$, $\phi=a$, and $\phi'=a'$, which are the solute molecular volumes (apparent and real) at infinite dilution. As concentration increases, these minimum values are added to by an amount proportional to the square root of the concentration. The values of a and b are found from a graph in which ϕ is plotted against $n^{1/2}$; b from the slope of the straight line and a by its extrapolation downwards to $n^{1/2}=0$.

A maximum conceivable value of n and the corresponding value of ϕ may be calculated from the pair of equations,

$$\phi_m=a+bn_m^{1/2} \quad \text{and} \quad \phi_m=\frac{1000}{n_m},$$

whence $an_m+bn_m^{3/2}=1000$. The solution of this last gives the theoretical upper limit to the straight line. ϕ_m is not

the molecular volume of the undissolved anhydrous solvend in its usual state, but that which it would have if it could be contracted (or expanded) by the "chemical" effect in the entire absence of water, or conceivably by a sufficient change of pressure, to cause n_m molecules to fill exactly one litre. But, as a fact, this point is never reached, for the "hydrate point" at which $\frac{n_w}{n}=x$, puts an end to the straight line at a smaller n value. If the solubility is large enough to allow this point to be reached and passed, the value of x can be at once detected by the abrupt transition from the straight line to a curve in a new direction at an indicated value of $p_H=\frac{M}{M+18{\cdot}016x}$; and the corresponding ϕ and n values can be exactly determined by the solution of the equations

$$\phi'_H=1000 \quad \text{and} \quad a'n_H+bn_H^{3/2}=1000.$$

Even though the hydrate point be not reachable, the values of p_H, n_H, and ϕ_H, corresponding to any assumed value of x, can be determined in this way; but, if too large a value of x be assumed and it fall within the experimental range, it will be found that the straight line passes undeflected through the point. It is by this means that a maximum value of x can be calculated when its actual value is beyond reach.

The ϕ'_H value is already affected to some extent by a partial "physical effect" as well as by the complete "chemical effect"; for only the anhydrous substance at the higher n_m value could, even theoretically, be wholly free from the former.

The course of the volume change and the ideas already set forth are well illustrated by the H_2SO_4 graph (fig. 1), which shows the whole range from pure water to pure acid, and by those for NaOH, NaCl, and K_2CO_3 (figs. 2, 3 *a* and *b*), which all illustrate the case of limited solubility. The NaOH case is specially interesting; for it is one of two, among those studied, which give negative values of ϕ in the more dilute solutions. A negative volume, even at infinite dilution, is a contradiction in terms; but the difficulty vanishes when it is remembered that the true solute is a hydrate whose molecular volume is

$$\phi'=\phi+\frac{18{\cdot}016}{d_w}x.$$

In the NaOH case x is probably 1 (it cannot be greater

Fig. 1.

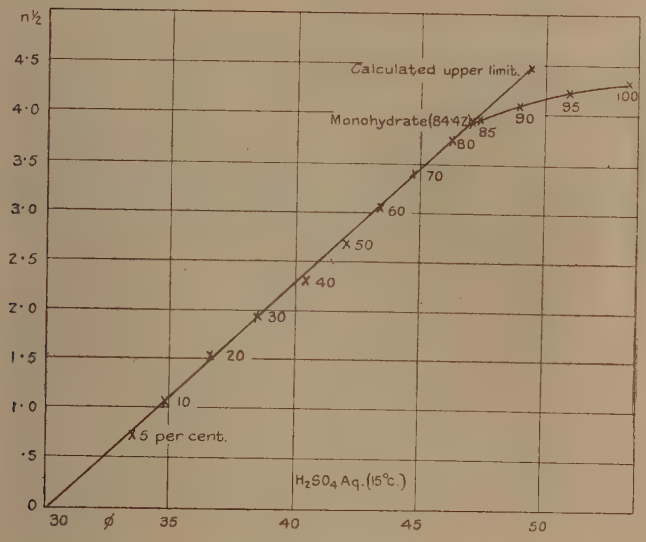
n½
4·5
4·0
3·5
3·0
2·5
2·0
1·5
1·0
·5
0
Calculated upper limit.
Monohydrate(84·47)
85
90
95
100
80
70
60
50
40
30
20
10
5 per cent.
H2SO4 Aq.(15°C.)
30
φ
35
40
45
50

Fig. 2.

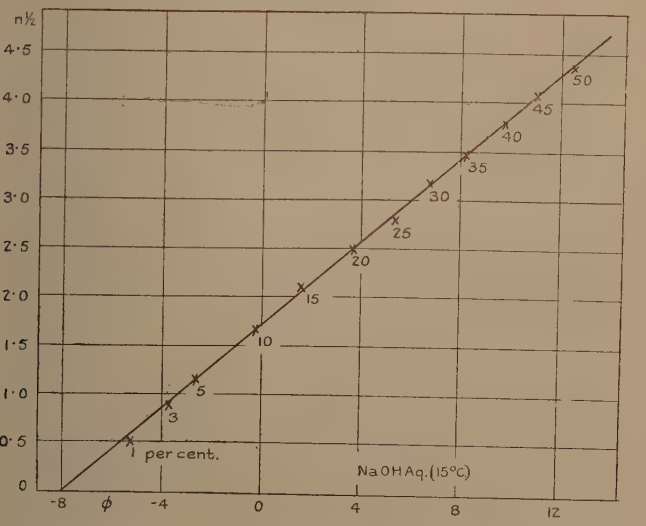
n½
4·5
4·0
3·5
3·0
2·5
2·0
1·5
1·0
0·5
0
50
45
40
35
30
25
20
15
10
5
3
1 per cent.
NaOH Aq.(15°C.)
-8
φ
-4
0
4
8
12

than 2), and this is sufficient to convert the negative a into a positive a'.

The Nature of the "Physical Effect" : the Cause of the Change of Molecular Volume with Change of Concentration.

The large diminution of ϕ (or ϕ') in direct proportion to the fall of $n^{1\cdot2}$ inevitably calls for some explanation of its cause ; and the suggestion is as inevitable that the hydrate exists in two forms, a greater and a smaller, and that ϕ', as measured, belongs always to a mixture of the two in a

Fig. 3.

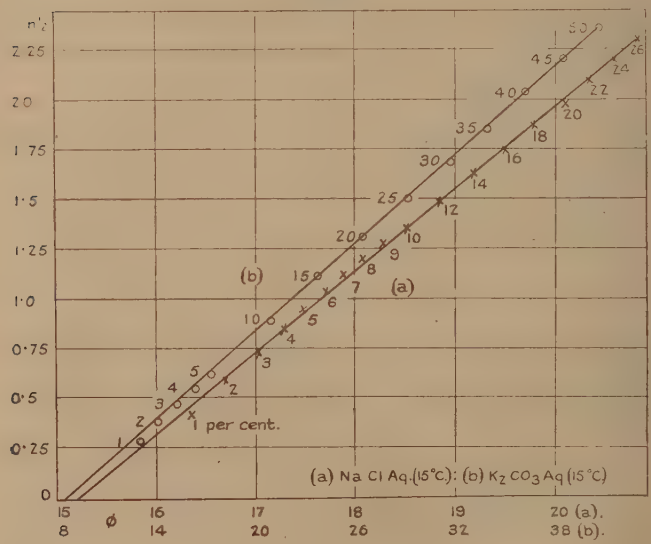

proportion determined by the concentration. The smaller form could exist by itself only if it were possible for the hydrate to exist at all in the complete absence of solute, *i. e.*, at infinite dilution. The larger form could exist by itself only if it were possible for the hydrate to exist at all in the complete absence of water, *i. e.*, at n_m (not at n_H), This puts the "physical" volume effect on a par with ionization, which is complete only at infinite dilution and may presumably be called nil only in the absence of water. Moreover, it is a generally accepted belief now that hydration of the solute is an accompaniment, or rather an

antecedent, of ionization. It seems quite probable, therefore, that the larger volume is that of the unionized molecule and the smaller one that of the molecule in its ionized state, *i. e.*, the sum of its ionic volumes. This hypothesis may or may not be true, but it at least calls for further examination.

The Ionic Theory of the Volume Change.

If α be the ionized fraction of the molecules at any given concentration, the theory may be put as follows:

$$\phi=(1-\alpha)\phi_m+\alpha\phi_i=\phi_m-\alpha(\phi_m-\phi_i)=\phi_i+(1-\alpha)(\phi_m-\phi_i).$$

When $n=0$,

$$\alpha=1 \quad \text{and} \quad \phi=\phi_i;$$

and when $n=n_m$,

$$\alpha=0 \quad \text{and} \quad \phi=\phi_m.$$

But

$$\phi=a+bn^{1/2};$$

hence

$$\phi_i=a, \quad \phi_m=a+bn_m^{1/2}, \quad \text{and} \quad b=\frac{\phi_m-\phi_i}{n_m^{1/2}}.$$

And, since

$$\phi=\phi_i+(1-\alpha)(\phi_m-\phi_i)=a+bn^{1/2},$$

it follows that

$$1-\alpha=\left(\frac{n}{n_m}\right)^{1/2}=kn^{1/2}, \quad \text{or} \quad \alpha=1-kn^{1/2}.$$

The fact that it is the hydrate which should be considered as the ionizing solute and that its x value is in most cases undetermined does not affect the conclusion as to the value of α; for, as already pointed out, the correction merely increases the constant term a (or ϕ_i) by $\frac{18{\cdot}016}{d_w}.x$ and leaves the equation otherwise unaffected.

We thus obtain (by hypothesis) a simple measure of the ionization factors at any concentration up to the hydrate point, if the solubility allows one to go so far; and it involves only one constant, $k=\frac{1}{n_m^{1/2}}$, which is easily evaluated in the manner already described. Beyond the hydrate point the formula can not apply; for, though there may still be some of the hydrate present and some ionization, as shown by conductivity, the solvent medium is a new one. But in the sulphuric acid case, if points on the curve beyond the hydrate point be recalculated as those of a solution of the

monohydrate in H_2SO_4, and the new $n^{1/2}$ and ϕ values so obtained be plotted, it is evident that here also the straight line rule obtains from infinite dilution (pure sulphuric acid) up to the monohydrate point. Confirmation has been obtained also in another case, which will be dealt with later. It seems likely, therefore, that further inquiry may show that ϕ and $n^{1/2}$ are rectilinearly related in solutions in other conducting solvents besides water, in which case the ionic interpretation will be applicable to them too.

The ionization fractions deduced from the volume study of aqueous solutions have to be compared with those obtained by the conductivity and other methods. To distinguish them, we may write β for $1-kn^{1/2}$, reserving α for the classic conductivity values. That they differ, especially at high concentrations, is not in itself a condemnation of β; for it is now generally recognized that $\lambda/\lambda\infty$ or α is in reality the product of the true ionization fraction and a mobility ratio, $\frac{u+v}{u_0+v_0}$ or $\frac{\mu}{\mu_0}$, and that the latter is not constant but changes with concentration in a manner related in some unknown way to the two ionic mobilities at infinite dilution. Should β make good the claim to represent the true ionization fraction, it should help to elucidate this mobility factor and its variation. The lack of any reliable method has led to the curious position that some investigators are claiming complete ionic dissociation for all good electrolytic solutions, while another school is inclined to dispute the truth of the fundamental principle of Arrhenius's theory—a theory that has done much for science and has certainly not been disproved.

Evidence based on published data of the Specific Gravity of Aqueous Solutions.

This is summarized in Table I., in which are given in consecutive columns (1) the formula of the anhydrous solute; (2) the temperature; (3) the highest concentration covered by the experimental work, in gram-mols. per litre; (4) $a=\phi_i$; (5) $b=\frac{\phi_m-\phi_i}{n_m^{1/2}}$; (6) ϕ_m; (7) n_m; (8) $n_m^{1/2}$; (9) $k=\frac{1}{n_m^{1/2}}$; (10) β when $n=1$; (11) β when $N=1$, which is $1-k$ when $N=n$ but $1-\frac{k}{2^{1/2}}$ when $N=2n$; (12) α when $N=1$; (13) the number of H_2O molecules (x) combined with one of the anhydrous substance in those cases where the composition

Table I.

Experimental :— $\phi_n = \frac{M}{d_w}\left(\frac{1}{ps} - \frac{1-p}{p}\right) = a + bn^{1/2}$.

Theory :— $\phi_n = \phi_i + \frac{\phi_m - \phi_i}{n_m^{1/2}} n^{1/2}$; $\beta_n = 1 - \left(\frac{n}{n_m}\right)^{1/2}$.

Anhydrous Solute.	$t°$.	Highest concentration, mols. litre.	$a=\phi_i$.	$b=\frac{\phi_m-\phi_i}{n_m^{1/2}}$.	ϕ_m.	n_m.	$n_m^{1/2}$.	$k=\frac{1}{n_m^{1/2}}$.	β when $n=1$.	β when N=1.	$a=\lambda/\lambda\infty$ when N=1.	Hydrate Point. w.	Hydrate Point. n_H.
NaOH	15	19·12	−8·00	4·667	22·86	43·74	6·614	·1512	·8488	·8488	·736		
KOH	15	14·25	2·88	4·131	27·70	36·10	6·005	·1664	·8336	·8336	·770		
H_2SO_4	15	18·71	30·30	4·275	49·51	20·20	4·494	·2225	·7775	·8427	·517	1	15·36
$(NH_4)_2SO_4$	17·5	4·9	51·00	10·133	85·63	11·68	3·417	·2926	·7074	·7967			
$MgSO_4$	15	2·6	−4·96	11·118	46·75	21·39	4·625	·2162	·7838	·8471	·26		
$ZnSO_4$	15	3·2	1·20	10·71	49·64	20·14	4·488	·2228	·7772	·8425	·24		
HCl	15	14·28	16·60	1·260	24·63	40·60	6·372	·1569	·8431	·8431	·793	3·5	11·90
LiCl	18	12·5	17·20	1·385	25·82	38·73	6·223	·1607	·8393	·8393	·626	10	4·985
NaCl	15	5·34	15·24	2·425	29·39	34·03	5·834	·1714	·8286	·8286	·676		
KCl	15	3·86	25·75	2·650	39·14	25·55	5·054	·1978	·8022	·8022	·755		
NH_4Cl	15	5·22	35·30	1·633	43·16	23·17	4·814	·2078	·7922	·7922	·748		
$MgCl_2$	15	4·9	13·57	6·170	43·24	23·12	4·809	·2080	·7920	·8530	·552		
$CaCl_2$	15	5·05	15·10	7·100	47·67	20·98	4·580	2183	·7817	·8456	·584		
$CdCl_2$	18	4·6	22·77	5·715	48·67	20·54	4·533	·2206	·7794	·8440	...		
HNO_3	15	23·5	27·80	0·925	32·90	30·40	5·513	·1814	·8186	·8186	·824	11	4·385
$NaNO_3$	20·2	8·32	28·90	2·105	39·49	25·32	5·03	·1987	·8013	·8013	·626	1	17·877
KNO_3	15	2·37	35·75	3·250	50·25	19·90	4·46	·2242	·7758	·7758	·637		
NH_4NO_3	17·5	10·43	45·45	1·764	53·10	18·83	4·34	·2304	·7696	·7696	...	7	5·686
$AgNO_3$	18	6·77	26·25	3·148	41·67	24·00	4·90	·2041	·7959	·7959	·582		
$NaClO_3$	? 15	4·2	34·20	2·688	46·64	21·44	4·63	·2160	·7840	·7840			
$Na_2S_2O_3$	19	2·6	25·00	12·23	70·33	14·21	3·77	·2653	·7347	·8124			
K_2CO_3	15	5·6	8·80	13·60	62·99	15·88	3·984	·2510	·7490	·8228			

of the hydrated solute is indicated by termination of the straight line; (14) the n value at which this occurs.

In further illustration, reference may be made again to figs. 1–3, which represent typical cases. Various points of general or special significance are dealt with in the following notes.

Limits of accuracy.—Most of the data employed were taken from the tables of percentage composition and specific gravity given in the Comey-Hahn 'Dictionary of Solubilities.' They are quoted there from various authors and are not of equal accuracy. None were useful for the present purpose that give S to less than 4 decimal places. Some give it to 5, and in one case (Pickering's NaOH table) it is given to 6. Though most of the tables begin at $p=\cdot01$, it is only in exceptional cases that values below $p=\cdot05$ are accurate enough to give correct results. This is obvious when it is remembered that the calculated value of ϕ depends on the difference between $\frac{1}{ps}$ and $\frac{1-p}{p}$, and that this means the difference between 19 and a fraction and 19 at $p=\cdot05$, but between 99 and a fraction and 99 at $p=\cdot01$. At higher concentrations points are seen to deviate more or less on both sides of the straight line which represents the prevailing rule (see fig. 1); but such deviations are, at least partly, to be ascribed to erroneous data. Each table represents a curve in which interpolated values of s are plotted against p and thus involves errors inherent in the experimental determinations of p and s and also those due to the smoothing process. In the few cases examined from this point of view, it has been found that the points calculated from interpolated values deviate from the straight line considerably more than those derived from the experimental ones. But, of course, any errors in the data are magnified in the ϕ, $n^{1/2}$ graph. In the sulphuric acid case, p and s have been calculated back from points on the straight line where the graph shows maximum deviation, and this has been found to be covered by a difference of 2 or 3 units in the third decimal place of S. Such a difference is barely noticeable in a p, s curve drawn on any ordinary scale. Fig. 3 *b* (K_2CO_3) shows a case with deviations at a minimum. There are others in which they are somewhat greater than in the H_2SO_4 case.

The ϕ_i values.—The relation of these to the true molecular volumes of hydrated solute at infinite dilution has already been explained, and the significance of the negative ϕ_i of NaOH and of $MgSO_4$ has been pointed out in illustrative

The ϕ_m and n_m values.—These were calculated from a and b as already described. Comparisons of the chlorides shows that ϕ_m increases, and n_m decreases correspondingly, in the order of, but not in proportion to, the molecular weights of HCl, LiCl, NaCl, KCl; that NH_4Cl has a greater ϕ_m than KCl; that it is almost the same for $MgCl_2$ as for NH_4Cl; and that $CaCl_2$ and $CdCl_2$ have larger values, in that order, but differ only slightly from each other. Closely similar relationship is shown by the nitrates of H, Na, K, NH_4, while $AgNO_3$ has a value between those of Na and K. The ϕ_m of $(NH_4)_2SO_4$ bears nearly the same ratio (1·77) to that of H_2SO_4 as NH_4Cl and HCl give (1·75), and in the case of the nitrates it is somewhat smaller (1·61). $MgCl_2$ and $MgSO_4$ occupy similar positions in their respective classes.

The β values.—Relations observed among the n_m values necessarily reappear in the comparison of $k=1/n_m^{1/2}$, and therefore also of $\beta=1=kn^{1/2}$ when $n=1$. It may be noted that H_2SO_4 has a considerably lower β than HCl when equimolar solutions are compared, but that they are practically equal in equivalent solutions.

Comparison with the corresponding α shows that β is uniformly higher. This is in accordance with the view that seems now to prevail, that the conductivity method puts the ionization fraction too low; but this matter will not be further discussed here.

The Indication of Definite Hydrates.

There are only five cases with entries in the last two columns of Table I., for the good reason that in those cases only does the rectilinear relation between ϕ and $n^{1/2}$ break down before the upper limit of the experimental range is reached—a range determined generally by the solubility of the substance. But they suffice to show that there is no uniform rule as to the complexity of the hydrate which forms the ionizing solute. They also show that it is not necessarily capable of separation as a crystalline solid, though some of those formed with contraction and heat production may be.

The first case is that of H_2SO_4, in which the rectilinear relation persists up to the monohydrate point. The p value here must be ·8442 and the other characteristics, calculated in the manner already indicated, are $n'_H=15·36$, $n_H^{1/2}=3·920$, and $\phi'_H=65·087=47·086\times18·031$ (at 15°). The curve from this point to that of pure H_2SO_4 has been discussed already.

The monohydrate, which may be called ortho-sulphuric acid, is well known. It readily separates from super-saturated solution in H_2SO_4 at low winter temperatures when reagent bottles of "strong" sulphuric acid are shaken.

The case of HCl is somewhat uncertain. There is no doubt that the straight line which holds up to over $p = \cdot35$ gives place to a curve in the neighbourhood of ·37, but, unfortunately, the specific gravities at all higher concentrations up to ·43 (the highest) are recorded as less accurate than those below. It is most probable, however, that the break-away from the line occurs when $p = \cdot3664$ and the solution has the composition of $HCl \cdot 3\frac{1}{2}H_2O$. This requires $n_H = 11\cdot897$, $n_H^{1/2} = 3\cdot449$, and $\phi'_H = 84\cdot055 = 20\cdot947 + 3\cdot5 \times 18\cdot031$ (at 15°). The curve from this point bends upwards in the direction that indicates it has been formed from its components with contraction, which accords with the marked exothermic reaction of hydrogen chloride and water. The only compound which has been isolated in the solid state is the monohydrate; but specific gravity data do not extend to such a high concentration ($p = \cdot6693$).

In the LiCl case the break-away from the straight line into a curve takes place at the point where the whole solution has the composition of $LiCl \cdot 10H_2O$, far below the saturation point, which extends to near $n = 12\cdot5$. The characteristics of this hydrate point are $p = \cdot1908$, $n_H = 4\cdot985$, $n_H^{1/2} = 2\cdot2327$, and $\phi'_H = 200\cdot60 = 20\cdot20 + 10 \times 18\cdot040$ at (18°). Both the line and the curve are accurately defined by points calculated from extensive experimental work done in the Melbourne laboratory (W. H. Green, Trans. Chem. Soc. 1908, p. 2036). The change from the line to the curve is fairly abrupt, so that there is small room for doubt as to the exact point at which it occurs. The case is very similar to that of H_2SO_4, except for the complexity of the hydrate indicated and for the fact that the curve bends away in the opposite direction, the hydrate in this case being formed from its components with expansion. $LiCl \cdot 10\ H_2O$ is not known in the solid state. Mono- and di-hydrates have been separated from more concentrated solutions, but the corresponding hydrate points are beyond the range of the experimental data.

The case of another very soluble salt is very similar. The straight line of NH_4NO_3 gives place to a curve at the hydrate point for $NH_4NO_3 \cdot 7H_2O$, for which the p value is ·3884 and $n_H = 5\cdot686$, $n_H^{1/2} = 2\cdot3845$ and $\phi'_H = 175\cdot87 = 49\cdot60 + 7 \times 18\ 039$ (at 17·5°). Here also the curve tends in the direction which shows that expansion occurred on the formation of the

hydrate from its components. No hydrate of NH_4NO_3 has been separated in the solid state.

The straight line in the case of HNO_3 is relatively short, the acid being soluble in water in all proportions and the greater part of the ϕ, $n^{1/2}$ graph showing as a decided curve. The break-away from the line occurs at the $HNO_3 . 11H_2O$ hydrate point, *i. e.*, at (or close to) $p = \cdot 2413$, for which $n_H = 4 \cdot 385$, $n_H^{1/2} = 2 \cdot 094$, and $\phi'_H = 228 \cdot 05 = 29 \cdot 71 + 11 \times 18 \cdot 031$ (at 15°). In this case the curve bends towards higher volume, showing that the hydrate has formed with contraction, like $H_2SO_4 . H_2O$. An attempt to straighten this curve by plotting ϕ against a higher power of n proved completely successful with $n^{3/2}$, for a straight line resulted which is defined by the equation $\phi = 28 \cdot 65 + \cdot 1225\, n^{3/2}$ and which, of course, does not include the points below the $11H_2O$ hydrate point. Again, however, there is a break-away from the line at a definite hydrate point; and this time it is the monohydrate, $HNO_3 . H_2O$, which requires $p = \cdot 7777$, $n_H = 17 \cdot 877$, $n_H^{1/2} = 75 \cdot 586$, and $\phi'_H = 55 \cdot 938 = 37 \cdot 907 + 18 \cdot 031$. Here another curve, itself nearly rectilinear, diverges in the direction of smaller volume. It is unbroken up to about $p = \cdot 98$, beyond which uncertainty attaches to the experimental data on account of the instability of very highly concentrated nitric acid. The whole range of concentrations is thus divisible into three stages, viz.: (1) from $n = 0$ to $n = 4 \cdot 385$, following the $n^{1/2}$ rule, with solutions of the $11H_2O$ hydrate in excess of water; (2) from $n = 4 \cdot 385$ to $n = 17 \cdot 877$, following the $n^{3/2}$ rule, with mixtures of the above hydrate and the monohydrate; (3) from $n = 17 \cdot 877$ to the end, with solutions of the monohydrate in the anhydrous acid. Pickering predicted and isolated as solids the monohydrate and trihydrate, but the present study of the solute volume has given no sign of the latter. The constitution of nitric acid in its higher concentrations has always been a problem. W. H. Hartley, from his study of the absorption spectra and other properties, was led to conjecture that it is a mixture of orthonitric acid (the monohydrate) and a polymerized anhydrous molecule, perhaps $H_2N_2O_6$, with oxidizing power but no acid characters. V. H. Veley, who did much work on the properties of nitric acid, held similar views. In the more dilute solutions, which, according to the theory given here, contain hydrates free from anhydrous acid, polymerized or otherwise, nitric acid closely resembles hydrochloric acid in its conductivity (α) values; but G. N. Lewis has shown that mobility considerations, based upon transport numbers, lead to somewhat lower

true ionization fractions for HNO_3 and the nitrates than for HCl and the corresponding chlorides. The β values given in Table I. accord well with this view.

Poor Electrolytes and Non-Electrolytes.

Of these, phosphoric acid, acetic acid, sucrose, and glycerol have been examined. Though conventionally distinguished as above, sucrose and glycerol have some small tendency to salt formation and should be classed in the same category with phosphoric and acetic acids. They all differ from the electrolytes already discussed, first in showing a much smaller percentage change of volume on dilution and, secondly and more radically, in not following the $n^{1/2}$ rule. All yield decided curves when ϕ is plotted against $n^{1/2}$. The

TABLE II.

Poor Electrolytes. $\phi = a + bn^{5/4}$.

Substance.	$t°$.	Highest concentration (mols per litre).	$a = \phi_0$.	$b = \frac{\phi m - \phi_0}{n_m^{5/4}}$	ϕm.	n_m.	n_m.	At hydrate point. x.	At hydrate point. n.
Phosphoric acid...	15°	8·8	45·16	·2024	53·10	18·833	39·233	—	—
Acetic acid	15°	17·58	50·91	·1385	55·99	17·86	36·713	1	13·77
Sucrose	17·5°	3·6	210·12	1·500	220·07	4·544	6·634	—	—

whole range in the case of glycerol, which is soluble in all proportions, yields a ϕ volume change of only about 4 per cent., and more exact p and s values than those available would be needed for any particular regularity to be disclosed. But the rather surprising fact has been ascertained that each of the others gives an undeniable straight line when ϕ is plotted against $n^{5/4}$. With lower powers (e. g., n itself) or higher powers (e. g., $n^{3/2}$) there is curvature one way or the other. Phosphoric acid, acetic acid, and sucrose, therefore, follow the rule that $\phi = a + bn^{5/4}$; but whether this is more generally true of the class to which they belong cannot be stated at present. The three cases are summarised in Table II.

In the case of phosphoric acid, the rule holds from $p = \cdot 15$ and $n = 1 \cdot 66$ to $p = \cdot 60$ and $n = 8 \cdot 8$, *i. e.*, through the whole range of available data, excluding those at the dilute end, where no certain conclusion can be drawn. In the sucrose

case the rule holds from $p=\cdot05$ and $n=0\cdot149$ to $p=\cdot85$ and $n=3\cdot6$ approximately,—again to the highest concentration for which data are available. But acetic acid, being soluble in water in all proportions, affords evidence up to $p=1$ and $n=17\cdot58$; and in its case the straight line runs from $p=\cdot10$, $n=1\cdot69$, to a point between $p=\cdot75$ and $p=\cdot80$, where regular curvature away from the line sets in. There is no doubt that this is the monohydrate (orthoacetic acid) point, for which the calculated characteristic values are $p=\cdot769$, $n_{\mathrm{H}}=13\cdot77$, $n_{\mathrm{H}}^{5/4}=26\cdot53$, $\phi'_{\mathrm{H}}=72\cdot622=54\cdot591+18\cdot031$ (at 15°) The case is like that of H_2SO_4 except for the different power of n. It is shown in fig. 4.

Fig. 4.

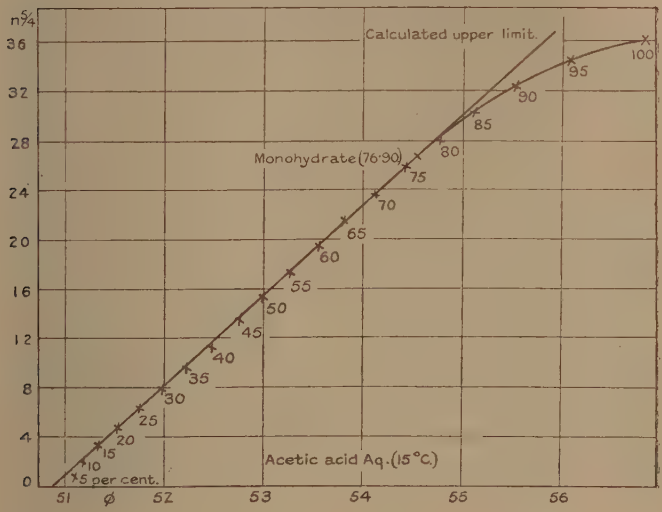

The curve between the monohydrate and anhydrous acid points has been examined as was done in the H_2SO_4 case, a few points being recalculated as solutions of $C_2H_4O_2\,.\,H_2O$ in $C_2H_4O_2$; and again it was found that the new ϕ values when plotted against the new $n^{1/2}$ values give points lying on or close to a straight line, from $p=0$ at the anhydrous acid end to $p=1$ at the hydrate point. These two cases give some evidence, therefore, that the square root holds for electrolytic solutions in other solvents besides water, provided that complicating conditions be absent.

That there are some such complicating conditions in the cases of acetic acid, phosphoric acid, and sucrose in aqueous solution is suggested by their substitution of the $n^{5.4}$ rule for the other. That acetic acid is prone to form associated molecules offers a possible explanation in its case, for gradual depolymerization as dilution increases may well swamp a simultaneous but smaller volume change due to ionization. A similar complication may, perhaps, be at work in the more concentrated solutions of nitric acid: but, whatever the cause, acetic acid, phosphoric acid, and sucrose follow the same rule. Further investigation seems to be called for.

Summary.

1. It is shown that, in the great majority of instances, the apparent solute molecular volume of an electrolyte in aqueous solution is a rectilinear function of the square root of the volume concentration. In most cases of limited solubility the straight line representing this relation holds through the whole range of experimental data; but in those in which this range extends to sufficiently high concentration it is shown that curvature sets in, the change seeming always to originate at a point corresponding to the composition of some definite hydrate. In the case of sulphuric acid the monohydrate is thus indicated, while various higher hydrates are shown by nitric acid, hydrochloric acid, ammonium nitrate, and lithium chloride.

2. From these facts and other evidence the conclusion has been drawn that, below the point at which curvature originates, the solution is always that of a hydrate in excess of water, but that, above that point, it is not truly an aqueous solution but either a solution of a monohydrate in excess of anhydrous substance or an intermediate mixture of hydrates, as the case may be.

3. From this view it follows that the true solute molecular volume, below the hydrate point, is that of the characteristic hydrate and is the sum of the apparent molecular volume and a quantity determined by its degree of hydration. It includes the plus or minus volume change that accompanies its formation from its components and also a contraction, the extent of which depends on the dilution. This true molecular volume has a definite value at infinite dilution, which increases linearly with the square root of the concentration up to the hydrate point. The apparent solute molecular volume in a few instances is negative at low

concentrations; the true volume—that of the hydrate—is always positive.

4. It is suggested that the true solute molecular volume at infinite dilution is that of the completely ionized hydrate and that the larger measured value at any given concentration is the average value of a mixture of ionized and unionized molecules. It is shown, also, how the unreachable value of the completely unionized hydrate may be calculated from the two constants of the straight line.

5. It is shown, further, that, if this hypothesis be correct, it necessarily follows that the ionization fraction (β) at any given concentration (n) is expressed by the equation $\beta = 1 - kn^{1/2}$, where k is a constant readily calculated.

6. While the facts cited as to the apparent solute molecular volumes involve no assumptions, their interpretation in the manner explained assumes that any excess of water which remains as solvent after formation of the characteristic hydrate retains its original specific volume practically unchanged.

7. In the case of three poor electrolytes, viz., acetic acid, phosphoric acid, and sucrose, it is shown that the apparent solute molecular volume is a rectilinear function of the $\frac{5}{4}$ power of the volume concentration, the square root rule not holding. In the last two cases the straight line extends through the whole range of the experimental data, but in the acetic acid case it gives place to a curve above the monohydrate point. In both this case and that of sulphuric acid, points on the curve above this point have been recalculated as those of solutions of the monohydrate in anhydrous acid, and are found to lie on a straight line when plotted as solute molecular volumes against the square root of the concentration, thus supplying some evidence that this rule is not confined to aqueous solutions.

8. Twenty-two cases of alkalis, acids, and salts, and the above three cases of poor electrolytes, are summarized in tabular form and their more striking features are discussed in detail.

Melbourne,
October 1929.

XXIX. *On the Acoustics of Large Rooms**. *By* Dr. M. J. O. Strutt †.

Abstract.

The theoretical proofs hitherto given in literature of Sabine's experimental result, that the duration of residual sound in a large room does not depend upon the shape but only on the volume and the absorbing power, and is the same (generally) if measured in different points with the source at different places, may be said to be incomplete. They start from considerations of reflexion at the walls, but phase relations are left out.

Moreover, often a homogeneous distribution of sound-energy over space at the moment the source stops is assumed, which will not be true in various cases that, on the other hand, experimentally check Sabine's law very well.

The present treatment discusses the problem of forced oscillations in a continuous medium with arbitrarily distributed absorption, and shows Sabine's law to be a general asymptotic property of such oscillations, if the quotient of the forced frequency over the lowest free frequency of the system tends to infinity.

In addition, various special experimental features are discussed from this point of view.

The prevalence of Sabine's law in other departments of physics, *e. g.*, with the electromagnetic radiation in closed spaces, is predicted from its general character.

Introduction.

In a series of fundamental experiments W. C. Sabine has shown ‡ that the acoustical properties of large rooms may often be very well defined by the duration of residual sound. This duration is measured in the following way :—A source of sound (*e. g.*, organ pipes), of frequency generally large with respect to the lowest free frequency of the room, is operated constantly during a time sufficient

* The essential contents of this paper coincide with a lecture delivered by the Author before the Dutch Physical Society at Amsterdam, January 26th, 1929.

† Communicated by the Author.

‡ Collected papers on Acoustics.

to reach the stationary state of affairs. Then the source is stopped abruptly, and the time from this moment until the sound has fallen to the minimum audible intensity is measured. By a series of measurements this time is reduced to a value giving the duration of residual sound with an intensity at the moment the source stops which is a known multiple of the minimum audible intensity (*e.g.*, a million-fold).

Many experiments lead to the conclusion (hereafter referred to as Sabine's law) that in general *the duration of residual sound measured in this way is proportional to the volume of the room over the total absorbing power* (the meaning of this latter term will appear hereafter), *but does not depend on the shape of the room, the places of source and experimenter, while the frequency does not change much after the source has stopped,* this law being checked best in large rooms.

I must add that Sabine has also performed experiments which seem to contradict this law, but these experiments may in general be easily explained by special conditions, causing a deviation from the law, which, as will appear shortly, is only *exactly* followed in certain "ideal" conditions.

In general, experiments must be said to check the law with remarkable accuracy, as is illustrated by graph 1, which is taken from a paper by Sabine.

After this experimental discovery, which enabled rooms with improved acoustical properties to be constructed, many theoretical papers were devoted to proofs of the law. The first of such papers was by Sabine himself.

In most of them (including Sabine's) a homogeneous distribution of sound-energy over space at the moment the source stops is assumed, which leads to a proof of the law if certain elementary considerations of reflexion at the walls are followed.

It is easy to give simple cases in which this homogeneous distribution of energy cannot exist. This happens, *e.g.*, in a spherical room with the source at the centre. Another case is a cylindrical room with the source at the centre. All these cases are automatically excluded from the considerations mentioned above, and one might conclude (this point of view has indeed been supported by certain authors) that Sabine's law will not hold in such cases.

Now experiments are known in which a non-homogeneous distribution of energy certainly exists—*e. g.*, the Sanders' theatre, discussed by Sabine. However, the point (1) in

graph 1, belonging to this theatre, lies beautifully on the straight line. Hence this assumption of special energy distribution cannot be essential for the validity of Sabine's law.

In all of the papers mentioned above, considerations of reflexion are applied to the *intensity*, leaving out phase relations. It is difficult, if not impossible, to rate the error brought into the calculation by this neglect.

A Law similar to Sabine's holding in Physics.

In various departments of physics a law exists which bears some resemblance to Sabine's. It has first been

Graph 1.

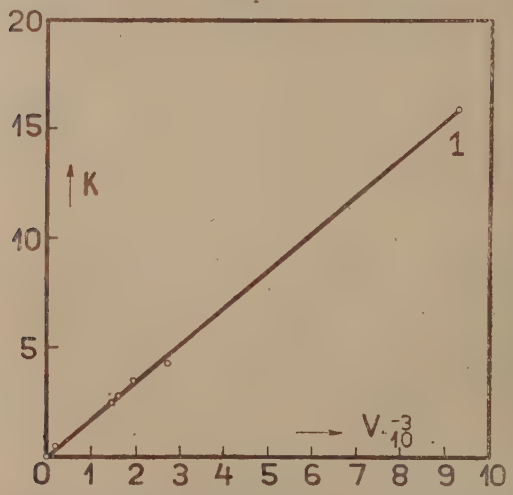

Vertical axis: Duration of residual Sound total absorbing Power.
Horizontal axis: Volume of room.

(Taken from a paper by Sabine.)

announced by H. A. Lorentz that the very high characteristic frequencies * (*i. e.*, the modes in which a system oscillates without outside forces acting constantly) of a continuous system *without* absorption will asymptotically depend only on the volume and the elastic properties, but be independent of the shape. This proposition has been proved mathematically by H. Weyl.

* Lorentz, 'Modern Physics,' p. 166 (1927).

Its physical plausibility is most easily seen by considering some applications.

J. H. Jeans and P. Debye have developed a theory of radiation in closed spaces, leading to Planck's experimental law. Herein the proposition must be supposed to hold, for otherwise Planck's law would not follow.

Similarly, in Debye's theory of specific heat * a cubic piece of metal would have a heat capacity different from a spherical piece of the same metal if Lorentz's proposition were not fulfilled.

A. Sommerfeld has pointed out that the proposition is also important for the acoustics of large rooms †.

In all of these theories systems without absorption were considered, and hence the angular frequencies in the notation

$$e^{j\omega t}$$

$$(j = \sqrt{-1}\,;\ t = \text{time})$$

are purely real. If we have absorption ω will have a real and an imaginary portion, the latter being of positive sign, so that any free oscillation once started in the system will die out after some time.

Lorentz's proposition, mentioned above, has been shown by Weyl ‡ to be an asymptotic property of the real characteristic values of the frequency ω belonging to systems *without* absorption.

In the present paper *Sabine's law will be shown to be an asymptotic property of the complex characteristic values of* ω *in systems with absorption.*

Once this analogy between Lorentz's and Sabine's laws has been formulated, the course which must be adopted in the analytical proof of the latter is quite clear. Firstly, it is necessary to calculate the complex characteristic values of ω in continuous systems with absorption distributed arbitrarily over space. As a special case we may then transport all absorbent matter to the walls, as is necessary for the acoustics of large rooms. In the second place, the forced and free oscillations of such systems must be studied in a general manner, for the process of residual sound involves a complete calculation of these oscillatory states. Combining the results of these two fundamental considerations, we shall be conducted to Sabine's law. Meantime we shall have

* Lorentz, *loc. cit.*

† *Physikalische Zeitschrift*, xi. p. 1057 (1910).

‡ *Mathematische Annalen*, lxxi. p. 441 (1912).

opportunity to define the exact conditions necessary for its validity. Also deviations from the law and special features, shown by experiments, must at once become clear from this point of view.

According to the general character of Sabine's law, indicated above, we shall be able to predict its existence in various other departments of physics, *e. g.*, with the electromagnetic radiation in closed rooms and with the oscillations of strings, bars, plates, etc.

Asymptotic Calculation of the Characteristic Frequencies in Continuous Systems with Absorption.

It is not my aim to go into mathematical details in the present paper. Of course, for a rigid proof these details become essential, but from a physical point of view they are quite unimportant. A special paper, entitled "Ueber das Daempfungsproblem der mathematischen Physik," which will appear in the *Mathematische Annalen*, is devoted to their discussion.

Improbable though it seems, I have found only one paper * in the mathematical and physical literature dealing with the problem of oscillating continuous systems with absorption distributed arbitrarily over the system. It gives the complete theory of such a system for *one dimension* (*e. g.*, string). The methods employed are such that no immediate generalization to more dimensions can be found. Moreover, the developments of Faber's do not permit us to prove Sabine's law for even one single dimension. On the contrary, they seem to indicate that no law such as Sabine's can exist in continuous systems with absorption.

For these two reasons it was necessary to start a completely new consideration, embodying the theory for more than one dimension and giving formulæ by which Sabine's law can be proved. Faber's development formula could be shown to be equivalent to the new one in the case of one dimension, its inability to prove Sabine's law being due to the special, and in this respect inefficient, form adopted by Faber.

As dependent variable in the analysis here given, I shall adopt a quantity u, referred to as "amplitude of oscillation." Afterwards this u may, in the acoustical case, be identified with the velocity potential or with the pressure at any one point.

* O. Faber, "Theorie der gedämpften Schwingungen," Dissertation Strassbourg (Referee: R. von Mises) (1914).

Let the amplitude of oscillation be given by the equation

$$\left(\frac{\partial^2}{\partial x^2}+\frac{\partial^2}{\partial y^2}+\frac{\partial^2}{\partial z^2}\right)u=\rho(xyz)\frac{\partial^2 u}{\partial t^2}+w(xyz)\frac{\partial u}{\partial t}, \quad . \quad (1)$$

which, by writing

$$u(xyzt)=v(xyz)e^{j\omega t},$$

yields

$$\left(\frac{\partial^2}{\partial x^2}+\frac{\partial^2}{\partial y^2}+\frac{\partial^2}{\partial z^2}\right)v+\omega^2\rho\left(1-j\frac{w}{\omega\rho}\right)v=0. \quad . \quad (2)$$

Here ρ is always supposed to be positive ($\rho > 0$), Equation (2) shows that for large values of ω the term between brackets reduces to 1, provided that w/ρ is nowhere infinite. By transferring (2) to an integral equation we may even see that the necessary condition is only that w/ρ integrated over the space considered does not become infinite, though w itself might be infinite at some points.

We require a solution of (2) which satisfies certain conditions at the boundary of the space considered, *e. g.*, the Newtonian condition

$$\sigma(xyz)u+\frac{\partial u}{\partial n}=0, \quad . \quad . \quad . \quad . \quad . \quad (3)$$

where n indicates the direction, normally outward, to the aforesaid boundary.

It is known that the problem (2), (3) can only be solved for certain values of ω, the characteristic frequencies. These values of ω will be complex, with positive imaginary part, so as to cause any free oscillation once started in the system to die out after some time :

$$\omega=\alpha+j\beta. \quad . \quad . \quad . \quad . \quad . \quad . \quad . \quad (4)$$

Now from (2) we may conclude that the imaginary part β of ω will be quite negligible in amount compared with α, if $\alpha\rightarrow\infty$:

$$\lim_{\alpha\rightarrow\infty}\frac{\beta}{\alpha}=0\left(\frac{1}{\alpha}\right), \quad . \quad . \quad . \quad . \quad . \quad . \quad (5)$$

where the symbol $0(1/\alpha)$ indicates that the right-hand side vanishes as a constant independent of α multiplied by α^{-1} for $\alpha\rightarrow\infty$.

This equation (5), in combination with (2) and a formula derived by Weyl in proving Lorentz's law, enables us to calculate α and β for large values of α.

Weyl's formula for the high characteristic frequencies

of (2) if the term within brackets is replaced by 1, *i.e.*, in the case of large values of α, is

$$\lim_{\alpha_n \to \infty} \alpha_n{}^3 = \frac{6\pi^2 n}{\iiint_v \rho^{\frac{3}{2}}\, dx\, dy\, dz} + 0(\alpha^2 \ln \alpha), \quad . \quad . \quad (6)$$

where the integral in the denominator is to be taken over the whole space V considered, n is a large integer, indicating the (according to our assumption large) order of the characteristic frequency α, and the symbol 0 has a meaning similar to that explained above.

From (5), replacing ρ in (6) by $1 - jw/\omega\rho$ according to (2), we find

$$\lim_{\alpha \to \infty} \beta = \tfrac{1}{2} \frac{\iiint w \sqrt{\rho}\, dx\, dy\, dz}{\iiint \rho^{\frac{3}{2}}\, dx\, dy\, dz} + 0\left(\frac{\ln \alpha}{\alpha}\right). \quad . \quad . \quad (7)$$

Hence the characteristic frequencies of very large order n have an imaginary part, which asymptotically tends to become independent of n (and hence of α) and depends only on w integrated over space divided by ρ times the volume considered, if we take ρ constant. This implies that the high free modes of oscillation in our system, once started, all die out at exactly the same rate, independent of the frequency α considered.

This, as we shall see, is one fundamental part in the proof of Sabine's law.

We now turn to the second part of this proof.

Proof of Sabine's Law.

In Sabine's experiments the system is operated by a force causing a stationary state of oscillation after some time. Hence, we proceed to consider the motion of our system under such a force, which differs from the equations above, as these only express the free motion without force. Let the force acting on the system be given by

$$\mathrm{F}(xyx)e^{j\omega t};$$

then the motion of our system is given by the equation

$$\left(\frac{\partial^2}{\partial x^2} + \frac{\partial^2}{\partial y^2} + \frac{\partial^2}{\partial z^2}\right) u = \rho \frac{\partial^2 u}{\partial t^2} + w \frac{\partial u}{\partial t} + \mathrm{F} e^{j\omega t}, \quad . \quad (1a)$$

the solution of which, in the stationary case here considered, can be shown to be

$$u = e^{j\omega t} \sum_{n=1}^{\infty} \frac{\iiint \mathrm{F} \,.\, v_n \,.\, dx\, dy\, dz}{\omega_n{}^2 - \omega^2} c_n v_n(xyz). \quad . \quad . \quad (8)$$

Here ω_n and v_n are the characteristic (complex) frequencies of (2) and the characteristic solutions of (2) respectively. The coefficients c_n do not contain ω, the *forced* frequency :

$$-\frac{1}{c_n} = \iiint \rho v_n^2 \, dx \, dy \, dz + \frac{j}{2\omega_n} \iiint w v_n^2 \, dx \, dy \, dz.$$

The derivation of (8) was carried out by application of a method, due to Poincaré, which is based on Cauchy's theory of residues. This rather lengthy method had to be adopted, as the ordinary method for the derivation of development formulæ of this type which is based on a property called orthogonality of the functions v_n could not be followed, the functions v_n in systems with arbitrarily distributed absorption being no longer orthogonal to each other, as may be proved from (2).

Faber, in his paper mentioned before, gives a formula equivalent to (8), but having in our notation $\omega_n - \omega$ in the denominator and, of course, somewhat different c_n which, as in our formula, does not contain ω. As will appear shortly, this formula of Faber's is unable to give Sabine's law.

Let us perform Sabine's experiment with our system, oscillating according to (8). We have to stop the source abruptly at an instant $t = t_0$ and see how the system behaves. From this instant onwards, as no force acts, the motion of our system can be described as an infinite sum of free motions, which are solutions of (2) and (3)

$$t > t_0 : \quad u = \sum_{n=1}^{\infty} A_n v_n e^{(-\beta_n + j\alpha_n)(t - t_0)} + \sum_{n=1}^{\infty} B_n \bar{v}_n e^{(-\beta_n - j\alpha_n)(t - t_0)}, \quad . \quad . \quad . \quad . \quad (9)$$

where $\bar{v}_n$ is the conjugate complex function to v_n. The coefficients A_n and B_n have to be determined from the state of the system at the instant $t = t_0$, *i. e.*, by u and $\partial u / \partial t$ at this instant. These quantities may be found from (8)

$$\left.\begin{aligned} (u)_{t=t_0} &= e^{j\omega t_0} \sum_{n=1}^{\infty} \frac{\iiint F v_n \, dx \, dy \, dz}{\omega_n^2 - \omega^2} c_n v_n(xyz) \\ \left(\frac{\partial u}{\partial t}\right)_{t=t_0} &= j\omega e^{j\omega t_0} \sum_{n=1}^{\infty} \frac{\iiint F v_n \, dx \, dy \, dz}{\omega_n^2 - \omega^2} c_n v_n(xyz) \end{aligned}\right\} . \quad (8a)$$

By differentiating (9) with respect to t, taking $t = t_0$, separating the real and imaginary parts of v_n and $\bar{v}_n$ and

comparing with (8 *a*), the coefficients A_n and B_n may be written down. We need not, however, write out this calculation, as we may at once see the result.

From (8 *a*) we see that the coefficients of v_n in both series differ from zero only by an arbitrarily small quantity up to a fixed but very large index n, if we take the forced frequency ω tending towards infinity $\omega \to \infty$. This implies the same property with the coefficients A_n and B_n of (9).

4. By combining this result with (7) we shall prove Sabine's law. Indeed, as the series (9) for $\omega \to \infty$ in (8 *a*) contains only terms of very large order n, these terms have all the same β by (7). In other words, we see that

$$e^{-\beta t}$$

may be placed before the sigmas in (9), so that the oscillation of the system dies out at a rate proportional to the volume over the total absorption independently of the shape, the places of the source and of the experimenter.

This is essentially what Sabine found.

Extension of the Theory.

Hitherto, for purposes of generality, I have considered a quantity u described as amplitude of oscillation. Before I proceed to show with exactly what quantity u has to be identified in the acoustical case, a slight extension of the considerations just exposed will be given.

In the first place, in the acoustical case the dissipation w is not distributed over the whole space, but is substantially localized at the walls. Hence we have to see how this will alter our formulæ.

From Weyl's derivation of (6) we may conclude that replacing the boundary condition (3) by any other condition will not alter this formula. The same may be said of (7).

If w vanishes everywhere except at the walls, the rate of decay β, however, remaining finite, the space integral in the numerator of (7) has simply to be replaced by a surface integral.

By going through the derivation of (7), as exposed above, it will be perceived that it is in no step essential to consider w as independent of ω. It may, indeed contain this frequency, but it may not become infinite if $\omega \to \infty$. In other words, it may be a *bounded function of the frequency*. As will appear shortly, this extension is of great importance for the acoustical problem, for now we are prepared to consider various hypotheses regarding the nature of the absorption.

It is at once clear that there will exist continuous systems with absorption in which w, in our notation, is no bounded function of the frequency. In such systems (7) is no longer true, and hence Sabine's law cannot exist. In the course of this paper an instance of such a system will be given.

Denoting the two series in (9) by Σ_1 and Σ_2 respectively and its differential quotients with respect to the time t by Σ_1' and Σ_2', whereas the expression (8) and its differential quotient with respect to t will be denoted by Σ_3 and Σ_3' respectively, the above derivation of Sabine's law can be written symbolically

$$\left.\begin{aligned} &\Sigma_1 + \Sigma_2 = \Sigma_3 \text{ for } t = t_0, \\ &\Sigma_1' + \Sigma_2' = \Sigma_3' \text{ for } t = t_0. \end{aligned}\right\} \quad . \quad . \quad . \quad . \quad (10)$$

Now consider the system at rest and a force F, defined as above, acting on it from $t = t_1$ onwards. If this force is not concentrated at a point, as real physical forces never are, we shall have for $t = t_1$

$$u = 0 \quad \text{and} \quad \frac{\partial u}{\partial t} = 0.$$

The state of our system for $t > t_1$ is described by

$$u = \Sigma_1 + \Sigma_2 + \Sigma_3. \quad . \quad . \quad . \quad . \quad . \quad (11)$$

Taking into account the conditions for $t = t_1$, we find

$$\left.\begin{aligned} &\Sigma_1 + \Sigma_2 = -\Sigma_3 \text{ for } t = t_1, \\ &\Sigma_1' + \Sigma_2' = -\Sigma_3' \text{ for } t = t_1. \end{aligned}\right\} \quad . \quad . \quad . \quad . \quad (12)$$

Comparing (12) with (10), it follows that in the present case the coefficients A_n and B_n of (9) are numerically the same as in Sabine's case, but of *reversed sign.*

Hence, in starting a system with absorption by an oscillatory source of high frequency, the rate of increase follows the same law as the rate of decay in Sabine's experiments. Moreover, from (11) we conclude that the increase of the oscillations in the system is *complementary* to the decay, *i.e.*, the sum of the amplitudes, taken at the same t, reckoned from the moment the source stops in one and the moment the source starts in the other case, equals the stationary amplitude as given by (8).

As will be shown in the following section, this theoretical conclusion has been borne out by experiments.

Acoustics of Large Rooms.

In applying the foregoing theory to the acoustics of large rooms (the condition "large" implies that the first free frequency of oscillation is very small with respect to the forced frequency), it is not clear from the start which quantity to take for our u.

From the theory of acoustics it is known that in systems *without* absorption the velocity potential and the pressure are given by equations as (1) with the term containing w left out. But in extending this to equation (1) *with* absorption w we should be forced to make very special hypotheses regarding the nature of the dissipation. This applies also to the boundary condition (3). Only very special walls would satisfy this condition.

Graph 2.

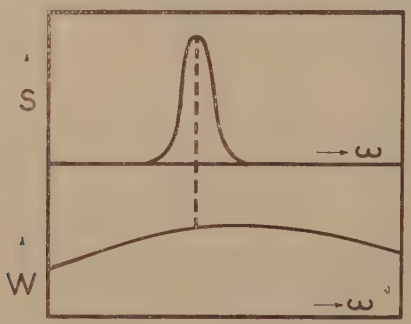

Upper part: magnitude of the terms in the series (9) as a function of ω.
Lower part: absorption w of eq. (1) as a function of ω for ω large.

In order to avoid these very narrowing and, in fact, for the present consideration not necessary restrictions, the theory has first to be extended in such way that a comparatively large degree of freedom is obtained regarding the boundary condition (3) and the function w in (1). This has been done in the foregoing section.

We may now take either the velocity potential or the pressure instead of our u, and can show from experiments that all remaining necessary conditions regarding w are fulfilled. This may be done in the following manner.

Let w be a function of ω, as in the lower part of graph 2. In the upper part of this graph, the magnitude of the terms in the series (9) is given as a function of ω. As we have

seen, all terms up to a certain ω_n in the neighbourhood of the forced frequency ω are very small. For ω_n about the same as ω they increase rapidly as a function of ω, but as the series converges they must decrease again if ω increases indefinitely. All that is required for our present consideration is that *w must be a slowly variable function of ω* as compared with the magnitude of the terms in (9) as a function of this ω. This is illustrated in graph 2. In this case, all β_n's in (9) are about of equal magnitude and our proof of Sabine's law holds.

On the other hand, if this is fulfilled we can, by measuring the rate of decay or of increase as a function of the forced frequency ω, find the absorption function w as a function of ω. Now Sabine has indeed performed such measurements, and we may see from his results that no experimental case is known where w is not a *bounded* function of ω. Reversing this reasoning, we conclude that, assuming the velocity potential or the pressure as our quantity u gives a satisfactory description of Sabine's results.

As the wave-length is in our considerations very small with respect to the dimensions of the room considered, we may treat the absorption by the walls in an elementary way, assuming an absorption coefficient A for the intensity of sound. In this way we find for w,

$$w = \frac{A c \rho}{4},$$

where c is the velocity of sound and ρ is the same as in equation (1).

Considering the absorption of, *e. g.*, a porous wall in the way adopted by the late Lord Rayleigh, we find w to be a bounded function of ω with a maximum. Other kinds of absorption also lead to such bounded functions w, and here we have another more direct proof that the theory may immediately be applied to the acoustics of large rooms.

Special Experimental Features.

According to the formula (7), in reality Sabine's law will never be valid exactly. With given forced frequency it will be followed better if the volume increases, for then the second term on the right-hand side of (7) decreases.

It is, of course, always possible to dispose the absorbent material in such manner that Sabine's law is not followed. This occurs, *e. g.*, if the arrangement is such as to coincide with the loops and nodes of a free mode of oscillation of

frequency in the neighbourhood of the forced frequency ω. In this case the one special mode of free oscillation will decay faster than any other mode, as was shown in previous analysis *. Hence, in such a case Sabine's law cannot hold. We should always consider distributions of absorbing matter of a structure large as compared with the wave-length of the forced oscillations. From Sabine's experiments we conclude that this condition is often fulfilled in practice.

The proof given above of Sabine's law shows that the frequency remains substantially the same during the decay. This holds better, if w in graph 2 is a slower variable function of ω.

With the ear, and still better in oscillograms, we can perceive that in reality the intensity of sound at any place

Graph 3.

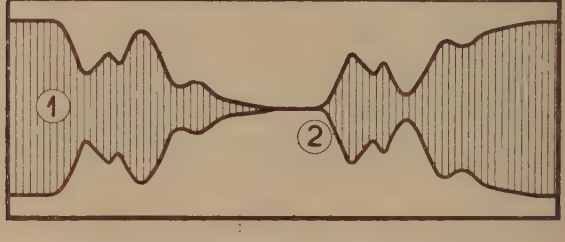

Oscillogram showing the decay of sound in a room to be exactly complementary to the increase.

does not die out in the simple exponential manner, as the above analysis seems to indicate. On the contrary, the intensity swells and decreases again more than once before it becomes inaudible. But this is exactly what equation (9) gives on a closer consideration. Although exp. $(-\beta t)$ may be placed before the sigma's, the terms under these signs are still oscillatory functions of the time. Hence their consonance, as the high free modes of oscillation lie very close together, will give large regions of interference, floating through space. What we perceive with the ear or the oscillograph is the passing of these regions.

This is illustrated in graph 3, drawn after such an oscillogram. At the point 1 the source stops, at 2 it starts again. We clearly see that the process of increase is

* *Annalen der Physik*, lxxxvii. p. 145 (1928).

complementary to the process of decrease, the duration of both being the same, as was described above *.

If we ask how to measure the duration of residual sound from an oscillogram, such as graph 3, the answer is that we have to take mean values over long intervals. The ear, recording the intensity logarithmically, is much more sensitive for small intensities than an oscillograph, and gives the ups and downs of intensity much less pronounced. Hence the process of taking mean values is much more easy to perform by the ear than from an oscillogram.

Sabine's Law in other Departments of Physics.

We have only proved Sabine's law to hold for systems the equations of which, by adopting a proper dependent variable, may be thrown in the form (1), with w a bounded function of the frequency.

In the first place, all closed electromagnetic systems belong to this type (even with w independent of the frequency). Here we may adopt any potential or field-strength function as dependent variable and always come to equation (1).

Hence the time of decay or of increase in a closed space, filled with electromagnetic radiation of frequencies all large with respect to the first characteristic frequency, is proportional to the volume over the total absorption and independent of the shape, the places of the sources and of the experimenter.

The oscillations of strings, membranes, etc. with dissipation proportional to the square of the velocity, are described by equations similar to (1). Sabine's law will be valid with these systems.

As an instance of a system which does not follow Sabine's law, we consider a column of liquid in a tube with dissipation by viscosity. Adopting Stokes's theory of viscous fluids, we have

$$\frac{\partial^2 u}{\partial t^2} = a\frac{\partial^2 u}{\partial x^2} + b\frac{\partial^3 u}{\partial x^2 \partial t},$$

where u is the velocity and a, b are constants, depending on the nature of the fluid.

* Oscillograms published by Trendelenburg (Siemens) and others do not show the exact complementary of decay and increase here described. This must, I think, be attributed to conditions not being *exactly* the same in oscillographing the decay and the increase. A series of oscillograms, taken in this laboratory by Dr. Zwikker, carefully observing the same conditions during the decay and the increase, all show the exact complementarity, which follows from the present theory.

With

$$u = v(x) \cdot e^{-j\omega t},$$

and

$$v(0) = v(l) = 0,$$

this equation yields

$$\omega = -j\frac{bn^2\pi^2}{2l^2} \pm \tfrac{1}{2}\sqrt{4a\frac{n^2\pi^2}{l^2} - \left(\frac{bn^2\pi^2}{l^2}\right)^2},$$

$$n = 1, 2, 3, 4 \ldots .$$

Hence we find that for large order n of the free oscillation considered, the imaginary part of ω increases proportional to n^2. As the asymptotic constancy (*i. e.*, independency of n) of the imaginary part of ω was necessary to prove Sabine's law (equation (7)), this law cannot hold in the present case.

Of course, other systems in which Sabine's law is not valid can be found.

The general importance of this law is, however, clear from the above considerations, showing its validity in the most common mechanic and electromagnetic systems.

Physical Laboratory of
Philips's Glowlampworks, Ltd.
Eindhoven, February 1929.

XXX. *Ionic Magnetic Moments.* *By* EDMUND C. STONER, *Ph.D.(Cambridge), Reader in Physics at the University of Leeds* *.

Introduction.

THE magnetic moment of an atom (or ion) may be calculated when its spectroscopic state is known. In many cases the normal spectroscopic state is not known from direct experiment, but it may be predicted with reasonable certainty. Of the *possible* states (determinable from the number of electrons), the deepest (corresponding to the normal state) is found with the aid of rules which were primarily suggested by the experimental facts, but which also have theoretical justification. Using this method,

* Communicated by Prof. R. Whiddington, F.R.S.

Hund calculated the magnetic moments of the rare earth ions, and obtained values which, with one exception, were in remarkable agreement with the values deduced from measurements of the susceptibility. For the ions of the first transition series, however, there was practically no agreement. This disagreement has not been removed by the more complete theory of Laporte and Sommerfeld.

A suggestion of Bose, that in the first transition series only the electron spin contributes towards the susceptibility, does give results which are in rather better agreement with experiment, but, as it stands, this suggestion cannot be regarded as completely satisfactory.

The problem arises as to why the behaviour of the ions of the first transition series and of the rare earths is different. The variability of magnetic moment is an associated problem. Although the magnetic moments of a particular ion (as deduced from susceptibility measurements on different salts, or even the same salt under different conditions) are grouped round a fairly definite value, the range in some cases is very much larger than can be accounted for by experimental errors.

These problems will be considered in this paper. Various theories which have been given will first be briefly reviewed in relation to the experimental results. A modified theory will then be put forward, which, although in some respects qualitative, does seem to remove a number of the present difficulties. The evidence for the view suggested, and some of its consequences, will be briefly discussed.

Theories.

For many "normal" paramagnetics the susceptibility varies with the temperature, over considerable ranges, according to the formula

$$\chi_M = \frac{C_M}{T-\theta}, \quad \ldots \ldots \quad (1)$$

where χ_M is the gram-molecular susceptibility and C_M the Curie constant per gram molecule. The classical Langevin-Weiss theory * then gives for the gram-molecular magnetic moment σ_M,

$$\sigma_M = \sqrt{3RC_M}.$$

* For further details see E. C. Stoner, 'Magnetism and Atomic Structure' (Methuen, 1926).

The calculated moment is usually expressed in terms of the Weiss magneton, M_W, as unit ($M_W = 1123{\cdot}5$), and is given as p Weiss magnetons:

$$p = \frac{\sigma_M}{1123{\cdot}5} = 14{\cdot}07\sqrt{C_M}. \quad . \quad . \quad . \quad . \quad (2)$$

On the quantum theory the average magnetic moment will depend on the quantum state of the atoms (or ions or molecules), and the most convenient procedure is to find an expression for p in terms of the quantum numbers defining the state. This theoretical value can then be compared with that found experimentally (or calculated directly from the experimental measurements on susceptibility by the standard method outlined above).

Following on earlier work of Pauli, Epstein, and Gerlach, Sommerfeld * calculated the p values corresponding to atoms or ions whose magnetic moments were integral multiples of the Bohr unit ($M_B = 5593$), assuming that the atoms orientated themselves in a magnetic field so that their resolved moments were the same as those of atoms in an S state, as revealed by the Zeeman effect. Let b be magnetic moment in Bohr units. (The resolved moments will be b, $b-2$, $b-4 \ldots -b$.) Then it may be readily shown that

$$p = \frac{M_B}{M_W}\sqrt{b(b+2)} = 4{\cdot}97\sqrt{b(b+2)}. \quad . \quad . \quad (3)$$

For $b = 1, 2, 3 \ldots$ this gives $p = 8{\cdot}6, 14{\cdot}1, 19{\cdot}3 \ldots$.

Assuming that for the ions with from 18 to 28 electrons b increased from 0 to 5 and then decreased to 0, the calculated values for p were found to be in rough agreement with the values found experimentally (except for the Co^2 ion).

There was, however, no reason to suppose that the ions were always in an S state, and Hund † showed that in general the p value is given by

$$p = 4{\cdot}97g\sqrt{j(j+1)}. \quad . \quad . \quad . \quad . \quad . \quad (4)$$

where g is the Landé splitting factor and j the inner quantum number characterizing the state. This result was given before the advent of the spinning-electron theory, but it is simpler to discuss it in the light of this.

* A. Sommefeld, *Zeits. für Phys.* xix. p. 221 (1923).
† F. Hund, *Zeits. für Phys.* xxxiii. p. 855 (1925).

The total angular momentum—and magnetic moment—of an atom is a resultant of the orbital and spin moments of the electrons. In general the orbital moments may be regarded as combining to give a resultant characterized by the quantum number l ($l=0, 1, 2$ corresponding to S, P, D ... terms) and the spins to a resultant s ($s=0, \frac{1}{2}, 1, 1\frac{1}{2}$ ... corresponding to multiplicities $r=1, 2, 3, 4$ ...); j is the resultant of l and s, assuming values from $l+s$ to $|l-s$. The spectroscopic symbol ${}^{r}\mathrm{L}j$ (*e. g.* ${}^{4}\mathrm{F}_{3/2}$) thus gives the spin moment s ($r=2s+1$), the orbital moment l (*e. g.* for F terms $l=3$), and the total moment j. The factor g may be expressed in terms of l, j, and s. An empirically correct expression for g, the ratio of the magnetic to the mechanical moment of the atom, was first given by Landé; with the assumption that the ratio of the magnetic to the mechanical spin moment is double that for the orbital moment, it has now been deduced theoretically, using the new mechanics. By Hund's method possible ${}^{r}\mathrm{L}$ states for an atom may be found by considering the resultant effect of the electrons in it, and making use of Pauli's exclusion principle. Experiment and theory * indicate that those with the highest r will be the deepest, and of these that with the highest l. In determining the j value corresponding to the deepest state (the ground state), it is taken to be the lowest j in the first half of a group and the highest in the second (corresponding to inverted multiplet intervals).

Following this procedure, and using the expression (4), Hund obtained p values which agreed closely with experiment for the rare earth ions. For the ions of the first transition group, however, the sequence of p values given by the theory was completely different from that observed.

Laporte and Sommerfeld † pointed out that if the multiplet intervals were small ($ch\Delta\nu_j$ comparable with $k\mathrm{T}$), the ions would not be all in the lower state, but that there would be a distribution of the ions among the different possible j states. They obtained the following general expression for p:

$$p=4{\cdot}97\sqrt{\left\{\Sigma(2j+1)g^2j(j+1)e^{-\frac{ch\Delta\nu_j}{k\mathrm{T}}}\Big/\Sigma(2j+1)e^{-\frac{ch\Delta\nu_j}{k\mathrm{T}}}\right\}}. \quad (5)$$

* F. Hund, 'Linienspektren und periodisches System' (Springer, Berlin, 1927).

† O. Laporte and A. Sommerfeld, *Zeits. für Phys.* lx. p. 333 (1926).

Two limiting cases were considered:

$$(a)\ \Delta\nu \geqslant kT\ (\Delta\nu \to \infty \text{ or } T \to 0)$$

$$p_z = 4{\cdot}97g\sqrt{j(j+1)}, \quad . \quad . \quad . \quad . \quad . \quad . \quad . \quad . \quad (5a)$$

$$(b)\ \Delta\nu \ll kT\ (\Delta\nu \to 0 \text{ or } T \to \infty)$$

$$p_0 = 4{\cdot}97\sqrt{\{\Sigma(2j+1)g^2j(j+1)/\Sigma(2j+1)\}}. \quad . \quad (5b)$$

The observed values of p should then lie between those given by $(5a)$ and $(5b)$. The limits are fairly wide, but some of the observed p values (for Ni^2 and Cu^2) still did not fall between them. More recently, by a process of extrapolation, Laporte * has estimated the multiplet intervals for the ions concerned and carried out a calculation of the p values, using the full expression (5). He finds that there is no agreement at all in the case of multiplet terms.

Van Vleck †, in his very complete treatment of paramagnetism on the basis of the new mechanics, obtains the same expression as $(5a)$ for the case where the multiplet intervals are large. When the multiplet intervals are small ($ch\Delta\nu$ comparable with kT), he shows that the spin and orbital moments (l and s) are quantitized separately relative to the axis of the field—in small as well as large fields, by the principle of spectroscopic stability—and obtains, in place of $(5b)$, the expression

$$p = 4{\cdot}97\sqrt{4s(s+1) + l(l+1)}. \quad . \quad . \quad . \quad (6)$$

The actual values differ little from those given by $(5b)$.

Bose ‡ assumes that the paramagnetic susceptibility of the ions of the first transition series is due entirely to the spin moment of the electrons. The number of electrons N_l in a complete group is $2(2l+1)$. (For the first transition series the elections concerned are those for which $l=2$.) If there are Z electrons in an incomplete group in the atom, the maximum magnetic moment is $Z\mu_1$, for $Z \leqslant 2l+1$; and for $Z \geqslant 2l+1$ the maximum moment is $Z'\mu_1$, where $Z' = N_l - Z$. In a magnetic field Bose supposes that the possible moments for the atom with a maximum $Z\mu_1$ are $Z\mu_1, (Z-2)\mu_1 \ldots -Z\mu_1$, corresponding to $Z, Z-1 \ldots 0$, electrons having their spin moments parallel to the field, and the rest antiparallel; when $Z > 2l+1$ the moments range from Z' to $-Z'$ at

* O. Laporte, *Zeits. für Phys.* lxvii. p. 761 (1928).
† J. H. Van Vleck, Phys. Rev. xxxi. p. 587 (1928).
‡ D. M. Bose, *Zeits. für Phys.* lxiii. p. 864 (1927).

intervals of 2. This assumption of a variable moment of the atom due entirely to the electron spins gives the result

$$\left.\begin{aligned} & p=4\cdot97\ \sqrt{Z(Z+2)} \\ \text{or} \quad & p=4\cdot97\ \sqrt{Z'(Z'+2)} \end{aligned}\right\} \cdot \cdot \cdot \cdot \cdot \quad (7)$$

If s is the resultant spin moment (corresponding to the multiplicity $r=2s+1$), this result may be written

$$p=4\cdot97\ \sqrt{4s(s+1)} \cdot \cdot \cdot \cdot \cdot \quad (7a)$$

when the relation to Van Vleck's expression (6) becomes clear.

The actual result obtained is the same as that given originally by Sommerfeld (3), while the procedure followed is equivalent to stating that the ions behave magnetically as though they were in S states. It has been noted before that this is so for the ions with a smaller number of electrons*, but exceptions remain which indicate that the theory is by no means completely satisfactory empirically even for the first transition series, and no suggestion is given as to why the rare earth ions behave differently.

Comparison with Experiments.

The magnetic moments for the ions of the first transition series, calculated by the methods outlined above, are given in Table I. (The ions with 18 and 28 electrons, with a $^1S_0$ ground term, should have a zero moment, and are, in fact, diamagnetic). The observed values are also shown. (The index gives the positive charge on the ion.) It is not necessary to discuss these in detail †, but a few points may be mentioned.

With solutions, the apparent ionic susceptibility in many cases varies with the concentration. Thus with cobalt salts the p value for Co^2 varies between about 24 and 25; the addition of acid may cause the apparent p value to fall below 23. On the other hand nickel chloride, in concentrations ranging from ·62 to 22·69 per cent., gives a p value for Ni^2 constant to within about ·4 per cent., the value being practically the same for different salts. There are indications that in solutions θ (in eq. (1)) is not always zero. Birch ‡ has found for $CuCl_2$ in solution that from 0°–40°, $\theta=+10$ and $p=9\cdot01$; from 40°–85° $\theta=-65$, $p=9\cdot98$.

* E. C. Stoner, Phil. Mag. iii. p. 336 (1927).

† See P. Weiss, *Journ. de Phys.* v. p. 129 (1924); also 'Magnetism and Atomic Structure.' Chaps. vi. and vii.

‡ Birch, *Journ. de Phys.* ix. p. 137 (1928).

The solutions with different ions have not all been studied so thoroughly, but there can be no doubt that the apparent moment is not generally constant. The table gives a summary of the data so far available from the more precise experiments.

With solid salts the $1/\chi$, T curves are usually linear, at least over limited ranges; but where the investigations have been carried out over a large range of temperature, changes of slope or curvatures are frequently found. The procedure has usually been to consider linearity as a test for the validity of applying the Weiss-Langevin theory, or as a test for "magnetic purity"—the presence of a single carrier

TABLE I.

Calculated and Observed Magnetic Moments of Ions of the First Transition Series.

Number of electrons ...	19	20	21	22	23	24	25	26	27
Ground term	$^2D_{3/2}$	$^3F_2$	$^4F_{3/2}$	$^5D_0$	$^6S_{5/2}$	$^5D_4$	$^4F_{9/2}$	$^3F_4$	$^2D_{5/2}$
$4{\cdot}97\sqrt{4s(s+1)}$	8·6	14·1	19·3	24·4	29·4	24·4	19·3	14·1	8·6
$4{\cdot}97g\sqrt{j(j+1)}$	7·7	8·1	3·9	0	29·4	33·6	33·2	28·0	17·7
p from (5 b)	14·5	21·6	24·7	26·0	29·4	26·0	24·7	21·6	14·5
$4{\cdot}97\sqrt{4s(s+1)+l(l+1)}$.	14·9	22·2	25·8	27·2	29·4	27·2	25·8	22·2	14·9
Observed values of p. Solutions			Cr^3. 18·2–19·1	Cr^2. 23·8	Fe^3. 26–29·5 Mn^2. 29·4	Fe^2. 26·5	Co^2. 23–25	Ni^2. 16·0	Cu^2. 9–10
Solid salts.....	V^4. 8·9		Cr^3. 18·9 M^4. 19·8		Fe^3. 29 Mn^2. 27–30	Fe^2. 25–27·5	Co^2. 22–26	Ni^2. 14·5–17	Cu^2. 9–11

then being indicated. Attention has been directed more to finding linear parts of curves, and calculating p values from them, than to studying in detail divergences from the linear character. That there is definite variability of magnetic moment with different salts containing the same ion is shown by the careful experiments of Jackson *, who found, for example, the following p values for different salts of nickel, studied in the same manner :—

$NiSO_4$ $p=16{\cdot}9$,
$NiSO_4 . 7H_2O$ $p=14{\cdot}62$,
$NiSO_4 . (NH_4)_2SO_4 . 6H_2O$ $p=15{\cdot}9$.

* L. C. Jackson, Phil. Trans. A, ccxxiv. p. 1 (1923).

The apparent p value, calculated by the standard method, for the same ion in different salts may vary considerably; also the same salt may behave differently magnetically according to its thermal treatment, and give different p values over different ranges of temperature. The extensive investigation of Chantillon * on the cobaltous ion shows how widely the magnetic moment may vary (from 22 to 26).

The calculated and observed results are also shown in fig. 1. It will be seen at once that there is no question of the observed results falling even approximately on curve (2) —the Hund curve for large multiplet intervals. (It is the

Fig. 1.

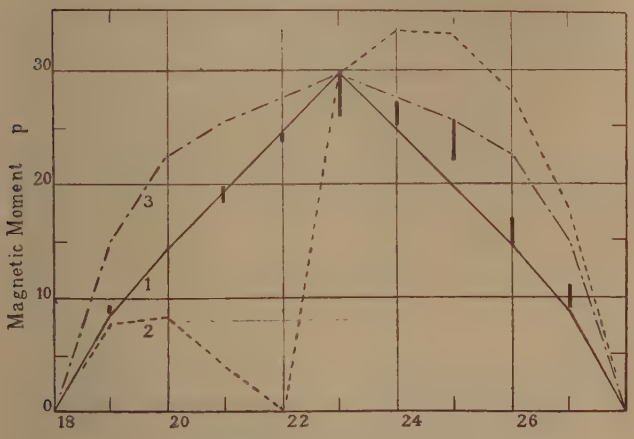

Calculated and observed magnetic moments.

Calculated { 1. ——— $p=4{\cdot}97\sqrt{4s(s+1)}$. 2. - - - - - - - - $p=4{\cdot}97g\sqrt{j(j+1)}$. 3. — — — — — $p=4{\cdot}97\sqrt{4s(s+1)+l(l+1)}$.

The thick vertical lines represent the range of observed values. (See Table I.)

corresponding curve which fits the results for the rare earth ions extremely well.) Moreover the observed values do not all fall between curves 2 and 3—notably Ni^2 26 and Cu^2 27. Curve 3 is that corresponding to small multiplet intervals (the Van Vleck expression is used). The suggestion

* A. Chantillon, *Annales de Phys.* ix. p. 187 (1928).

that the multiplets for the ions at the end of the series might be regular instead of inverted—so that the end part of curve (2) should be similar to the initial part—cannot be reconciled with the experimental spectroscopic facts, besides being at variance with the general theory. None of the suggestions put forward by Laporte seem adequate to explain the discrepancy.

The assumption of Bose, that only the electron spin contributes to the paramagnetism, leads to curve (1), which does agree fairly well with the experimental results; but the ions with 24 to 27 electrons certainly have moments greater than those indicated by the theory.

In short, none of the suggestions so far made seem adequate to account even qualitatively for some of the distinctive magnetic characteristics of the ions of the first transition series.

Modified Theory of Ionic Susceptibility.

Difference between ions of the two series.—For an ionic *gas* there can be little doubt that the treatment of Hund, as developed by Laporte and Sommerfeld, and by Van Vleck, is satisfactory, the p value, for large multiplet intervals, being given by

$$4{\cdot}97g\sqrt{j(j+1)},$$

and for small by

$$4{\cdot}97\sqrt{4s(s+1)+l(l+1)}.$$

That the first of these expressions gives results in agreement with experiment for the rare earth ions indicates not only that the multiplet intervals must be large, as is anticipated, but also that there is little disturbing interaction, and that the ions (in solids and solutions) behave in a magnetic field as though they were effectively independent.

In the ions of the first transition series it is the incomplete group of d electrons ($l=2$) which gives rise to the paramagnetism; in the rare earths the incomplete group of f electrons ($l=3$). The following numbers show the electronic constitution for two typical ions:—

n	1	2	3	4	5
l	0	0 1	0 1 2	0 1 2 3	0 1
Fe^3 23	2	8	8 5		
Gd^3 61	2	8	18	18 7	8

Numbers of electrons in groups in Fe^3 and Gd^3.

There is another difference besides that in the "orbital" character of the electrons in the incomplete groups. In the ions of the Fe^{5} type the incomplete group of electrons belongs to the group with the highest total quantum number in the ion ($n=3$); in the ions of the Gd^{3} type the incomplete group does not belong to the highest quantum number group. It is suggested that, just as it is the electrons of the highest total quantum number which are responsible for the ordinary valency properties (polar or homopolar) of atoms, so, in an ion, it is the group with the highest total quantum number which is primarily responsible for the interaction forces resulting in the formation of crystals or of aggregates in solutions.

The effect of interaction.—In an ion there is a strong interaction between the "orbital" moments of the different electrons, and also between the spin moments; these interactions between the l's of different electrons and the s's being much greater than the interaction between the l and s of a single electron. In a free ion the resultant l and s combine to give the total moment j, which is quantized with respect to an applied field. Where there is little interaction between an ion and its neighbours, in a solid or solution, the ion will still behave as "free." From a magnetic point of view an ion will behave as free if the group of electrons giving rise to the magnetic moment does not take part in the interaction. This is apparently the case in the rare earth ions.

If the magnetic group of electrons forms part of the "interacting" group, the ion will no longer behave as free. It may be anticipated that just as there is a strong l interaction between the electrons in a single atom, so there will be an l interaction between the different ions and atoms in a solid or solution. The ion may still behave as relatively free as far as the spin moment is concerned, for the "electrostatic" symmetry of an ion depends on the l moment, but not on the s moment. The suggestion is equivalent to supposing that the l moment of the ion (if this is due to electrons in the group of highest total quantum number) tends to assume a definite orientation with respect to neighbouring ions (or atoms or molecules). It would seem that this must be so in a crystal, where there is a definite arrangement of the centres of the electronic systems. Indeed, one of the main difficulties of the older theories of paramagnetic susceptibility was that they implied that the carriers of the magnetic moment were as free to change their orientation in a solid as in a gas. In a solution it might be thought that the ions had a greater

freedom for reorientation; but here the l moment of the ion may still tend to assume a different orientation with respect to the molecules or ions with which it is surrounded, even when these do not form a definite chemical complexion. In some cases there is very convincing evidence that similar associations are formed both in crystals and in solution. A study of the absorption spectra of cobalt compounds, for example, leads to the conclusion that both in solids and solutions the cobalt atom is associated with four groups in the blue compounds and with six in the red *.

It is suggested, then, that whereas in the rare earth ions there is a strong ls coupling, so that the resultant j is quantized with respect to an external field, in the ions of the transition series there may be a relatively weak ls coupling, while the l moment is subject to relatively strong interatomic coupling forces. With very strong interaction the s moment only may be quantized with respect to an external field H. The interaction field may be approximately regarded as a virtual magnetic field with direction distributed at random. The l quantization will then be with respect to the resultant of the external field and the random internal field. The limiting cases arise when the interaction field is very strong or very weak. For strong interaction

$$p=4\cdot97\sqrt{4s(s+1)}.$$

For weak interaction

$$p=4\cdot97\sqrt{4s(s+1)+l(l+1)}.$$

In general, it would be anticipated that, when there are no other disturbing factors, the observed magnetic moment would lie between these two values.

Comparison with experiment.—As may be seen from fig. 1, the observed moments generally fall between these not widely separated limits. For the ion 23, however, where there should be no variability for the reason under discussion (since $l=0$), the range is quite considerable. This is mainly due to the variation in the apparent moment of the Fe^3 ion in solution with concentration and amount of acid. The extraordinary variability in this case is probably due to chemical effects—possibly to the partial formation of complex ions of lower magnetic moment. It is noteworthy that Mn^2 23 has a remarkably constant moment. In a careful study of solutions of the chloride, sulphate, and nitrate Cabrera and his collaborators have found in each case a

* R. Hill and O. R. Howell, Phil. Mag. xlviii. p. 833 (1924).

value close to 29·35, independent of the concentration *. Bearing in mind the experimental difficulties and the uncertainty in the correction for the coexisting diamagnetism, the agreement between the observed and anticipated values is remarkably good.

Interaction equivalent to an initial virtual field.—The interaction between ions and surrounding ions and molecules is presumably of the same quantum type as that considered by Heitler and London in connexion with the formation of simple molecules. The general problem is a very complex one. It seems reasonable, however, to consider the initial interaction as similar to that resulting from an initial virtual magnetic field, with direction distributed at random. Such an assumption has proved remarkably fruitful in Kapitza's theory of the change of electrical conductivity in magnetic fields †. To see the general character of the effect of such initial field, the simplest possible case will be considered.

Consider a group of N ions, each a magnetic moment μ, and suppose that in a magnetic field the resolved moments are $\pm\mu$. Instead of supposing the initial field H_i to be distributed at random, it will be supposed to be parallel or anti-parallel to an external field H, the direction of which is taken as positive. The ions may be divided into two groups, N/2 in each, for one of which H_i is positive and for the other negative.

Let $\mu H_i/kT=x, \qquad \mu H/kT=h.$

The mean resolved moment may be obtained by the usual treatment:

(1) $H_i=0$:

$$\frac{\bar{\mu}}{\mu}=\frac{e^h-e^{-h}}{e^h+e^{-h}}=\tanh h \doteq h, \quad \bar{\mu}=\frac{\mu^2 H}{kT} \quad . \quad . \quad . \quad (8)$$

(This is the well-known quantum-theory result for the case where μ is one Bohr unit. According to the classical theory,

$$\bar{\mu}=\frac{\mu_c^2 H}{3kT}.$$

Thus

$$p=\frac{\mu_c}{M_W}=\frac{1}{M_W}\sqrt{\frac{3kT\bar{\mu}}{H}}=\frac{1}{M_W}\sqrt{\frac{3kT\mu^2 H}{kTH}}$$

$$=\frac{M_B}{M_W}\sqrt{3}=4{\cdot}97\sqrt{3}=8{\cdot}6.$$

* See Weiss, *l. c.* p. 141.

† P. Kapitza, P. R. S. cxxiii. p. 342 (1929).

(2) $H=0$. Considering the two groups,

$$\frac{\bar{\mu}}{\mu}=\frac{e^{x}-e^{-x}}{e^{x}+e^{-x}}-\frac{e^{x}-e^{-x}}{e^{x}+e^{-x}}=0.$$

(3) Both H and H_i present:

$$\frac{\bar{\mu}}{\mu}=\frac{1}{N}\cdot\frac{N}{2}\left\{\frac{e^{x+h}-e^{-x-h}}{e^{x+h}+e^{-x-h}}-\frac{e^{x-h}-e^{-x+h}}{e^{x-h}+e^{-x+h}}\right\}$$

$$=\tfrac{1}{2}\{\tanh(x+h)-\tanh(x-h)\}. \quad . \quad . \quad . \quad (9)$$

For $h\ll x$ this gives

$$\frac{\bar{\mu}}{\mu}=\operatorname{sech}^2 x\times h. \quad . \quad . \quad . \quad . \quad . \quad (10)$$

For $\mu H_i<kT$, let $\phi=\mu H_i/k$. Approximately

$$\bar{\mu}\doteq\left\{1-\left(\frac{\phi}{T}\right)^2\right\}\frac{\mu^2 H}{kT}. \quad . \quad . \quad . \quad . \quad . \quad (11)$$

The expressions (9)–(11) indicate the general character of the effect of the initial field. The nature of the variation with temperature may be summarized by writing

$$\bar{\mu}=f\left(\frac{T}{\phi}\right)\bar{\mu}_0, \quad . \quad . \quad . \quad . \quad . \quad . \quad (12)$$

where $\bar{\mu}_0$ is the value when $H_i=0$. As T approaches zero, $\bar{\mu}$ approaches 0. In general μ will be a fraction of $\bar{\mu}_0$, the fraction increasing as the temperature rises. In the limit it has the value 1. (For from (9), when x and h are both small, $\bar{\mu}/\mu\doteq\frac{1}{2}\{(x+h)-(x-h)\}=h$, as in (8)).

The general expression for the susceptibility must now be considered for the case where the ion has an s and l moment, the s moment being "free" and the l moment subject to the initial interaction field.

The Weiss-Langevin formula for the variation of the susceptibility with temperature is

$$\chi_M=\frac{C_M}{T-\theta}$$

$$=\frac{\mu_M^2}{3R(T-\theta)}=\frac{p^2 M_W^2}{3R(T-\theta)}. \quad . \quad . \quad . \quad (13)$$

Writing the quantum expression under consideration for p, this becomes

$$\chi_M=\frac{M_W^2(M_B/M_W)^2\{4s(s+1)+l(l+1)\}}{3R(T-\theta)}. \quad . \quad (14)$$

This requires modification in the light of the above view. The value of θ is not necessarily the same for the l and s moments. (θ arises from the Weiss "molecular field," which manifests itself when the substance is magnetized; that this field is a quantum interaction field has been shown by Heisenberg's treatment of ferromagnetism; it is probably related to the initial field, whose effect is represented by ϕ in (11).) Further, owing to the interaction field, the l moment may not be fuliy effective. The general expression may now be written:

$$\chi_M = \frac{M_B^2}{3R}\left[\frac{4s(s+1)}{T-\theta_s} + f\left(\frac{T}{\phi}\right)\frac{l(l+1)}{T-\theta_l}\right]. \quad . \quad . \quad (15)$$

If $\theta_l = \theta_s$, the expression is simplified, and p is given by

$$p = 4{\cdot}97\sqrt{\{4s(s+1) + f(T/\phi)\, l(l+1)\}}. \quad . \quad . \quad (16)$$

According to equation (15), the $\left(\frac{1}{\chi}, T\right)$ curves will not necessarily be linear, though the divergences from linearity may be relatively small if ϕ (corresponding to the l interaction field) is either very large or very small. In general the effective p value increases with the temperature, and the $\left(\frac{1}{\chi}, T\right)$ graph will show a curvature with the concave side towards the T axis. This type of variation is frequently found. As the results for the nickel and copper ions have not fitted in with previous theories, some of the results given by Weiss for these may be quoted. The measurements of Théodoridès on nickel chloride give $p = 16{\cdot}03$ between 15°·2 and 125°, and $p = 16{\cdot}92$ between 150° and 500°. Honda and Ishiwara find $p = 9{\cdot}2$ for $CuCl_2$ between $-140°$ to $+20°$, and $p = 10{\cdot}0$ from 20° to 500°. More recently Birch has found that $CuSO_4$ gives a non-linear curve between 10° and 537°—a curvature which is compatible with an s moment corresponding to $p = 8{\cdot}6$, and a partly effective l moment. The copper salts generally, with moments between 9 and 11, fit in well with the theory put forward, which gives 8·6 and 14·9 as the limits; moments from 14·5 to 17 are observed for nickel, the theory giving 14·1 and 22·2 as limits.

In the region of very low temperatures, the $\left(\frac{1}{\chi}, T\right)$ curves frequently show peculiar curvatures, indications of "cryomagnetic anomalies." A qualitative explanation of these has been given by Foëx * on a non-quantum theory which

* G. Foëx, *Ann. de Phys.* xvi. p. 174 (1921).

simply assumes the existence of a potential energy depending on the orientation of the magnetic carrier with respect to the crystal lattice. This theory may obviously be brought into relation with the assumption of an initial field.

It should, perhaps, be noted that the "initial" field has been taken to modify the effective l moment, having no effect on the s moment; this simply means that it has been assumed that there is a strong l interaction. As the s moment is a intrinsic property of the electron—in contradistinction to the l moment, which has reference to a nucleus or aggregate of nuclei—the s interaction will presumably be weak, though not necessarily non-existent. There may, therefore, be an initial field for the s moment, which, though small, may be effective at low temperatures in disturbing the susceptibility from its ideal value. This must be borne in mind in any more detailed consideration of cryomagnetic anomalies.

Complex salts.—Following Sidgwick, for a typical complex ion, it is possible to assign an effective atomic number to the central atom. The magnetic moment depends on the effective atomic number, which gives the number of electrons associated with the central atom. Let Z be the effective atomic number. When Z=36, the substance is diamagnetic (as in cobaltammines), 36 electrons presumably giving the argon configuration. The following p values have been found:

Z	32	33	34	35
p (obs.) ...	24	17–21	13–15	9–10

There is difficulty in interpreting these results, because it is not known how the Z electrons are distributed. The 33 configuration, for example, may consist of a closed group of 30, with $3p$ electrons ($n=4$, $l=1$) giving a $^4S_{3/2}$ ground term, or of a closed group of 18, an incomplete group of $7d$ electrons ($n=3$, $l=3$), and a closed group of 8 ($n=4$, $l=0$, 1), giving a $^4F_{9/2}$ ground term. For $[Fe(N_2H_4)_2]Cl_2$, with Z=32, Ray and Bhar * have found $p=24{\cdot}1$. If there are $2p$ electrons, in addition to closed groups, the corresponding ground term $^3P_0$ gives the limits as 14·1–15·8; with $6d$ electrons ($^5D_4$) the limits are 24·4–27·2. This suggests that it is the $n=3$ group which is incomplete. The experimental data available, however, are not sufficient to decide between the various possibilities, and, although the problem of the complex ions is an interesting one, it would not be profitable to discuss it further at present.

* See D. M. Bose, *Zeits. für Phys.* xliii. p. 878 (1927).

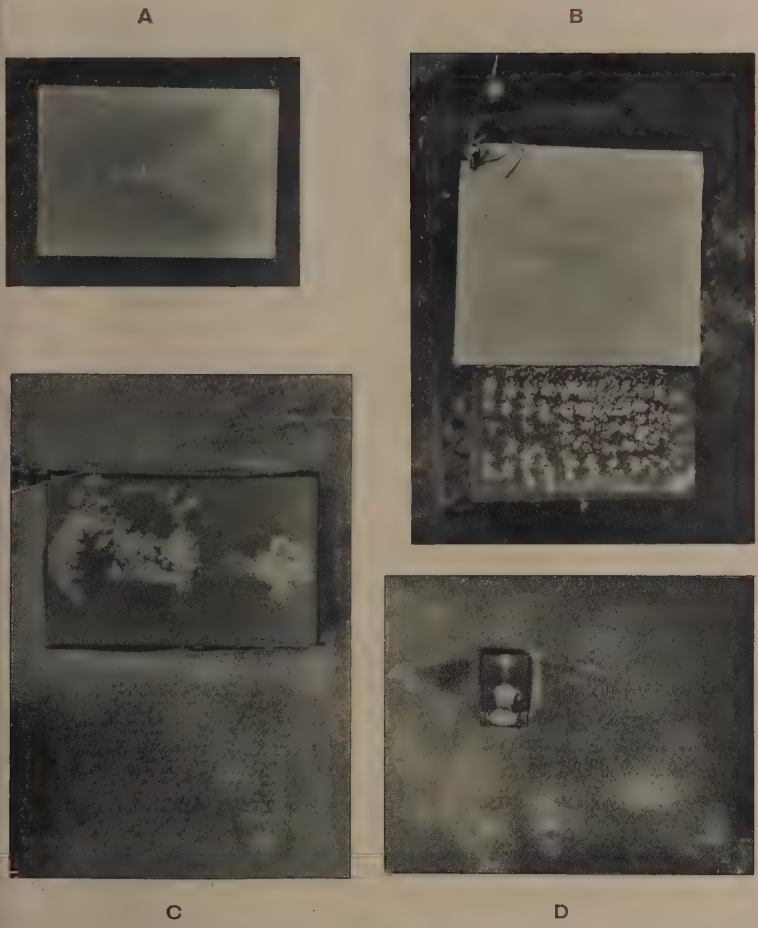

Dust-figures. Field parallel to E axis.
Longitudinal vibrations.

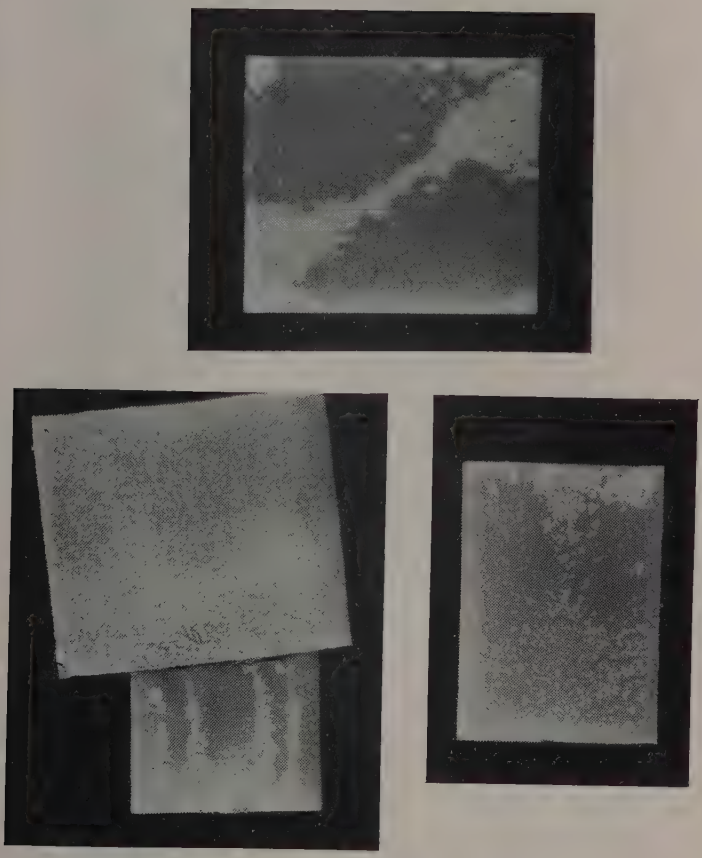

Dust-figures. Field parallel to B axis.
Longitudinal vibrations.

A

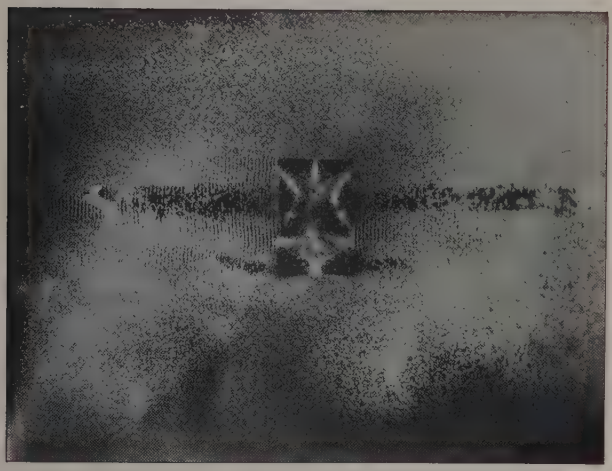

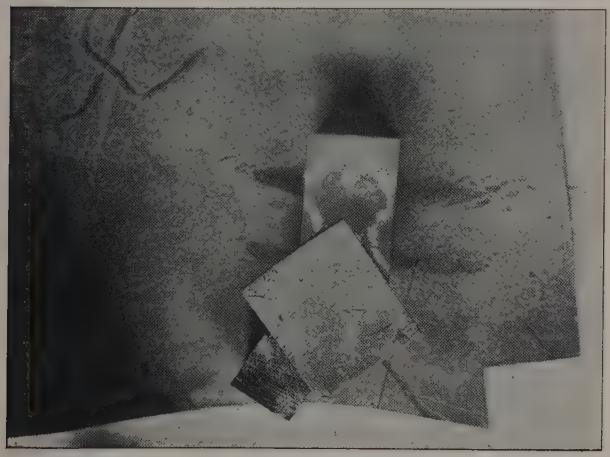

B

Dust-patterns showing air-streams and standing waves.

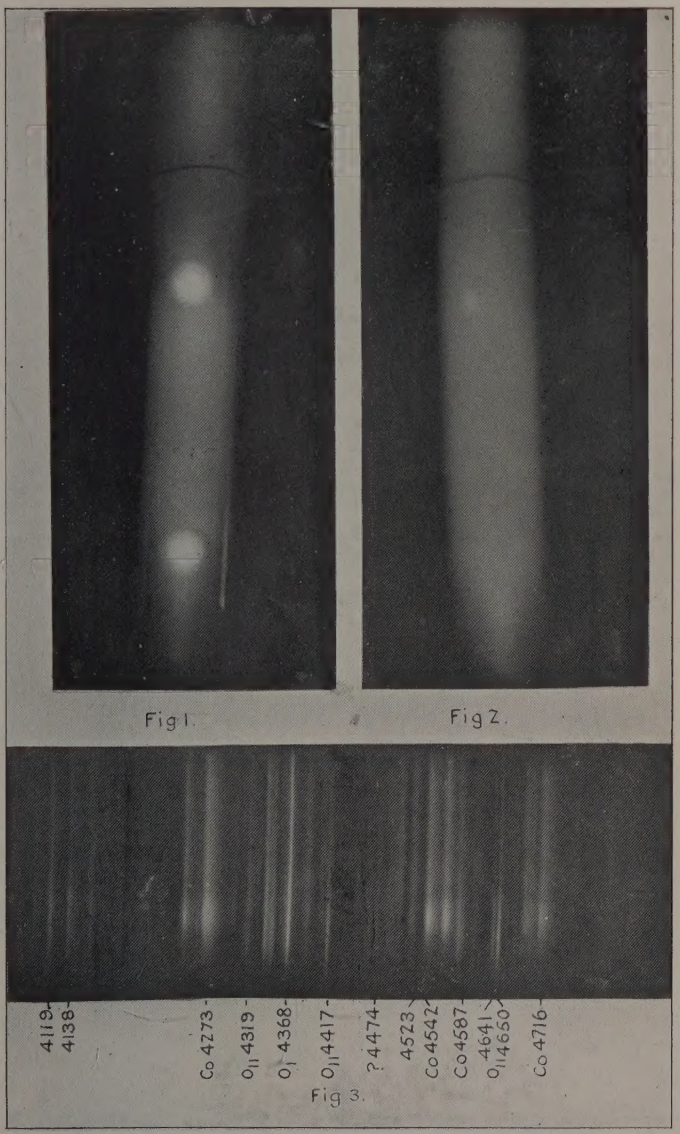
Fig 1.
Fig 2.
4119
4138
Co 4273
O II 4319
O I 4368
O II 4417
? 4474
4523
Co 4542
Co 4587
4641
O II 4650
Co 4716
Fig 3.

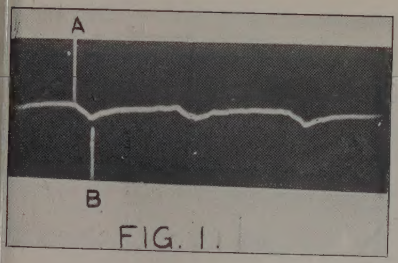

FIG. 1.

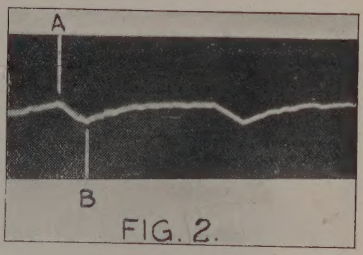

FIG. 2.

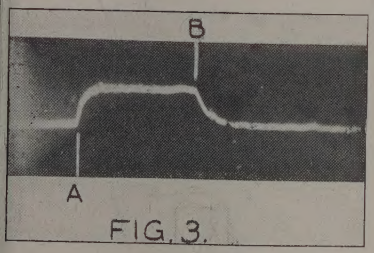

FIG. 3.

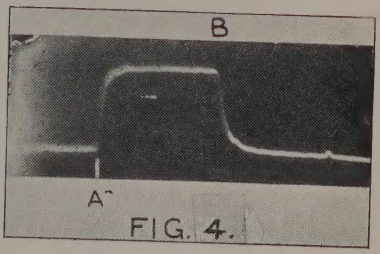

FIG. 4.

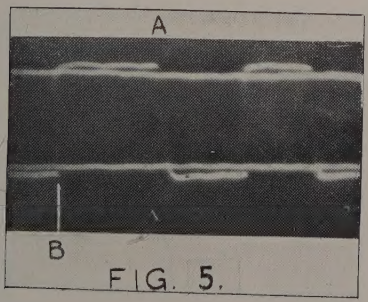

FIG. 5.